MASSACHUSETTS INSTITUTE OF TECHNOLOGY

THEORETICAL ANALYSIS OF GIMBALLESS INERTIAL REFERENCE EQUIPMENT USING DELTA-MODULATED INSTRUMENTS

by

THOMAS FREUD WIENER

MARCH 1962

DOCTOR OF SCIENCE

T-300

THEORETICAL ANALYSIS OF GIMBALLESS INERTIAL REFERENCE EQUIPMENT USING DELTA-MODULATED INSTRUMENTS

by

THOMAS FREUD WIENER

Lieutenant (junior grade), United States Navy
Sc. B. (E), Brown University, 1958

SUBMITTED IN PARTIAL FULFILLMENT
OF THE REQUIREMENTS FOR THE DEGREE OF
DOCTOR OF SCIENCE IN INSTRUMENTATION

at the

MASSACHUSETTS INSTITUTE OF TECHNOLOGY
March 1962

THEORETICAL ANALYSIS OF GIMBALLESS INERTIAL REFERENCE EQUIPMENT USING DELTA-MODULATED INSTRUMENTS

by

Thomas Freud Wiener

Lieutenant (junior grade), U.S. Navy

Submitted to the Department of Aeronautics and Astronautics on 1 March 1962 in partial fulfillment of the requirements for the degree of Doctor of Science in Instrumentation.

ABSTRACT

Gimballess inertial reference equipment might provide six possible advantages over conventional stable member systems. These are savings in power, size, weight, and expense, flexibility of packaging, and ease of maintenance. The theoretical problems involved in gimballess equipment are the question of what inertial instruments measure, and how best to use the information they generate. The engineering problems concern the difficulty of torquing gyroscopes with accuracies approaching one part in a hundred million, and the design of inertial instruments to withstand the high angular rates they will experience in this application. The inertial package to be considered contains three delta-modulated integrating gyros and three delta-modulated integrating accelerometers.

Delta modulation is a pulse modulation system which delivers output pulses, representing increments of the input or one of its integrals or derivatives, in synchronism with a clock. The analysis of delta-modulated loops with either a two- or three-level relay is a straightforward matter using z-transforms and modified step-by-step transient methods. Application of delta modulation to integrating gyros and accelerometers leads to instruments whose output pulses represent increments of rotation and velocity.

Transformation of a vector from one Cartesian coordinate frame to another may be represented in three essentially different ways: through matrix-tensor operations, four-parameter techniques, and vector algebra. Comparison of these to determine which is most suitable for machine computation, both from the standpoint of generating the transformation parameters and of accomplishing the transformation, shows that a matrix transformation, with straightforward generation of direction cosines, is best. The most attractive choice of machine for the computation is the digital differential analyzer, since the angular and linear motion information is in incremental form. High-order integration rules with larger angular increments cannot be used to reduce computer speed while maintaining accuracy because of an irreducible uncertainty in the digital angular information.

The transformation computer may be analyzed using frequency domain techniques. With these techniques, a signal flow graph representing the computer can be developed, which gives great insight into the dominant mode of operation of the computer, and which provides an estimate of truncation error. Quantization may be treated statistically.

This investigation has considered one way of instrumenting gimballess inertial reference equipment in detail, and has provided a survey of some of the possibilities in this field. It has shown the theoretical feasibility of such equipment, and has also indicated that the major development effort required to permit practical realization of such equipment with a specified accuracy must be concerned with inertial instruments designed especially for this application.

Thesis Supervisor: Wallace E. Vander Velde, Sc. D.

Associate Professor of
Aeronautics and Astronautics

ACKNOWLEDGEMENTS

I would like to express my appreciation to my thesis committee, Professor Wallace E. Vander Velde, Professor Walter Wrigley, Professor Yao Tzu Li, and Professor William W. Seifert for their helpful comments and suggestions. Especial thanks is due to Professor Vander Velde, who as chairman of the committee provided untold hours of stimulating discussion and guidance.

Also, I would like to thank my friend, John E. Miller, for his continued interest in this work and for his many contributions along the way.

The Faculty of the Institute and the Staff of the Instrumentation Laboratory were always willing to give freely of their energies in my behalf. Joan Phillips, Ruth Hession, and Claire Caram were most helpful in doing a great deal of tedious computation. Ann DeCarlo, Anne Rubin, and Joan Rogers performed heroically in typing the thesis.

I am indebted to the U.S. Navy, who made my graduate education possible.

Finally, I would like to thank my wife, Louise, for her editorial and other services.

T. F. W.
February, 1962

CONTENTS

LIST OF FIGURES

LIST OF TABLES

LIST OF SYMBOLS

Symbol	Meaning	Appearing
A	Output of linear plant of delta-modulated loop	2, A, B
	Angle of rotation about $\bar{r}$	4
A_c	Half-width of zero level of relay in delta-modulated loop	2, B
A_i	Value of A at i^{th} sampling instant	A, B
A_L	Euler angle; rotation about line of nodes	4
A_{min}	Minimum detectable angle of instrument float	3
A_o	Initial derivative of A	2, A, B
A_{OA}	Angle through which instrument float has turned with respect to the case about its output axis	3
$\overline{A}_{OA}$	Average value of A_{OA}	3
A_Z	Euler angle; rotation about Z axis	4
A_z	Euler angle; rotation about z axis	4
$A_{\Delta\theta}$	Value of A_{OA} representing one increment in the output	3
a_{IA}	Acceleration of accelerometer with respect to inertial space along its input axis	3
a_{max}	Maximum acceleration system will experience	6
a_{PRA}	Acceleration of accelerometer with respect to inertial space along its pendulum reference axis	3
B	Feedback signal in delta-modulated loop	2, A, B
b	Subscript deonoting body coordinate frame	4, 5
C	Output of delta-modulated loop	2, A, B
	Square matrix of direction cosines	4, 5, C
	Damping coefficient of instrument	3

Symbol	Meaning	Appearing
$C(O)$	Initial value of matrix C	5, C
$C_{ij}(O)$	Initial value of matrix element C_{ij}	5
C^T	Transpose of matrix C	4
C^{-1}	Inverse of matrix C	4
D	Drive level of relay	2, A, B
$d\theta_i$	Differential of rotation about i^{th} body axis	5
E	Error signal of delta-modulated loop	A, B
E_n	Truncation at n^{th} step	5
E_p	Allowable error in position	6
e_{ijk}	Cyclic tensor	4
f_a	Frequency of accelerometer clock	6
f_g	Frequency of gyro clock	6
f_{IA}	Frequency of vibratory motion about input axis	3
f_{SRA}	Frequency of vibratory motion about gyro spin reference axis	3
G	Linear plant in delta-modulated loop	2, A, B
G_1	Portion of G in forward path	2
G_2	Portion of G in feedback path	2
G_2'	G_2 excepting zero order hold if one is present	2
H_{sp}	Spin angular momentum of gyro	3
I	Identity matrix	C
$_I$	Subscript denoting inertial coordinate frame	4, 5
I_{IA}	Moment of inertia of instrument float about input axis	3
I. M.	Impulse modulator	2, 3, A, B
I_{PA}	Moment of inertia of instrument float about pendulum axis	3
I_{SA}	Moment of inertia of instrument float about spin axis	3
I_S	Information stored in float	3
i, j, k	Quaternion unit space vectors, $i^2=j^2=k^2=-1$	4
J	Polar moment of inertia of instrument float	3

Symbol	Meaning	Appearing
j	Unit imaginary number, $j = \sqrt{-1}$	2, 4, A, B
K	Number of periods in a given mode	A
	Elastic restraint constant	3
k	$k = \omega/\omega_1$	5
ℓ	$\ell = \omega/\omega_2$	5
M	Torque level of torque generator	3
M(z)	Numerator of terms containing $(1-\alpha z)$ in denominator	A, B
M_{app}	Torque applied to instrument float about its output axis	3
M_{tg}	Torque applied by torque generator	3
m	integer	3
	$m = \omega/\omega_3$	5
N	Number of pulses in an output sequence	2
N(A, ω)	Describing function	2
N^+	Number of positive pulses in an output sequence	2
N^o	Number of zero pulses in an output sequence	2
N^-	Number of negative pulses in an output sequence	2
n	Number of sampling periods	A, B
	Integer	3
	Number of bits in R and Y registers	5, 6
n_1	Number of sampling periods of opposite sign	A
OA	Subscript denoting output axis	3
P	Pendulosity of accelerometer	3
PA	Subscript denoting pendulum axis	3
PRA	Subscript denoting pendulum reference axis	3
Q	Matrix of Cayley-Klein parameters	4
Q^A	Adjoint of matrix Q	4
Q^*	Complex conjugate of matrix Q	4
$\|Q\|$	Determinant of matrix Q	4
Q_q	Quantizer with grain size q	5

Symbol	Meaning	Appearing
q	Quaternion	4
	Quantization grain size	5
q_o	Zero quanternion, $q_o = (0, \bar{0})$	4
$q(t)$	Quantization noise	5
q_u	Unit quaternion, $q_u = (1, \bar{0})$	4
$\overline{q_{ij}^2}$	Mean squared quantization noise at ij^{th} node	C
q^{-1}	Inverse quaternion, $q^{-1} = q^*/\lvert q^2 \rvert$	4
q^*	Conjugate quaternion	4
R	Input to delta-modulated loop	2, A, B
	Remainder of Z in DDA	5
r	$r = R/D$	2, A, B
$\bar{r}$	Unit vector along right hand axis of rotation	4
S	Strength of impulse	A, B
s	Laplace complex frequency variable	2, 5, A, B
$_s$	Subscript denoting sampling	2, 5, A, B
T	Period of oscillation	2
	Time required for float to travel through $A_{\Delta\theta}$	3
T_f	Time of flight	6
T_s	Sampling period	2, 5, A, B
t	Time	2, A, B, C
U	Numerator of fraction describing step input	2
$u_{-1}(t)$	Step function	A, B
V	Complex matrix representing $\overline{V}$	4
$\overline{V}_b$	Column vector with components resolved into body-fixed coordinates	4
V_{co}	Velocity at thrust termination	6
$\overline{V}_I$	Column vector with components resolved into inertially fixed coordinates	4
V_{max}	Maximum velocity system will attain	6
W	Denominator of fraction describing step input	2
W_{ca}	Angular velocity of instrument case about its output axis with respect to inertial space	3

Symbol	Meaning	Appearing
$\delta R/\delta V$	Velocity range derivative	6
ϵ_T	Percentage error in time of output pulse	3
ζ	Root of characteristic equation of transformation computer	5
θ_{IA}	Rotation of instrument about its input axis	3
θ_{ind}	Indicated value of θ_{IA}	3
λ	Scalar part of quaternion	4
$\bar{\rho}$	Vector part of quaternion	4
$\bar{\sigma}$	Vector representing rotation	4
$\bar{\sigma}'$	Alternate vector representing rotation $\bar{\sigma}' = -\bar{\sigma}/\sigma^2$	4
τ_i	Time constant of linear plant of delta-modulated loop	2, 3, A, B
Φ_{qq}	Power spectral density of quantization noise	5, C
ϕ_{qq}	Autocorrelation function of quantization noise	5
ϕ_s	Maximum phase shift due to sampling delay, $\phi_s = 2\pi \frac{T_s}{T}$	2
Ω	Angular velocity matrix	4, 5
ω	Angular frequency	2, A, B
$\bar{\omega}$	Angular velocity vector	4
ω_i	i^{th} component of $\bar{\omega}$ resolved into body-fixed frame	4, 5, C
ω_s	Angular sampling frequency of delta-modulated loop	2, 3, A, B
$\bar{1}$	Unit vector	4
$\dot{}$	Time differentiation, $\dot{A} = dA/dt$	2, 3, 4, 5, A, B

Symbol	Meaning	Appearing
W_{IA}	Angular velocity of instrument float about its input axis with respect to inertial space	3
W_{max}	Maximum angular velocity	3, 6
W_{PA}	Angular velocity of instrument float about its pendulum axis, with respect to inertial space	3
W_{SA}	Angular velocity of instrument float about its spin axis, with respect to inertial space	3
W_{SRA}	Angular velocity of instrument float about its spin reference axis with respect to inertial space	3
X	Variable of integration in DDA	5
X,Y,Z	Inertial axes	4
x, y, z	Body axes	4
Y	Integrand of DDA integration	5
Z	Output variable of DDA integration	5
z	Unit delay, $z = e^{-sT_s}$	2, 5, A, B, C
z_i	Unit "delay" in transformation computer $z_i = e^{-s\frac{\Delta\theta}{\omega_i}}$	5, C
$\alpha,\beta,\gamma,\delta$	Cayley - Klein parameters	4
α_i	Decay constant, $\alpha_i = e^{-\frac{T_s}{\tau_i}}$	2, A, B
γ	Phase angle	3
Δ	Prefix denoting increment	2, 3, 5, 6, A B, C
ΔV	Velocity increment	3, 5
$\Delta\theta$	Rotation increment	3, 5, C
δ	Variable delay due to samping	2
$\delta(t)$	Dirac delta function; unit impulse	A, B
δ_{ij}	Kronecker delta	4

CHAPTER 1

INTRODUCTION

1.A Background

The problem of arriving at a destination has been important to man from the beginning. At first, getting there was merely a matter of following a line of sight to the destination. Later, landmarks whose position with respect to the destination were known were used as guideposts in making journeys out of sight of the destination. The stars, which can be used out of sight of land, represent an important class of these reference points. Celestial bodies can be observed only on clear nights, and of course, other landmarks, by and large, must be visible to be useful. With the invention of radio, and later radar, man-made radiation could be used to distinguish landmarks during periods of reduced visibility. In modern military and transport applications many situations exist in which terrestrial and celestial reference points are either unavailable or unreliable as a basis for guidance. In such cases there is a need for navigation systems which do not depend on any external information. Inertial navigation systems, which deduce the position of a vehicle from on-board measurements, are systems of this type. The measured acceleration is integrated twice with respect to time to give displacement for an initial position.

The majority of inertial navigation systems today use two or three single-axis accelerometers mounted on a stable platform to measure acceleration. The platform is either kept non-rotating with respect to inertial space or precessed so that the input axes of the accelerometers are kept coincident with some slowly rotating set of coordinate axes, such as local geographic coordinates. The stabilized platform is

articulated with respect to its support by a system of gimbals. The gyros mounted on the platform detect the angular motion of the platform, and the gimbals are torqued in response to gyro signals to drive the platform back to its null position.

Another configuration for inertial navigation systems has the inertial instruments fixed to the vehicle and hence is gimballess. Single axis accelerometers measure vehicle acceleration and resolve it into vehicle coordinates. The guidance equations may be solved in body coordinates, in which case gyro information about vehicle rotations is used directly in the guidance equations; or they may be solved in an inertial coordinate frame, in which case the gyro information is used to generate a coordinate transformation which operates on the accelerometer data to give acceleration resolved into inertial axes.

There are six possible advantages available in gimballess guidance systems. With the removal of gimbals, weight, space, and power required are reduced. Further, the not inconsiderable expense of gimbals is eliminated. Since the inertial package in a gimballed system must assume practically a spherical shape, it is necessary to find a spherical space in the vehicle in which to put the guidance system. Without gimbals to dictate packaging, much more flexibility in packaging is available. Finally, assembly and maintainence of the inertial package is easier without the encumbrance of gimbals.

1.B The Problem of Gimballess Inertial Reference Equipment

1.B.1 Theoretical Aspects

The theoretical problems of gimballess inertial navigation are two: the measurement of acceleration in body fixed coordinates and the determination of the orientation of the body fixed coordiante frame with respect to the inertially fixed coordinate frame from gyro information.

The three single axis accelerometers measure inertial acceleration and resolve it into components along body-fixed axes. Coriolis effects are not inherently present in the measured acceleration components; they arise only in the intepretation of these components in non-inertial reference frames. If such frames are used in the guidance equations, the Coriolis terms must be computed separately using angular information from the gyros. If the guidance equations are set in inertial coordinates,

the three measured components need only be transformed into the inertial coordinate system.

The generation of a vector transformation from gyro information is a straightforward process. The differential equation governing the transformation parameters may be derived and instrumented in any convenient way.

1.B.2 Engineering Aspects

The engineering problems involved in gimballess applications of inertial guidance are many, but the two most important involve the environment to which the inertial instruments will be subjected and the speed of computation required to keep the computed orientation of the body-fixed coordinate frame close to its actual orientation.

While inertial instruments mounted on a stable platform are isolated from the angular motions of the vehicle carrying them, they do experience all the linear motion and most of the vibrations of the vehicle. Body-mounted instruments, in contrast, experience both the angular and linear motions, but they may be effectively shock mounted to minimize the vibrations present. Although much effort has been expended in developing instruments whose performance does not deteriorate under acceleration, practically none has been devoted to designs which might experience large angular velocities. For this reason no instruments are available at present which can be used in a gimballess application.

In gimballess inertial reference equipment, the gyros are used to measure angular orientation of the body-fixed coordinate frame with respect to some reference. This may be done either by using a pick-off arrangement with free gyros, or by torquing single-degree-of-freedom gyros to make them follow body rotations. If free gyros are used, the pick-offs must be accurate to about five thousandths of a degree. The required accuracy of torquing for single-degree-of-freedom gyros may be shown by the following considerations. If the gyro is to have a drift rate of one meru (about $7 \cdot 10^{-8}$ radians per second), the uncertainty in applied torque must not exceed this level. The maximum angular velocity which a typical vehicle might experience is about one radian per second, so that the maximum torque available must be able to precess the gyro

at that rate. Comparison of these two numbers shows that for gimballess applications, and the above specifications, the torquing must be accurate to about seven parts in a hundred million. For higher acceptable drift rates or lower maximum velocities, this accuracy requirement is less stringent.

The orientation of the body-fixed coordinate frame must be known to a high degree of accuracy (about five thousandths of a degree); thus at reasonable angular velocities very high computer speeds are required to keep up with the vehicle rotation. If a single adder is to be used, add times on the order of five microseconds per word are required. This is near the limit of available performance.

1.C Scope of the Investigation

A gimballed inertial reference system delivers acceleration information in stabilized inertial coordinates. This investigation will consider an inertial reference system with single axis integrating accelerometers and single-degree-of-freedom integrating gyros fixed to a vehicle. All the instruments will be pulse torqued. The gyro information is to be used to generate a coordinate transformation which will operate on accelerometer information to give inertially stabilized data. Thus it is proposed that the gimballed inertial package be replaced by a body-mounted inertial package and a transformation computer.

This investigation assumes that the guidance equations will be solved in inertial coordinates; no examination is made of the possibility of doing all or part of the computation in body-fixed coordinates. Further, no consideration is taken of the feedback through the guidance computer and vehicle autopilot.

There are no studies available which compare the attractiveness of various coordinate frames available for computation in gimballess guidance. For this reason, the present investigation of the performance and design of a system which provides inertially stabilized information from a gimballess inertial package is a useful one. Further, since the action of the inertial package and transformation computer is much faster than the feedback present, the equipment may profitably be examined as an open loop device.

Since the inertial package consists of three delta-modulated single-axis integrating accelerometers and three delta-modulated single-degree-of-freedom integrating gyros, the theory of delta modulation and its application to inertial instruments will be considered in some detail. Methods for determining the zero-input behavior of delta-modulated loops will be reviewed, and the response of such loops to impulses and steps will be found. Criteria for the choice of loop parameters will be set forth.

The available methods of transforming a vector from one Cartesian coordinate frame to another will be examined. There are essentially three ways of viewing the transformation: the matrix of direction cosines, the four parameter representations, and the vector representation. The properties of each will be considered and the differential equations governing the transformation parameters will be derived. Finally, the transformations will be compared to determine their suitability for machine computation, considering the form of instrument output.

The transformation computer will be designed to instrument the transformation found to be best for machine computation. The possibility of accumulating a number of increments from the gyros and instrumenting more complicated algorithms to permit the use of a computer with a slower clock rate and reduction of error will be examined. With the design of the computer fixed, a detailed analysis will be carried out to determine the dominant mode of the computer and estimates of truncation and quantization errors.

Finally a few typical values will be used to illustrate the method of determining the basic system parameters and at the same time to provide a feel for the order of magnitude of the numbers involved.

1.D Previous Results

Delta-modulation was originated as a transmission system (Refs. 2, 5, 6, 14) with little attention being paid to the feedback aspect of the transmission loop. Later, with interest developing in control systems using relays, control theory was applied to delta-modulated loops (Refs. 1, 3, 4, 6-13, 15-19) under the names bang-bang, on-off, and contactor control systems. The zero-input behavior of these loops

received most of the attention, with phase plane methods playing an important part (Refs. 8-11). In 1960 a method for determining the exact zero input behavior of a loop of any order by means of difference equations was presented by Torng and Meserve (Ref. 19) and the z-transform equivalent of this method was suggested by Bergen in his discussion of their paper (Ref. 1). Schwartz elaborated Bergen's method and applied it to the determination of the loop's response to step inputs (Ref. 15). Beyond this, no work has been done previously in determining the response of the loop to step inputs.

The application of delta modulation to inertial instruments first took place in 1957, and development work has continued so that these instruments are now a very attractive choice for any inertial system which requires instrument outputs in digital form (Refs. 4, 7, 8, 17, 18).

Coordinate transformations have received only cursory examination in connection with gimballess inertial reference equipment. Although some reports consider the possibility of using transformations other than direction cosines, they do not examine them in any detail. Of course, the literature on coordinate transformations is available in almost any text or reference on classical mechanics or mathematical physics (Refs. 30-39).

The analysis of numerical processes has a fairly long history, and most techniques are easily applied to digital computers (Refs. 41, 44, 46, 48, 51-53). However the application of frequency domain methods to the analysis of computers is quite rare (Refs. 49-51, 55, 61), and thus most analysis to date is quite cumbersome. No attempt has yet been made to apply frequency domain analysis to digital computers in which the vairable of integration has not been time.

A number of private companies have worked in the field of gimballess guidance, both on their own initiative and under contract. Their studies have mostly provided a brief survey of the possibilities in this field, but no detailed analyses. Very little of this work is available in the open literature (Ref. 66).

CHAPTER II

DELTA-MODULATED LOOPS

2.A Introduction

Delta modulation is a pulse modulation system patented in France in 1946 (Ref. 6) and first described in the literature by de Jager (Ref. 5) and others (Ref. 14) in 1952 as a system for speech transmission. In 1957, a similar system was developed giving digital outputs directly from instruments and interest in such instruments has remained active. (Refs. 4, 7, 8, 12, 17, 18)

2.B Description of the Loop

The input is translated into a sequence of pulses, each having the same value, but with either polarity being possible. The pulses are obtained by means of the negative-feedback loop shown in Fig. 2-1. One or the other of the linear plant functions may be unity. When the loop is used for transmission, the linear plant in the forward path is usually unity, while in instrumentation applications the feedback plant usually contains a zero-order hold. In any case, an integration occurs somewhere in the linear plant to assure zero average error (Ref. 3, p. 53). The relay may have either two levels or three levels. The mathematical model for the sampler is an impulse modulator synchronized with a clock.

Each impulse appearing at the output represents a unit change in the input or one of its integrals or derivatives. This representation of a signal in terms of increments leads to the name "delta modulation". If the integration appears in the forward path, each output pulse represents a change in the integral of the input. If the integration appears in the feedback path, each pulse represents a change in the input itself. Two integrations in the feedback path cause each pulse to represent a change

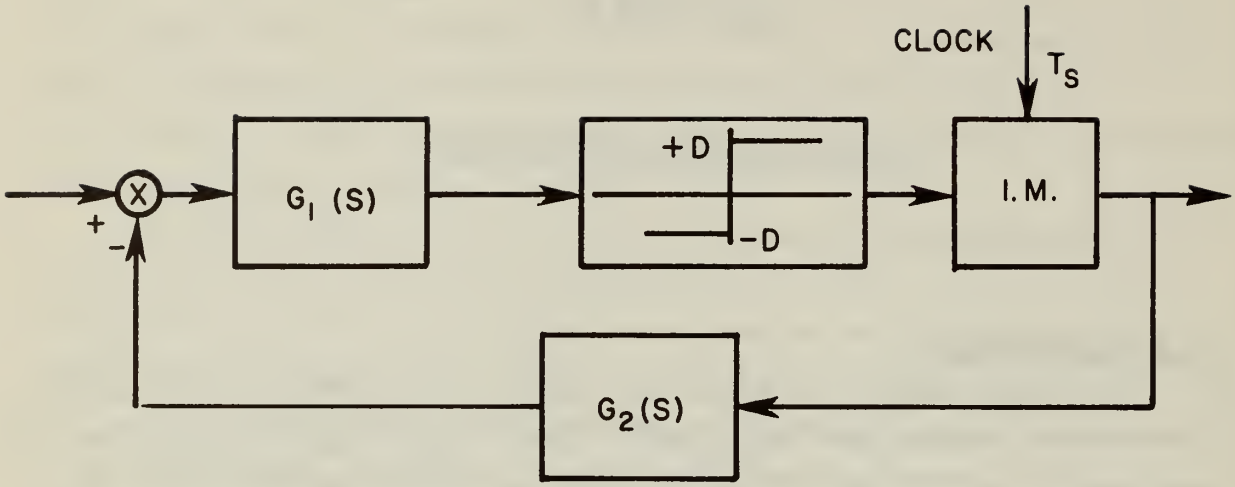

(a)

Two Level Relay

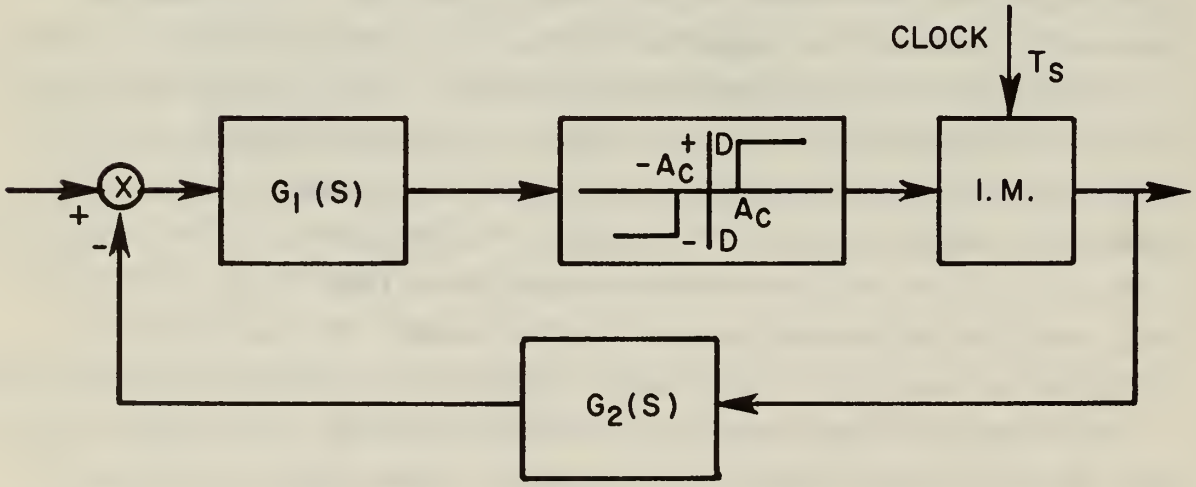

(b)

Three Level Relay

Fig. 2-1 Delta-Modulated Loops

in the slope of the input.

2.C Analysis for Zero Input

With no input, a loop with a two-level relay will experience a self-excited oscillation or limit cycle, and if the zero level is narrow enough, a loop with a three-level relay may also have a limit cycle. From physical considerations, it is clear that the periods of these limit cycles are integral multiples of the sampling period. Further, if the linear plant contains an integration, the number of positive pulses in a cycle will equal the number of negative pulses (Ref. 3, p. 53).

2.C.1 Moding

Each limit cycle exhibited by delta-modulated loops produces a characteristic sequence of output pulses. These sequences are referred to as the modes of the system and are very important in the analysis of input-output relationships. The modes of a system are designated by the output sequence they produce. For example, if the limit cycle in a loop with a two-level relay produces a single positive pulse followed by a single negative pulse, the mode designation is 1-1. Similarly, a mode producing two positive pulses followed by two negative pulses is designated 2-2. If the loop contains a three-level relay and has a limit cycle producing two positive pulses followed by two negative pulses and one zero pulse, the mode is termed 2-0-2-1. The zero for the second digit indicates that no zero pulse occurs between the positive and negative pulses. Note that the mode designations always begin with the positive pulses.

The concept of moding is applicable only to systems with no input, since the limit cycle is disturbed by inputs. The description of outputs in response to inputs is discussed in Section 2.D.

2.C.2 Describing Function Analysis

In his famous paper(Ref. 58) Kochenburger presented a method of steady-state sinusoidal analysis applicable to non-linear systems in which non-linear elements are represented as linear gains. These gains are determined as functions of the amplitude and frequency of the inputs to the non-linear element. Chow (Ref. 3) and Russell (Ref. 13)

first used the describing function to determine limit cycles in delta-modulated loops. Their interest was in adjusting the width of the zero level in a three-level relay to eliminate limit cycles, but their analysis is applicable to any sampled-data loop containing any non-linearity.

Their method of analysis is the same as the standard describing function analysis applied to continuous time systems with the addition of a variable delay due to sampling. This variable delay, δ, arises because the output pulses can occur only at sampling instants, even though the relay had switched earlier. This delay, which ranges from zero to a full sampling period, T_s, is easily understood from an examination of Fig. 2-2. The marks on the time axis indicate clock pulses. In each

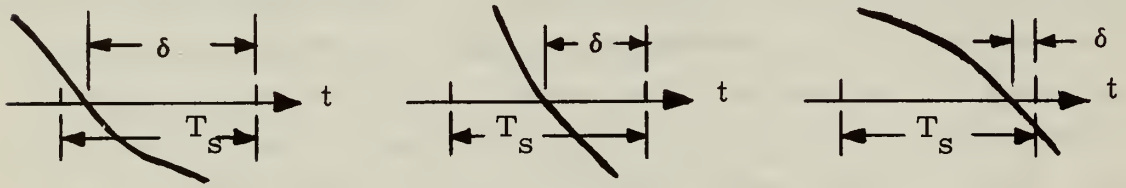

Fig. 2-2 Time Delay due to Sampling

case, the negative output pulse occurs with the second clock pulse shown and δ ranges from almost an entire sampling period in Fig. 2-2(a) to practically zero in Fig. 2-2(c). The maximum phase shift due to sampling, ϕ_s, is the product of frequency and sampling period, and is given by

$$\phi_s = \omega T_s = 2\pi \frac{T_s}{T} = 2\pi \frac{\omega}{\omega_s} \qquad (2\text{-}1)$$

where T is the period corresponding to the input angular frequency ω.

Standard describing function analysis (Ref. 63, Ch. 10, pp. 559-580) is carried out by graphical solution of the equation

$$1 + G(j\omega)N(A, \omega) = 0 \qquad (2\text{-}2)$$

$G(j\omega)$, the transfer function for the linear part of the system, is plotted on a Nyquist diagram with $-\frac{1}{N(A, \omega)}$, the negative of the reciprocal of the describing function for the non-linear element. Intersection of the

two curves indicates a root of Eq. (2-2) and predicts a limit cycle. In the analysis of delta-modulated loops the phase shift due to sampling must be added to the plot; this is most conveniently done by adding ϕ_s as a phase lag at frequencies on the G(jω) locus for which a limit cycle is possible, that is, at submultiples of the sampling frequency. In this application, a log polar plot is most convenient for making the Nyquist plot. It is termed a "moding plot".

In Fig. 2-3, a moding plot for $G(j\omega) = \frac{1}{j\omega(j\omega\tau + 1)}$ is shown. The negative reciprocal describing function for a two-level relay covering the whole negative real axis is shown. As can be seen from this plot, limit cycles are predicted for angular frequencies of $\omega_s/2$, $\omega_s/4$, and $\omega_s/6$. At $\omega_s/8$ the sampling phase is at most $\pi/4$, which is not sufficient to reach the negative real axis. It is clear that limit cycles will not exist at lower frequencies; thus the modes predicted are 1-1, 2-2, and 3-3. For a three-level relay, the describing function reaches a maximum when the amplitude of the relay input is $\sqrt{2}$ times the zero level half-width, A_c. Thus the reciprocal of the describing function has a minimum, and the zero level half-width may be adjusted so that no limit cycle is predicted. An example of this calculation is shown in Appendix B.

2.C.3 Detailed Analysis

The describing function is only an approximate tool, albeit a powerful one. For this reason attempts were made to achieve exact answers. The step-by-step transient method was discarded as being too cumbersome. Phase-plane methods received more attention, and although limited to second order systems became quite elegant (Refs. 9-11). Torng and Meserve (Ref. 19) presented a method for determining the exact output of the linear plant of a delta-modulated loop at sampling instants using discrete orthogonal functions. Bergen (Ref. 1), in his discussion of their paper, outlined a similar method using z-transform techniques. His method allows the possibility of determining no-transient initial conditions for the limit cycle. By manipulation, the state of the linear plant at each sampling instant may also be determined.

Each method assumes a mode at the relay and applies it as an input

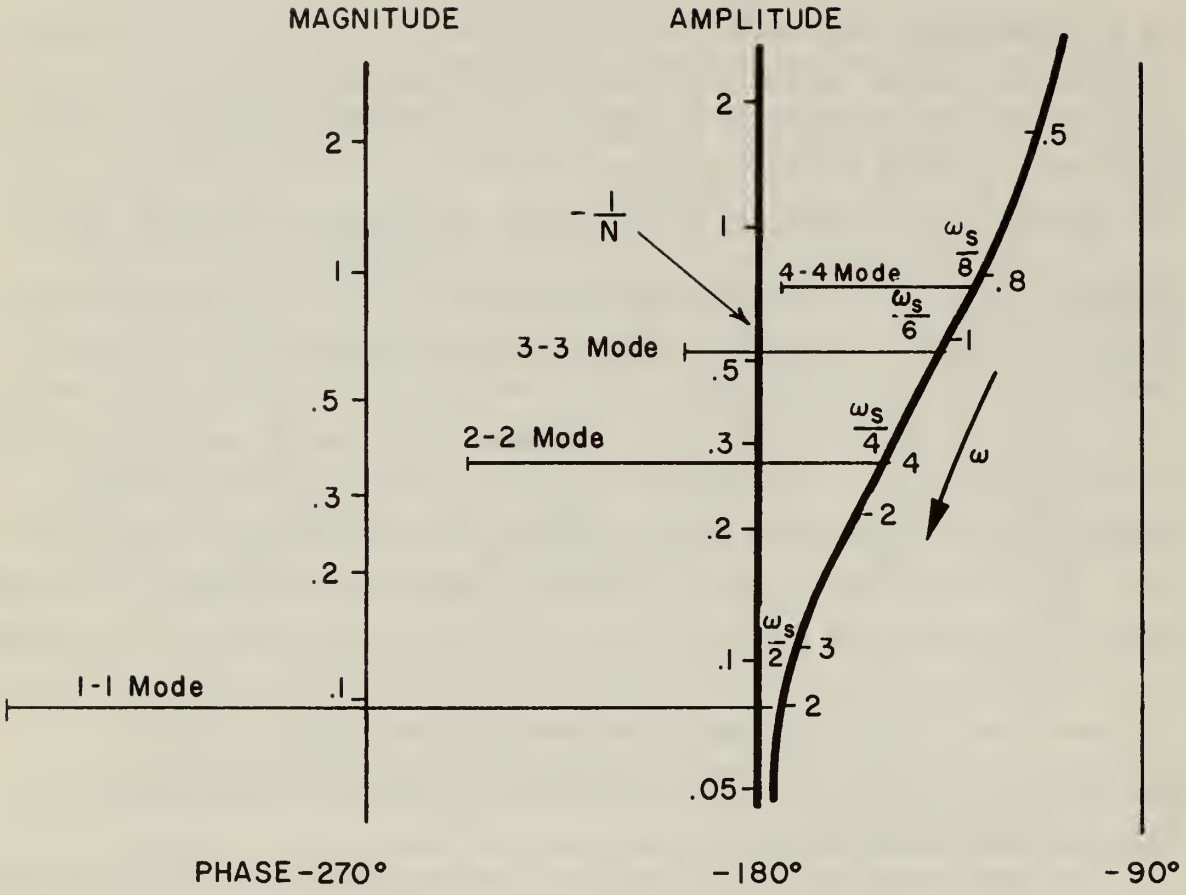

MODING PLOT

Fig. 2-3 Moding Plot

to the linear plant. The output of the linear plant resulting from this input is examined at the sampling instants to see if the signal has the proper polarity to sustain the postulated mode. Thus if the 1-1 mode be possible, the linear plant output at sampling instants must be a repeating sequence of two numbers: the first positive, the second negative. Torng and Meserve do this using discrete orthogonal functions in the time domain. Bergen operates in the frequency domain with z-transforms, and introduces initial conditions in this way.

The modes which must be investigated are limited, and may be determined by a describing function analysis as carried out above (Sec. 2.C.2). Torng and Meserve list the modes which must be investigated for limit cycles with periods of two, four, six, and eight sampling periods (Ref. 19, Table II, p. 303).

For a loop with a three-level relay, choice of the zero-level width so that a describing function analysis predicts no limit cycle may be made. However, for fast systems ($T_s/\tau > 1$), this choice of zero-level width may not eliminate low energy limit cycles. To eliminate these, a transient analysis is the easiest. The linear plant output is assumed to be just at the edge of the zero level of the relay. Thus one feedback pulse drives the linear plant back toward null. For no limit cycle to occur, the limit of the linear plant motion must not reach the outer edge of the zero level, even for very long times. The result of this analysis for any linear plant containing an integration is that the zero level width should be chosen greater than the product of the sampling period and the steady state velocity of the plant under the action of the relay alone.

2.C.4 Compensation

As Schwartz (Ref. 15) and Sliwkowski (Ref. 16) point out, in limit cycling loops inputs may not be sensed until one full period of the prevailing mode has elapsed. Another view of this problem is that in limit cycling, the loop is storing information; the amplitude of the limit cycle, indicated by the moding, is a measure of the information storage. This information storage should be kept to a minimum if the system is to be used to best advantage. In a loop with a three-level relay the

width of the zero level is a measure of stored information, and for slow systems ($T_s/\tau < 1$) may become quite large. For this reason it may be desirable to compensate the system so that all but the 1-1 mode are eliminated, or so that the zero level of a three-level relay is reduced to a reasonable size. There are three methods of compensation which suggest themselves: dc analog, ac analog, and discrete or digital.

Compensation is best viewed in terms of the moding plot (Fig. 2-3). To eliminate the 2-2 mode, more than 90° phase margin must be provided for $G(j\omega)$ at $\omega_s/4$. Similarly to eliminate the 3-3 mode 60° of phase margin must be provided at $\omega_s/6$ and so on. With these conditions met, the extended $G(j\omega)$ locus will not intersect the describing function except at the 1-1 mode. For a three-level relay, the zero level width may be adjusted so that the reciprocal describing function reaches down to just above the 1-1 level.

Dc analog compensation methods are covered in detail in most elementary automatic control textbooks (Ref. 57, Vol. I, Ch. 12; Vol II, Ch. 4; Ref. 64, Ch. 6; for example). Adjusting the moding plot to achieve the objectives listed above is a straightforward task. Ac analog compensation is also treated in many texts (Ref. 63 Ch. 6; Ref. 64 Ch. 6; for example). The desirability of this form of compensation stems from the fact that the relay is often a phase-sensitive switch operating on information in a supressed-carrier wave; thus, if dc compensation were used, the signal would have to be demodulated. However, the signal frequencies used in practice are very close to the carrier frequencies, and demodulation is very difficult under these conditions. For this reason, ac compensation is quite attractive. It should be noted that the use of low-pass to band-pass transformations do not provide sufficiently accurate compensation for this application.

Discrete or digital compensation has received little attention in the literature. The advantage of this form of compensation is that there is no problem of drift as compared to analog compensation, and non-linear or logical compensation is possible. Most books on sampled-data systems include sections on the techniques of linear discrete compensation and Tou (Ref. 62, pp. 444 ff) lists three methods for realizing linear discrete

transfer functions: computers, delay lines, and pulsed RC circuits.

The point in the delta-modulated loop at which the signal is discrete is after the sampler; it is here that the discrete compensator must be inserted. If a pulsed RC circuit is used, a second sampler must follow it.

Linear discrete compensation is best viewed in the G(z) plane. The locus of the linear plant has extensions similar to those in the moding plot, because of sampling delays. The compensation must be chosen so that the extended $G^*(s)$ locus does not intersect the negative reciprocal describing function locus.

Logical discrete compensation, using branching operations which influence the relay on the basis of past output pulses, has been tried only once (Ref. 20) with little success. It would seem that there are great possibilities for this type of compensation.

2.D Input-Output Relationships

As explained above, each output pulse represents a unit change in the input or one of its integrals or derivatives. Thus with a finite input, the algebraic sum of the output pulses should average to the input or one of its integrals or derivatives or, in the case of zero input, to zero. The system overloads when the rate of change of the input (or one of its integrals or derivatives) exceeds that value which requires all the output pulses to be of one sign (Ref. 2, p. 145). Therefore a convenient way of expressing the input is as a fraction of the maximum permissible signal.

Since the position and number of integrators in the loop change input-output relationships, a general analysis is very cumbersome. For this reason, the analysis discussed here considers a loop with one integrator in it. The linear plant in the feedback path is moved to the forward path, with the exception of zero-order hold, if one is present, which is left in the feedback path. This requires the reciprocal of the moved plant to be placed in front of the loop. Fig. 2-4 shows the rearranged loop. The dotted lines around the hold indicate that it may or may not be present. $G_2'(s)$ is the part of the linear plant moved out of the feedback path. The analysis which follows ignores the $1/G_2'(s)$ in front of the

loop since it tends to confuse the issue.

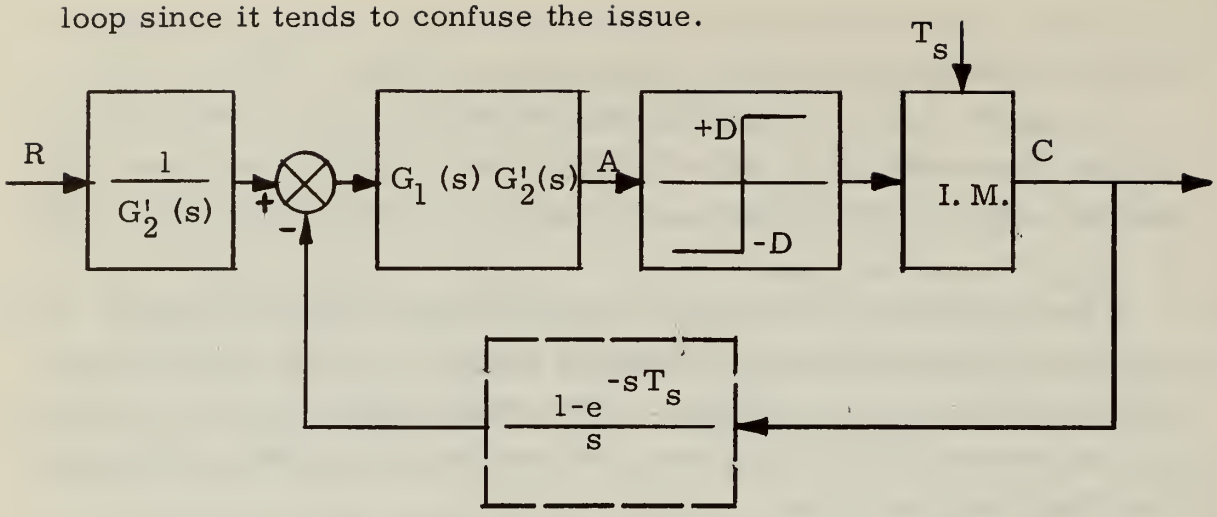

Fig. 2-4 Delta-Modulated Loop, Rearranged

2.D.1 Transient Response

The following analyses are exact determinations of the inpulse and step responses of delta modulated loops. With the exception of Schwartz's work (Ref. 15) on step inputs for loops with two-level relays, they have not been previously described.

2.D.1.a Impulse Response

The height of an impulse (infinity) exceeds the capacity of the system; the best output makes up the integral of the impulse a step at a time to within the quantization error of the loop. Clearly if the value of the impulse is too low, no output will appear, except for the limit cycle.

The analysis of the loop's impulse response is best done by a step-by-step transient method. The applied impulse drives the linear plant some distance from null; calculation of this excursion in the presence of the feedback signal is a simple task. The linear plant output at sampling instants is examined for the time at which the feedback signal changes sign. If the loop has a two-level relay, the state of the linear plant is compared with the set of initial conditions corresponding to each mode to determine into which mode the system will settle. Usually this will be the highest mode. The output of the linear plant plant in a loop containing a three-level relay is examined to see if it will cause the relay to have an output of opposite sign from the input. If not, the

computation is complete; if so, it must be carried further.

2.D.1.b Step Response

A step input of magnitude D, where D is the drive level of the relay, will saturate the system. For this reason the magnitudes of step inputs are given as a fraction, r, of D.

For a periodic sequence to appear at the output, the input must be expressed as a rational fraction of the saturating input. This is not a serious limitation, since any number less than one may be well approximated by a rational number with a small denominator

Suppose the input is a rational fraction, say U/U, of the saturating signal. Then the output will be a sequence of NW pulses. For a loop with a two-level relay, there will be $N^+ = (W+U)/2$ positive pulses and $N^- = N(W-U)/2$ negative pulses. This may be shown by a short computation. The relationship between U, W, N^+, and N^- is

$$\frac{N^+ - N^-}{N^+ + N^-} = \frac{U}{W} \qquad (2\text{-}3)$$

Rearrangement of this ratio yields

$$\frac{N^+}{N^-} = \frac{W+U}{W-U} \qquad (2\text{-}4)$$

A loop with a three-level relay may have N^O zero pulses. In this case, the required relation between U, W, N^+, N^-, and N^O is

$$\frac{N^+ - N^-}{N^+ + N^- + N^O} = \frac{U}{W} \qquad (2\text{-}5)$$

If U is positive, and there are no negative pulses, then

$$\frac{N^+}{N^O} = \frac{U}{W-U} \qquad (2\text{-}6)$$

With ratios, of positive, negative, and zero pulses determined, it only remains to determine the organization of these pulses within the sequence. This may be done by determining bounds on the number of consecutive pulses of one sign under various conditions. Different bounds are of interest depending on whether the loop has a two-level or a three-level relay.

For a loop with a two-level relay, the bounds that are important are the maximum number of pulses of one sign that are possible and the minimum number of pulses of one sign that are possible following a given number of pulses of the opposite sign.

The upper bound is found by observing the greatest possible excursion from null and counting the number of clock periods required to drive the linear plant back across null. The maximum excursion from null occurs when the linear plant output travels away from null at maximum rate for a full sampling period.

The lower bound is found by assuming minimum initial conditions. The minimum displacement is clearly zero plus, and the minimum derivatives result from maximum velocity at the previous switching time a given number of sampling periods earlier. Under these initial conditions, the number of sampling periods required for the system to cross null is found.

The bounds to be determined in the case of a loop with a three-level relay are the maximum number of pulses of the same sign as the input and the maximum number of opposite sign.

Determination of the maximum number of pulses of the same sign as the input proceeds from the assumption that the linear plant has travelled at maximum rate under the influence of the input alone for a full sampling period. At this point, positive pulses begin to drive the plant back to null. The pulses required to bring the linear plant output within the zero level are counted.

The possibility of pulses of a polarity opposite to the input may be examined by a similar analysis. It is assumed that the linear plant is driven across the zero level under the influence of the feedback signal and input for a full sampling period starting from just outside the zero level. The feedback signal switches off, and the system output is examined at successive sampling times to see whether it gets outside the zero level on the other side.

Examples of the above computations are shown in Appendices A and B.

With these bounds set, the sequences having the required average

may be written down. These sequences are designated in a way similar to that used for modes. For example, a sequence from a loop with a two-level relay consisting of three positive pulses followed by a negative pulse is designated 3, 1; one having four positive pulses, one negative pulse, two positive pulses, and another negative pulse is designated 4, 1, 2, 1. A loop with a three-level relay having an output sequence of a positive pulse followed by a zero pulse would have that sequence designated 1, 1, 0, 0. Nothe that each of these sequences has an average of one-half. The permissible sequences, which are few because of the elimination process just described, may be tested by Bergen's method to see if they can actually occur. The sequence, with the input, is assumed to drive the linear plant, and the signs of the linear plant output are examined at sampling times to see if the postulated sequence is sustained.

With inputs smaller than about one-tenth of the saturating signal, the period of the output sequence becomes rather too long for the analysis above to handle conveniently, and a modified step-by-step transient procedure is preferable.

In a loop with a two-level relay and a small input, the prevailing mode will continue for a number of cycles. The feedback signal has zero average over a full period of the mode, and its effect may be ignored. This is perhaps best visualized in phase space with the mode trajectory moving slowly through the space under the influence of the input. When the position coordinate of one of the sampling points of the trajectory moves to a new region of phase space (from positive to negative, for example), the prevailing mode will change. The mode changes either by dropping a pulse or by adding a pulse. In any case, the total state of the linear plant after the mode changes may be found and compared with the initial states of the other modes. Thus the new mode of the system is found. The trajectory of the new mode is assumed to move under the influence of the input, with a new initial position and an initial velocity which is the velocity of the plant relative to the new prevailing mode. This process is continued until the entire sequence is determined.

For the loop with a three-level relay, the appropriate calculation is a step-by-step transient response. Assume an initial condition, and

follow the plant through until the sequence is determined. In almost all cases only one positive output pulse will occur between zero pulses.

2.D.1.c Effects of Imperfect Integration

Thus far, it has been assumed that the integrator has been perfect. In some cases, the integrator is in reality a first order lag with a long time constant. This may be viewed as a small elastic restraint. With an elastic restraint present, there is a limit below which inputs cannot be detected. This is also best seen in terms of the mode trajectory in phase space. If the steady-state response of the linear plant to a small input is insufficient to move the trajectory far enough to cause the mode to change, no input will be detected. Of course, with a three-level relay, this critical value of linear plant output is the edge of the zero level.

2.D.1.d Ramps and Higher Order Inputs

Ramps and higher order inputs (e.g. parabolic) cannot be followed by the loop over infinite time since the amplitude of such a signal increases without limit. A sawtooth wave may be analyzed in terms of the frequency response described below. For ramps which rise to a certain value and then remain constant, a step-by-step transient computation seems to be the most convenient. The bounds on number of pulses are useful in this computation.

2.D.2 Frequency Response

Since the frequency response method of servomechanism design is familiar to most engineers, the following modification of the describing function is presented.

A sinusoidal signal is assumed at the relay. The standard describing function is used to represent the relay, assuming enough low pass filtering in the loop to make the describing function valid. The fundamental of the relay is passed through the sampler and hold, giving the feedback signal. With the input to the relay, which is the output of the linear plant, known, the error signal can be determined. The input to the loop is the sum of the error and feedback signals. With the relay output taken as the loop output, the describing function for the entire loop is determined as the ratio of relay output to loop input.

Three comments must be made about the above analysis. First,

the output of the loop has been taken as the relay output, with no limit cycle present. Thus, this analysis, for frequencies approaching the limit cycle frequency, is open to question. Second, there is a minimun amplitude of signal which can be detected, corresponding either to the limit cycle amplitude or the zero-level width of the relay. Third, the bandwidth of the loop is limited by the sampling frequency, and signals above this frequency will not be passed; instead they appear as steps. (Ref. 19).

CHAPTER III

DELTA-MODULATED INSTRUMENTS

3.A General Comments

The delta-modulated loops discussed in Chapter II are to be applied to two inertial instruments, the gyroscope and the accelerometer. The gyro to be used is the single-degree-of-freedom floated integrating gyro described by Draper, Wrigley and Grohe (Ref. 21). The accelerometer is a single-axis floated integrating pendulum type described by Hutchings and others (Refs. 4, 7, 8, 12, 17).

3.A.1 Brief Description of the Instruments

The integrating gyro, when behaving in an ideal manner, is described by the following differential equation:

$$J\ddot{A}_{OA} + C\dot{A}_{OA} = H_{sp}W_{IA} + M_{tg} \qquad (3\text{-}1a)$$

where J is the moment of inertia of the gyro float about its output axis;

C is the damping coefficient of the fluid damper;

H_{sp} is the spin angular momentum of the gyro;

W_{IA} is the angular velocity of the gyro case about its input axis, with respect to inertial space;

M_{tg} is the torque applied to the instrument float by the torque generator;

and A_{OA} is the angle through which the float has turned with respect to the case avout the instrument output axis.

A dot over a quantity (e.g. $\dot{A}_{OA}$) denotes time differentiation.

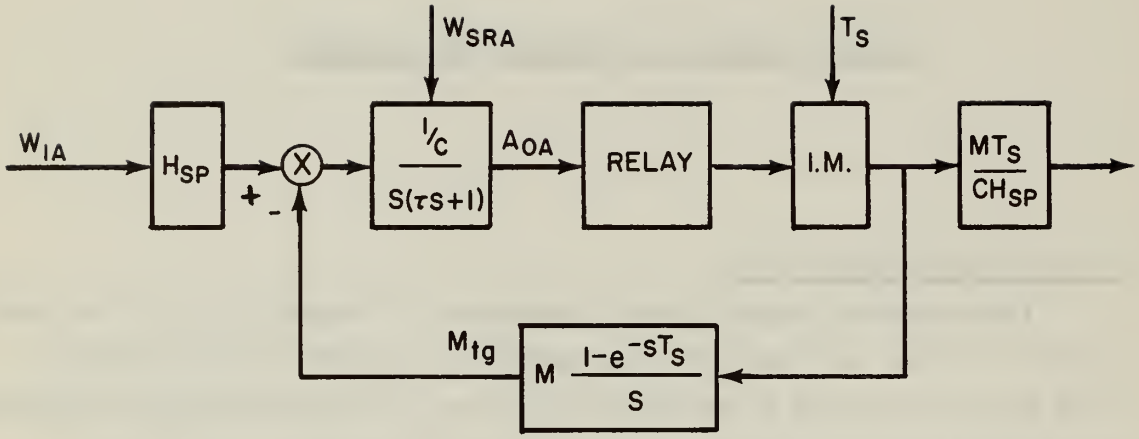

DELTA-MODULATED GYRO
(a)

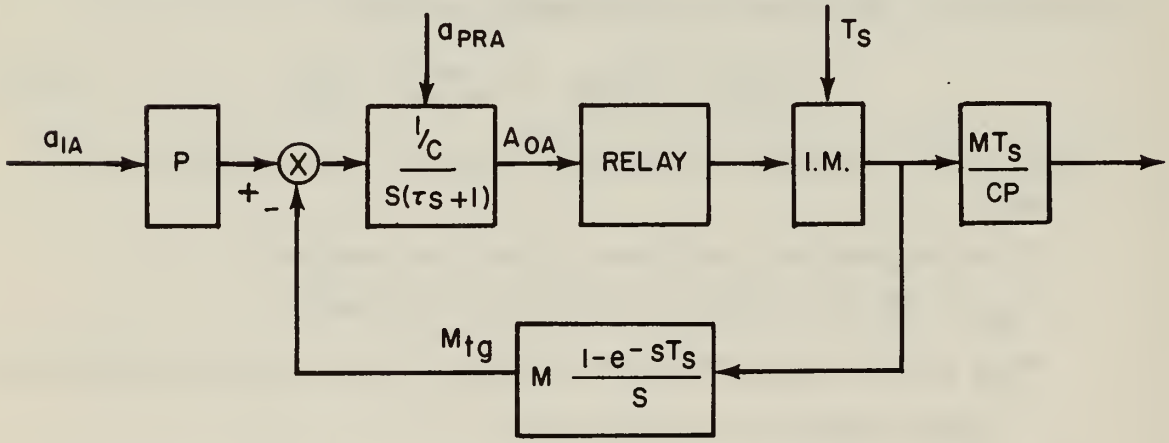

DELTA-MODULATED ACCELEROMETER
(b)

Fig. 3-1 Delta-Modulated Instruments

Eq. (3-1a) may be rewritten as

$$\tau \ddot{A}_{OA} + \dot{A}_{OA} = \frac{H_{sp}}{C} W_{IA} + \frac{M_{tg}}{C} \qquad (3\text{-}1b)$$

where $\tau = J/C$ is the characteristic time or time constant of the gyro.

The differential equation describing the accelerometer is

$$J\ddot{A}_{OA} + C\dot{A}_{OA} = Pa_{IA} + M_{tg} \qquad (3\text{-}2a)$$

where the symbols above are similarly defined; where P is the pendulosity of the accelerometer; and a_{IA} is the non-gravitational acceleration of the instrument with respect to inertial space along its input axis.

Eq. (3-2a) may be rewritten as

$$\tau\ddot{A}_{OA} + \dot{A}_{OA} = \frac{P}{C} a_{IA} + \frac{M_{tg}}{C} \qquad (3\text{-}2b)$$

where again $\tau = J/C$.

The torque generators are fed from a constant current source, with the current switched between two opposing windings to produce torque of different signs, or switched to a dummy load or off to produce zero torque. The required sign of the torque is determined at sampling times and is either opposite to the sign of the float angle or zero, depending on the logic of the loop. Therefore, the torque generator acts as a zero-order hold in the feedback path.

3.A.2 Form of the Loops

The delta-modulated instruments may be represented as shown in Fig. 3-1. These loops are identical in form to each other and to the loops analyzed in Appendices A and B. The output pulses represent changes in the integral of the input, so that the gyro's output pulses indicate changes in the angular orientation of the gyro case about its input axis, and the accelerometer's output pulses indicated changes in velocity along the accelerometer's input axis.

3.B Delta-Modulated Gyros

3.B.1 Detailed Description

A detailed physical description of the single-degree-of-freedom

floated integrating gyro is presented in Reference 21. Current practice is to center the gyro float in the case with a magnetic suspension system similar to that described in Reference 26, as well as to float it. Nominal values of the characteristics of some gyros are given in Reference 25. Fig. 3-2 shows a schematic drawing of the instrument.

The differential equation governing the gyro may be derived from Euler's equations of motion for a rigid body about principal axes. It is assumed that the bearings of the gyro are infinitely stiff, so that only motions about the output axis need be considered. The bearing stiffness assumption is quite well satisfied for gyros even under high angular velocities. The set (IA, OA, SRA) forms a right-handed triad. The equation is

$$M_{app} = -H_{sp}(W_{IA} \cos A_{OA} - W_{SRA} \sin A_{OA}) + J(\ddot{A}_{OA} + \dot{W}_{ca})$$
$$+(I_{IA} - I_{SA})(W_{IA}^2 - W_{SRA}^2) \sin A_{OA} \cos A_{OA}$$
$$+(I_{IA} - I_{SA})(\cos^2 A_{OA} - \sin^2 A_{OA}) W_{IA} W_{SRA} \qquad (3\text{-}3a)$$

$$M_{app} = M_{tg} - C\dot{A}_{OA} \qquad (3\text{-}3b)$$

where M_{app} is the torque applied to the instrument float about its output axis;

W_{SRA} is the angular velocity of the gyro float about its spin reference axis, with respect to inertial space;

W_{ca} is the angular velocity of the case about its output axis, with respect to inertial space;

I_{IA} is the moment of inertia of the gyro float about its input axis;

I_{SA} is the moment of inertia of the gyro float about its spin axis.

These equations may be rewritten as

$$\tau\ddot{A}_{OA} + \dot{A}_{OA} - \frac{H_{sp}}{C} W_{SRA} \sin A_{OA} = \frac{H_{sp}}{C} W_{IA} \cos A_{OA} +$$

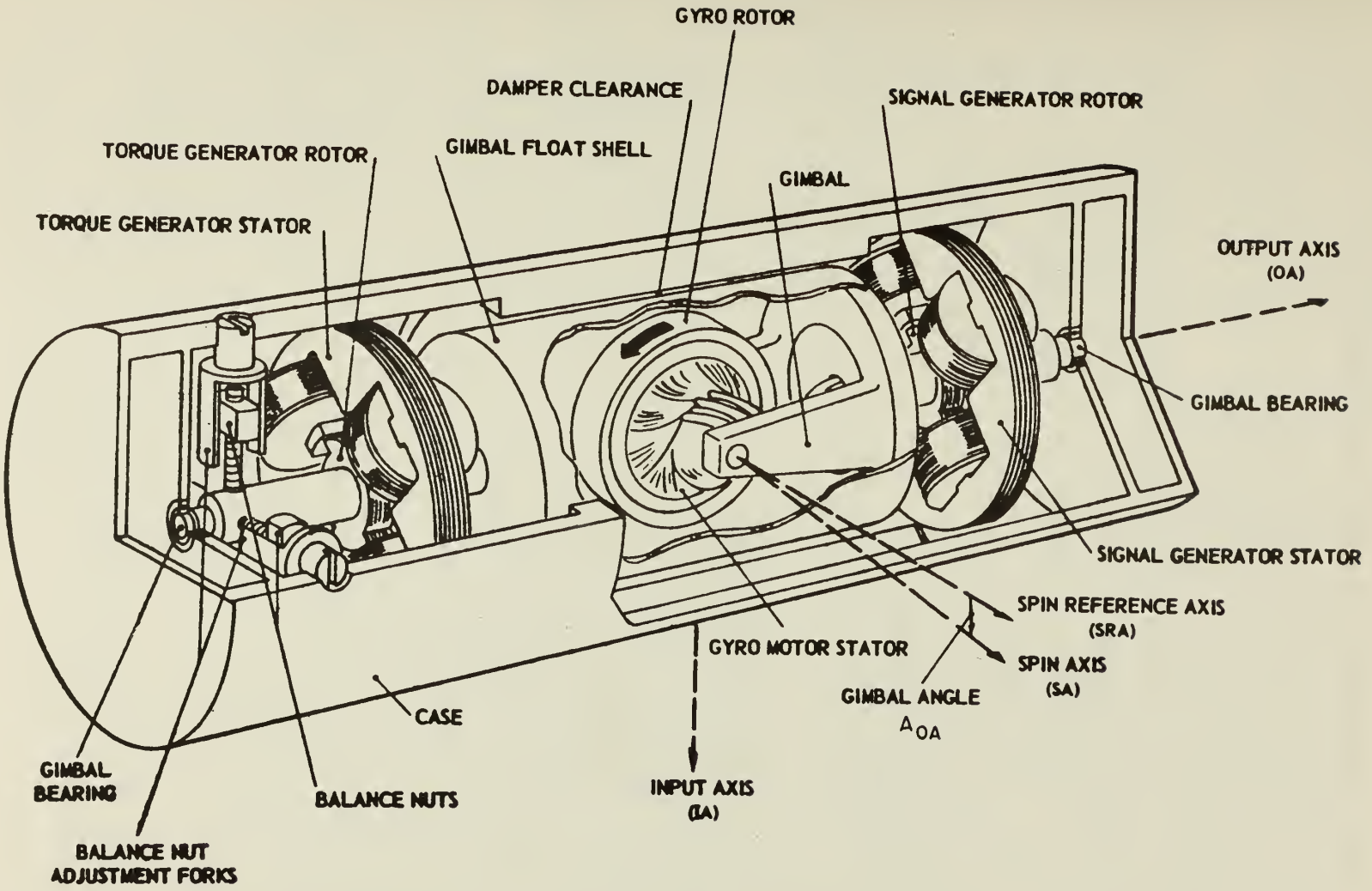

Fig. 3-2 Pictorial Diagram of Floated Single-Degree-of-Freedom Integrating Gyro

$$-\tau\dot{W}_{ca} + \frac{M_{tg}}{C} + (I_{SA} - I_{IA})(W^2_{IA} - W^2_{SRA}) \sin A_{OA} \cos A_{OA}/C$$
$$+ (I_{SA} - I_{IA}) (\cos^2 A_{OA} - \sin^2 A_{OA}) W_{IA} W_{SRA}/C \qquad (3\text{-}3c)$$

The last two terms on the right side of Eq. (3-3c) are anisoinertia effects and are negligible in practical gyros. They will not be considered further here.

Since A_{OA} stays well below a degree in practice, the standard small angle approximations may be made in Eq. (3-3c):

$$\tau\ddot{A}_{OA} + \dot{A}_{OA} - \frac{H_{sp}}{C} W_{SRA} A_{OA} = \frac{H_{sp}}{C} W_{IA} - \tau\dot{W}_{ca} + \frac{M_{tg}}{C} \qquad (3\text{-}3d)$$

For $W_{SRA} = \dot{W}_{ca} = 0$, Eq. (3-3d) is identical with Eq. (3-1b).

3.B.2 Rotational Coupling

Eq. (3-3d) shows that rotations of the gyros about all axes affect its motion. The coupling effects of these motions will be considered in detail.

3.B.2.a Non-Reversing Rotations

Examination of Eq. (3-3d) shows that an angular velocity about the spin reference axis appears as an elastic restraint term in the gyro equation. This elastic restraint causes imperfect integration in the loop. As noted in Chapter II, Section 2.D.1.c, imperfect integration in the loop produces a dead zone, and inputs within this dead zone cannot be detected. This is a significant phenomenon in gimballess inertial reference equipment, since large angular velocities may occur about any axis.

Angular acceleration of the case about its output axis produces a torque on the instrument float of the inertia reaction category. As can be seen from Eq. (3-3d), this torque is proportional to the gyro time constant and acts as a spurious input to the gyro.

These torques may be compensated out either directly in the gyro or in the computer, if it is found that they seriously affect the performance of the gyro, in a manner similar to that used for compensation of compliance effects in present gyros.

3.B.2.b Vibratory Rotations

Vibratory rotations of the gyro about one axis at a time do not affect the performance of the instrument. When this type of motion occurs about two axes at a time, however, it can produce a drift.

Consider sinusoidal motion of the case about the spin reference axis and the input axis. With sinusoidal motion, the gyro equation of motion, ignoring torque generator torque, is

$$\tau A_{OA} + A_{OA} - \frac{H_{sp}}{C} W_{SRA} \sin(2\pi f_{SRA} t) A_{OA} = \frac{H_{sp}}{C} W_{IA} \sin(2\pi f_{IA} t + \gamma) \tag{3-4}$$

A solution for this equation using series techniques, which coverges for $W_{SRA} H_{sp}/C < 1$, has been given by Haff and Meltzer (Ref. 27, Ch. 5). A further discussion of the series solution and its convergence is given in Reference 29.

Haff and Meltzer show that if $nf_{SRA} = mf_{IA}$, a constant drift is predicted by the series solution which they propose. A similar effect occurs if a vibration about the output axis occurs with the vibration about the spin reference axis. Further, if f_{SRA} is harmonically related to the clock frequency, drift may also be present, as can be seen by writing the Fourier series expansion for the torque generator torque.

Angular vibrations of the gyro about any two axes produce a conical motion. Computation of the orientation of the gyro may be made in such a way as to introduce a constant angular velocity about the cone axis in the computed orientation, when none actually exists. Haff and Meltzer present a general treatment of this effect for a stabilized platform (Ref. 27, Ch. 3, Sec. 3.4). It is clear from their discussion how the computation implied by a stable platform leads to this error. This coning error does not exist in gimballess systems.

3.B.3 Linear Motions

Many writers (Ref. 22, for example) have treated the effects of linear motions on gyros and they will not be considered here.

3.B.4 Choice of Loop Parameters

While the parameters of the loop must be chosen so that production

gyros and available electronic components may be used, a certain amount of latitude exists in choosing some parameters.

The spin angular momentum of the gyro is chosen on the basis of the allowable drift rate. The higher the drift acceptable, the lower the angular momentum may be.

The torque level, M, required in the torquer depends on the maximum angular velocity that the system must follow, W_{max}. The product of angular momentum and W_{max} gives the lower bound on M. For gyros with drift characteristics acceptable in inertial guidance applications, this bound may be quite high, and torquers other than microsyns may be required.

The clock frequency may be determined from the maximum angular velocity expected and the increment size in the loop, $\Delta\theta$,. The quotient $W_{max}/\Delta\theta$ gives the lower bound on clock frequency. If an ac signal generator is used, the carrier must be a multiple of the clock frequency. This requirement follows from the desirability of peak detection in the switch. If the carrier frequency is not a multiple of the clock frequency, the phasing of the clock and the carrier will not remain constant, and the clock pulses cannot be adjusted to appear at the peaks of the carrier sinusoid.

Since it is desirable to have the uncompensated mode of the loop as low as possible, or alternatively to have the relay zero-level width as narrow as possible, the gyro time constant, J/C, should be as low as possible. Since the polar moment of inertia of the float is usually fixed by the choice of angular momentum, the time constant depends only on the damping coefficient, C, which can be varied by varying the operating temperature of the instrument and the clearances between float and case. The higher the damping, the lower the time constant, but the smaller the angle through which the float travels. There is a certain value, A_{min}, below which the polarity of the signal cannot be determined, so that an indefinite increase in damping is not practicable. A short computation, suggested by J. E. Miller of the

M. I. T. Instrumentation Laboratory, gives an expression for the optimum damping in a loop with a two-level relay, considering only the dynamics of the gyro, which usually dominate.

The differential equation governing the gyro is

$$J\ddot{A}_{OA} + C\dot{A}_{OA} = H_{sp}W_{IA} + M_{tg} \qquad (3\text{-}5a)$$

Integration of this expression over an integral number of sampling periods, and assumption of zero initial conditions for A_{OA} gives

$$J\dot{A}_{OA} + CA_{OA} = H_{sp}(\theta_{IA} - \theta_{ind}) \qquad (3\text{-}5b)$$

where θ_{IA} is the angle through which the gyro case has turned about its input axis; and

θ_{ind} is the indicated value of θ_{IA}, obtained by counting output pulses.

The quantity $(\theta_{IA} - \theta_{ind})$ may be recognized as information stored in the float (see Ch. II, Sec. 2.C.4). When the torque switches sign, the value of A_{OA} is A_{min} and the value of $\dot{A}_{OA}$ is $M(1-\alpha^n)/(1+\alpha^n)C$. Here $\alpha = e^{-\frac{T_s}{\tau}}$ and the loop is assumed to be moding n-n. Thus at switching,

$$I_s = \frac{JM(1-\alpha^n)}{H_{sp}C(1+\alpha^n)} + \frac{C}{H_{sp}}A_{min} \qquad (3\text{-}5c)$$

By differentiating Eq. (3-5c) with respect to C, and setting the derivative equal to zero, an extreme value of I_s may be found, which can be shown to be a minimum. The dependence of α and n on C may be neglected.

$$\frac{dI_s}{dC} = \frac{JM(1-\alpha^n)}{H_{sp}C^2(1+\alpha^n)} + \frac{A_{min}}{H_{sp}} = 0$$

or

$$C = \sqrt{\frac{(1-\alpha^n)\,JM}{(1+\alpha^n)A_{min}}} \tag{3-6}$$

To show that this value of C indeed provides a minimum in I_s, $\frac{d^2 I_s}{dC^2}$ is computed:

$$\frac{d^2 I_s}{dC^2} = 2\,\frac{JM\,(1-\alpha^n)}{H_{sp} C^3 (1+\alpha^n)} > 0$$

which indicates a minimum.

This optimum value of C has been chosen to minimize stored information. The corresponding time constant is

$$\tau = \frac{J}{C} = \sqrt{\frac{(1+\alpha^n)JA_{min}}{(1-\alpha^n)M}} \tag{3-7}$$

For loops with a three-level relay, the damping should be chosen so that

$$A_c = A_{min} \tag{3-8}$$

The expressions for A_c are derived in Appendix B, Sec. B.1.

It is possible to show a relationship between the elastic restraint present in a gyro and the threshold of the instrument. The differential equation of the gyro is

$$JA_{OA} + CA_{OA} + KA_{OA} = H_{sp} W_{IA} + M_{tg} \tag{3-9}$$

where K is the elastic restraint acting on the float from all causes, including electromagnetic reaction torque and the effect of angular velocity about the spin reference axis. If the inertia-reaction torque is neglected (it is usually much smaller than the damping torque) and the average angle of the float, $\overline{A}_{OA}$, is considered, limit cycles may be ignored (See Ch. II, Sec. 2.D.1.b) Under these assumptions, the solution of Eq. (3-9) is

$$\overline{A}_{OA} = \frac{H_{sp} W_{IA}}{K}\left(1 - e^{-\frac{K}{C}t}\right) \tag{3-10}$$

In time T, the average angle of the float reaches a value $A_{\Delta\theta}$, which represents one increment in the loop's output. This value is given by

$$A_{\Delta\theta} = \frac{M}{C} T_s$$

Writing Eq. (3-10) for t = T and solving for T yields

$$T = -\frac{C}{K} \ell n \left(1 - \frac{A_{\Delta\theta}}{H_{sp} W_{IA}} K\right) \tag{3-11}$$

T becomes very large as $(A_{\Delta\theta}/H_{sp}W_{IA})K$ approaches unity. For this term greater than or equal to one, T is not defined. Physically, this corresponds to the case where elastic restraint completely masks the input (See Ch. II, Sec. 2.D.1.c). Using only the first and second order terms in the series expansion of the logarithm, for small K, gives

$$T \approx \frac{CA_{\Delta\theta}}{H_{sp}W_{IA}} \left(1 + \frac{1}{2} \frac{A_{\Delta\theta}}{H_{sp}W_{IA}} K\right) \tag{3-12}$$

Since $MT_s = H_{sp}\Delta\theta$, this may be written

$$T = \frac{\Delta\theta}{W_{IA}} \left(1 + \frac{1}{2} \cdot \frac{\Delta\theta}{W_{IA}} \cdot \frac{K}{C}\right) \tag{3-13}$$

Thus the percentage error in time of occurrence of an output pulse is

$$\epsilon_T = \frac{1}{2} \cdot \frac{\Delta\theta}{W_{IA}} \cdot \frac{K}{C} \tag{3-14}$$

By manipulating Eq. (3-14), many interesting relations between the time error and the loop parameters can be seen. The error in time decreases with elastic restraint and maximum input angular velocity. It is inversely proportional to the actual input angular velocity and the square of the damping coefficient. Since the optimum damping coefficient depends inversely on A_{min}, decreasing A_{min} decreases ϵ_T.

3.C Delta-Modulated Accelerometers

3.C.1 Detailed Description

A detailed physical description of a pulse-restrained accelerometer is given in Reference 8. Present practice is to center the float in the case by a magnetic suspension system described in Reference 25. Reference 4 gives some parameter values for a typical accelerometer. Fig. 3-3 shows a schematic drawing of the instrument.

The accelerometer's differential equation is

$$J\ddot{A}_{OA} + C\dot{A}_{OA} + Pa_{PRA} \sin A_{OA} = Pa_{IA} \cos A_{OA} - J\dot{W}_{ca}$$

$$+ (I_{IA} - I_{PA})W_{IA}W_{PA} + M_{tg} \qquad (3\text{-}15a)$$

where PA and PRA refer to the pendulum axis and pendulum reference axis respectively. (IA, PRA, OA) is a right-handed triad.

The last term on the right hand side of Eq. (3-15a) is an anisoinertia term which is negligible in practical accelerometers and it will not be considered further here. Making the small angle approximation for A_{OA} and dividing by C gives

$$\tau\ddot{A}_{OA} + \dot{A}_{OA} - \frac{P}{C}\, a_{PRA}A_{OA} = \frac{P}{C}\, a_{IA} - \tau\dot{W}_{ca} + \frac{M_{tg}}{C} \qquad (3\text{-}15b)$$

When $a_{PRA} = \dot{W}_{ca} = 0$, Eq. (3-15b) becomes Eq. (3-2b). As in the case of the gyro, infinite bearing stiffness has been assumed, and torques considered only about the output axis.

3.C.2 Rotational Coupling Effects

As can be seen from Eq. (3-15b), only rotations of the instrument about its output axis affect it, because of the assumed stiffness of the bearings. As in the case of the gyro, angular accelerations of the case about the output axis look like inputs.

If the case motion about its output axis is vibratory and a vibratory linear motion along the pendulum reference axis occurs, an equation of the form of Eq. (3-4) governs the accelerometer motion. As noted above, if the frequencies of the two motions are harmonically related, a drift in the loop's output may appear.

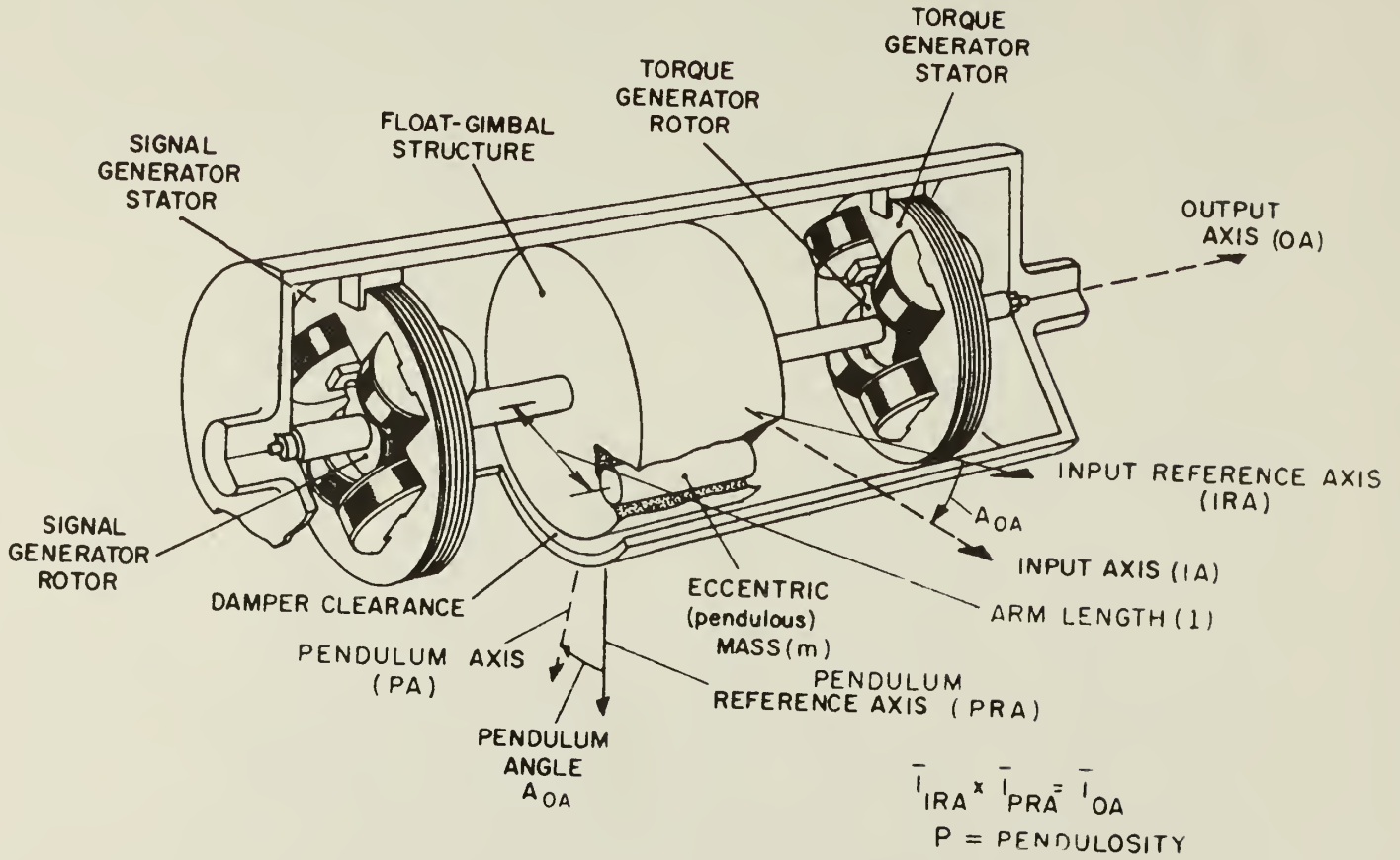

Fig. 3-3 Pictorial Diagram of Floated Single-Axis Pendulum

3.C.3 Linear Coupling Effects

Eq. (3-15b) shows that an acceleration along the pendulum reference axis appears as an elastic restraint. Imperfect integration results and a dead zone appears in the instrument. This is important in any application of this accelerometer since it may experience acceleration in any direction.

If a vibration occurs along the pendulum reference axis in conjunction with a vibratory input, a drift may result as described above. A similar situation may arise if vibrations along the pendulum reference axis are related to the clock frequency.

3.C.4 Choice of Loop Parameters

Parameters for delta-modulated accelerometers may be chosen in a way similar to that used when choosing gyro parameters. Those which may be chosen are pendulosity, torque level, clock frequency, and damping.

The pendulosity of the accelerometer is chosen on the basis of the level of torque uncertainties expected. The lower the torque uncertainty, the lower the pendulosity may be. This choice involves the same sort of compromise as the choice of angular momentum for a gyro.

The required torque level is the product of the pendulosity and the highest level of input acceleration expected. This value is practically always lower than the corresponding value for a gyro.

The clock rate is determined from the maximum acceleration expected and the velocity increments used. Their quotient gives the lower bound on clock frequency.

The choice of damping coefficient for the accelerometer is made just as in the case of a gyro. For a limit cycling accelerometer, the optimum damping is

$$C = \sqrt{\frac{(1-\alpha^n)JM}{(1+\alpha^n)A_{min}}} \qquad (3\text{-}16)$$

which gives a time constant

$$\tau = \sqrt{\frac{(1+\alpha^n)JA_{min}}{(1-\alpha^n)M}} \qquad (3\text{-}17)$$

For an accelerometer with a three-level relay, the damping coefficient should be chosen so that

$$A_c = A_{min} \qquad (3\text{-}18)$$

The remarks about elastic restraint made with respect to the gyro apply to the accelerometer as well. The equation corresponding to Eq. (3-14) is

$$\epsilon_T = \frac{1}{2} \frac{\Delta V}{a_{IA}} \frac{K}{C} \qquad (3\text{-}19)$$

3.D Non-Ideal Components

Up to this point, very little has been said about the non-ideal behavior of any components. The following sections consider some of the more serious hardware problems.

3.D.1 Gyros

In most applications, floated, single-degree-of-freedom integrating gyros do not experience significant angular velocities about any axis. In any environment in which they do, their performance will deteriorate, simply because they were not designed to take such punishment. A high angular velocity environment affects present-day gyros in two ways. First, they are not structurally strong enough to withstand the bending and torsion they experience. When torque is applied by the torque generator, the float experiences a torsional and bending stress because of the high spin angular momentum it has. In gimballess applications, the high torques involved may literally tear the instrument apart. A second effect of high angular velocities is high bearing loading. The bearings must be able to supply reaction forces strong enough to counter a torque equal to the torque generator torque. This cannot be done for long periods of time, but in a floated instrument the floatation fluid provides temporary additional bearing support, so that for short times the float will stay reasonably well centered. While at the present time floatation provides necessary additional support for the instrument,

magnetic supports are becoming capable of handling the entire load alone.

3.D.2 Torque Generator and Current Source

In the analysis above, it has been assumed that the time constant of the torque generator was negligibly small. This assumption is violated as the torque from a given instrument is increased. Torque rises as the square of the input current. To increase this current, either the voltage must be increased or the impedance of the torquer decreased. Increasing the voltage is not an attractive solution, since, in general transistors drive the torquer, and their voltage limit is quite low. Lowering the impedance requires lowering the resistance, which in turn raises the time constant of the torquer, L/R. As the time constant of the torque motor increases, the effect of the lag makes itself felt in the moding plot. The value of the torquer time constant above which the lag must be considered is about $\tau_{tg} = \frac{1}{5} T_s$. More torque can, of course, be obtained by increasing the size of the torquer, but it is desirable to have small instruments.

Microsyn torquers (Ref. 28) have been successfully used in pulse torquing applications. However, they are not high torque instruments, and their dependence on current squared makes them non-linear when used with a three-level relay.

Flapper-type torquers (Ref. 23) provide about ten times as much torque as a corresponding size microsyn. Their main disadvantage is the presence of a fairly large negative elastic restraint, which makes the torquer positionally unstable. This might be eliminated by providing a positive mechanical or electrical spring, or using ac voltage for torquing and tuning out the restraint term. The ac torquer provides a double frequency term as well as a constant average, so that the frequency used must be well above the clock frequency, and above the mechanical break point of the system.

Moving-coil, or d'Arsonval, instruments also provide large torques for small size. This type of torquer usually uses a permanent-magnet field. The difficulty with permanent magnets is that measurement techniques are not yet accurate enough to determine the stability of the field.

A problem that all three kinds of torquers share is the stability

of their sensitivities. Good operation of the instruments requires that the same angular impulse be applied to the float for each electrical impulse applied to the torquer. If this is not the case, the instrument scale factor will vary with time, and errors will appear from this source.

A related problem is the variation in torquer time constants with direction of torque. If the time constants are different, more impulse will be applied in the direction of the smaller time constant. Eventually a change in the output will be indicated although the input has been zero.

To achieve the required accuracy in torquing a very stable current source must be used. If a three-level relay is used, either the current must be turned off, or it must be fed into a dummy load. Turning off the current, while achieving great savings in power, causes stability problems in the current source above those already present. Ac current sources can be made more stable, but ac torquers are less sensitive than dc torquers.

3.D.3 Signal Generator

With ac signal generators, the output is a supressed-carrier wave. Thus, careful attention must be paid to the effects of circuitry which operates on the signal generator signal so that the gain for each sideband frequency is the same, and the phase shifts at each sideband are the negative of each other. If this is not the case, a quadrature component,which will cause a larger uncertainty in the position of the float with respect to the case, will be introduced into the signal. The end result will be an increase in the minimum angle of the float which can be detected. For this reason, the low-pass to band-pass transformations commonly used in ac compensation are not sufficiently accurate to be used in this application.

As noted above (Sec. 3.B.4) when ac signal generators are used, the carrier and clock pulse phases are adjusted so that the clock pulses occur at the peaks of the carrier sinusoid. This adjustment is usually made by shifting the ac signal at either the primary or the secondary winding of the signal generator. For the reasons noted above this

phase shifting should be done on the primary to avoid adding a quadrature component to the signal generator and increasing the minimum discernable angle.

Flapper-type (Ref. 24) and d'Arsonval signal generators provide attractive alternatives to microsyn signal generators, because of their small size.

CHAPTER IV

KINEMATICS OF ROTATING COORDINATE FRAMES

4.A Introduction

In a conventional inertial guidance system, the inertial space reference is preserved physically by the gimballed stable platform. The gimbals isolate the platform from the motion of the vehicle through servo drives, operating to null the output of gyros mounted on the stable platform. In a gimballess system, the inertial space reference may be preserved analytically in a transformation computer. This computer operates on a vector measured in body-fixed coordinates (the ΔV vector) to give the components of the vector in an inertially fixed frame of reference. The computer uses angular information obtained from gyros mounted on the vehicle to generate the rotational transformation.

In this chapter, the properties of the transformation and the relations between the angular velocity of the body-fixed coordinate system with respect to inertial space and the rates of change of the transformation quantities will be adduced.

There are essentially three methods of representing rotational transformations. Probably the most familiar is the matrix of direction cosines. This matrix, or alternatively, this second-order tensor, may have its elements written in terms of the nine direction cosines explicitly, in terms of a set of Euler angles, or in terms of the axis and magnitude of the rotation. Quaternions, invented by Sir William Hamilton in 1853 (Ref. 31), use four parameters to describe a rotation. The vector to be transformed is cast in quaternion form, pre-multiplied by a quaternion representing a rotation, and post-multiplied by the conjugate quaternion. The result

is a quaternion representing the rotated vector. A variation on this, the Cayley-Klein parameters, uses the same four parameters in a slightly different form. The third transformation uses a vector to represent the rotation, and performs the transformation by means of purely vector and algebraic operations.

These three types of transformation will be compared to determine which is most useful for machine computation.

4.B Direction Cosines: Matrices and Tensors

4.B.1 Direction Cosines

The most familiar of the rotation transformations is the matrix transformation (Ref. 30; p. 95ff)

$$\overline{V_I} = C\overline{V_b} \tag{4-1}$$

where V_I is a column vector with components measured in an inertial coordinate frame.

V_b is the same vector with components measured in a body-fixed coordinate frame, and

C is the square matrix of direction cosines of the inertial axes relative to the body axes.

The first component of Eq. 4-1 in vector notation is

$$\begin{aligned} V_{Il} &= \overline{l}_{Il} \cdot \overline{V}_b \\ &= (\overline{l}_{Il} \cdot \overline{l}_{b1})V_{b1} + (\overline{l}_{Il} \cdot \overline{l}_{b2})V_{b2} + (\overline{l}_{Il} \cdot \overline{l}_{b3})V_{b3} \end{aligned} \tag{4-2}$$

where l_{Il} is the unit vector along the inertial X axis, etc. Since the vectors involved are unit vectors,

$$\overline{l}_{Il} \cdot \overline{l}_{b1} = \cos(l_{Il}, l_{b1}) = C_{11} \tag{4-3}$$

and in general, the elements of the matrix C are

$$C_{ij} = \cos(l_I, l_{bj}) = \overline{l_{Ii}} \cdot \overline{l_{bj}} \tag{4-4}$$

The rate of change of the elements of C may be found by differentiating Eq. (4-4) directly:

$$\frac{d}{dt} C_{ij} = \frac{d}{dt}\left(\overline{l}_{Ii} \cdot \overline{l}_{bj}\right) = \frac{d}{dt}\left(\overline{l}_{Ii}\right)_I \cdot \overline{l}_{bj} + \overline{l}_{Ii} \cdot \frac{d}{dt}\left(\overline{l}_{bj}\right)_{I}$$

$$= \bar{l}_{Ii} \cdot [(\frac{d}{dt} \bar{l}_{bj})_b + \bar{\omega} \times \bar{l}_{bj}]$$

$$= (\bar{l}_{Ii} \cdot \bar{l}_{bj+1})\omega_{j+2} - (\bar{l}_{Ii} \cdot \bar{l}_{bj+2})\omega_{j+1} \quad (4\text{-}5)$$

or using a dot ($\cdot$) to denote time differentiation,

$$\dot{C}_{ij} = C_{ij+1}\,\omega_{j+2} - C_{ij+2}\,\omega_{j+1} \quad (4\text{-}6)$$

Note that ω_j is the j^{th} component of angular velocity of the body-fixed coordinate frame measured in body coordinates.

Eq. (4-6) may also be derived by differentiating Eq. (4-1) directly:

$$\dot{\bar{V}}_I = \dot{C}\bar{V}_b + C\dot{\bar{V}}_b$$
$$= C(\dot{\bar{V}}_b + C^{-1}\dot{C}\bar{V}_b) \quad (4\text{-}7)$$

This is the Law of Coriolis in matrix form. If the term $C^{-1}\dot{C}\bar{V}_b$ be identified with $\bar{\omega} \times \bar{V}_b$, and the angular velocity matrix Ω be defined by

$$\Omega = \begin{pmatrix} 0 & \omega_3 & -\omega_2 \\ -\omega_3 & 0 & \omega_1 \\ \omega_2 & -\omega_1 & 0 \end{pmatrix} \quad (4\text{-}8)$$

then

$$\bar{\omega} \times \bar{V}_b = -\Omega\bar{V}_b = C^{-1}\dot{C}\bar{V}_b \quad (4\text{-}9)$$

Thus, the differential equation for C is

$$\dot{C} = -C\Omega. \quad (4\text{-}10)$$

which expands to give Eq. (4-6).

There are nine direction cosines. Since a rotation involves only three degrees of freedom, there must be six constraints on these nine quantities. These constraints arise from the fact that during a rotation, the magnitude of a vector remains unchanged. This condition requires that

$$C^T = C^{-1} \quad (4\text{-}11)$$

where C^T is the transpose of C
and C^{-1} is the inverse of C.
Another, more useful, form of the orthogonality condition is

$$C^T C = C C^T = I \qquad (4\text{-}12)$$

where I is the identity matrix. Thus it is possible to write the nine direction cosines as functions of any three of them, using six independent orthogonality relations from Eq. (4-12). Another solution involves the use of Euler angles.

4.B.2 Euler Angles

There are many ways of defining Euler angles; the definition shown in Figure 4-1 follows the most common usage (Ref. 30 p. 104ff., and Ref. 39, p. 23, for example). The first rotation is about the Z axis of magnitude A_Z. The second rotation is about the displaced x axis, which becomes the line of nodes, by an amount A_L. The final rotation is about the z axis by an amount A_z. In example being used, the capital letter axes correspond to the inertially fixed frame, while the lower case axes are the body-fixed set.

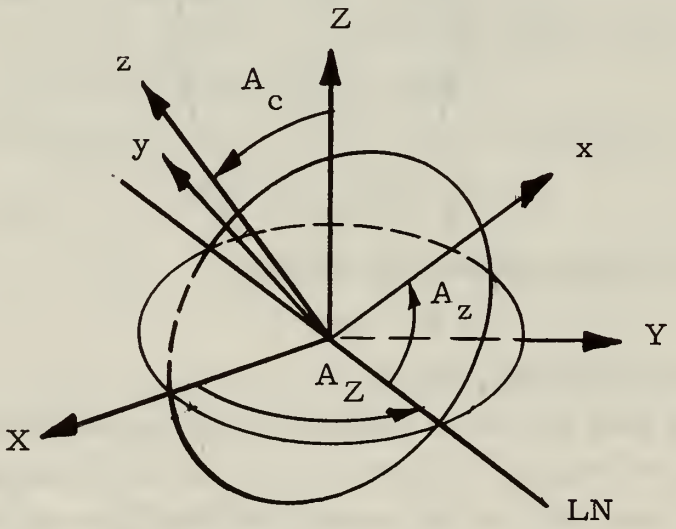

Fig. 4-1 Euler Angles

In terms of these Euler angles, the direction cosine matrix is

$$C = \begin{pmatrix} \cos A_Z \cos A_z - \sin A_Z \cos A_L \sin A_z & -\cos A_Z \sin A_z - \sin A_Z \cos A_L \cos A_z & \sin A_L \sin A_z \\ -\sin A_Z \cos A_z - \sin A_Z \cos A_L \cos A_z & -\sin A_Z \sin A_z + \cos A_Z \cos A_L \cos A_Z & \sin A_L \cos A_z \\ \sin A_z \sin A_L & -\cos A_Z \sin A_L & \cos A_L \end{pmatrix} \qquad (4\text{-}13)$$

The rates of change of the Euler angles in terms of the angular velocity of the body-fixed set measured in the body-fixed coordinates may be determined by resolution, and are (Ref. 39; p. 24)

$$\dot{A}_Z = \omega_1 \frac{\sin A_z}{\sin A_L} + \omega_2 \frac{\cos A_z}{\sin A_L}$$

$$\dot{A}_L = \omega_1 \cos A_z + \omega_2 \sin A_z$$

$$\dot{A}_z = \omega_1 \cot A_L \sin A_z - \omega_2 \cot A_L \cos A_z + \omega_3 \qquad (4\text{-}14)$$

This computation suffers from two disadvantages; trigonometric functions must be determined, and a singularity exists at $\sin A_L = 0$. The singularity corresponds to gimbal lock in a three-gimbal system (see Ref. 39, Figure 8-37, p. 25) and can be eliminated by including a fourth parameter in the description of the rotation, just as gimbal lock may be eliminated by the addition of a fourth gimbal.

4.B.3 Tensors

A third expression for the direction cosines is most conveniently cast in tensor form. It should be remarked here that since the transformation involves only Cartesian coordinates, no distinction between covariant, contravariant, and physical components of vectors and tensors need by made (Ref. 35, p. 170). The direction cosine tensor is

$$C_{ij} = \cos A\, \delta_{ij} + (1-\cos A)\, r_i r_j - \sin A\, e_{ijk} r_k \qquad (4\text{-}15)$$

where the rotation which carries the body-fixed axes into the inertial axes is about an axis with direction cosines r_i (the same with respect to either coordinate system) with magnitude A. Here δ_{ij} is the Kronecker delta

$$\delta_{ij} = \begin{cases} 1 \text{ if } i = j \\ 0 \text{ if } i \neq j \end{cases} \tag{4-16}$$

e_{ijk} is the cyclic tensor

$$e_{ijk} = \begin{cases} +1 \text{ if ijk positive cyclic (e.g. 123)} \\ -1 \text{ if ijk negative cyclic} \\ 0 \text{ if } i = j, \ j = k, \text{ or } i = k \end{cases} \tag{4-17}$$

and the convention of summing on repeated indices is observed (Ref. 34, p. 96 for example). Using the tensor formulation, Eq. (4-1) is

$$V_{Ii} = C_{ij} V_{bj} \tag{4-18}$$

and Eq. (4-10) becomes

$$C_{ij} = -C_{ik} e_{kjm} \omega_m \tag{4-19}$$

4.C Four Parameter Representation

The direction cosine computations are six-fold redundant; the Euler angle computations carry no redundancy but have a singularity. The use of four parameters to describe a rotation eliminates the singularity and diminishes the redundancy. There are two practically identical ways of describing a rotation with four parameters. These are Hamilton's quaternions (Refs. 31-33, 36, 38, 40) and Cayley-Klein parameters (Refs. 30, 40).

4.C.1 Quaternions

Hamilton developed quaternions as an extension of complex numbers. In representing a vector in two dimensions as a complex number, the unit real number 1 represents one direction, and the unit complex number $i = \sqrt{-1}$, the other. In analogy with this, Hamilton let the unit space vectors be i, j, k, with multiplication rules similiar to those for $\sqrt{-1}$:

$$i^2 = j^2 = k^2 = -1 \quad ij = -ji = k, \text{ etc.} \tag{4-20}$$

Thus, a space vector may be represented as $V = iV_1 + jV_2 + kV_3$, and

a general quaternion, with the unit real 1, the fourth direction, as

$$q = a + ib + jc + kd \tag{4-21}$$

Conjugation is defined by

$$q^* = a - ib - jc - kd \tag{4-22}$$

and length is given by

$$\ell^2 = q^* q = a^2 + b^2 + c^2 + d^2 \tag{4-23}$$

A simpler notation follows from representing a quaternion as a scalar and a vector:

$$q = (\lambda, \bar{\rho}) = \lambda + i\rho_1 + j\rho_2 + k\rho_3 \tag{4-24}$$

Thus,

$$q^* = (\lambda, -\bar{\rho}) \tag{4-25}$$

and if $q_1 = (\lambda_1, \bar{\rho}_1)$ and $q_2 = (\lambda_2, \bar{\rho}_2)$, then

$$q = (q_1 q_2) = (\lambda_1, \bar{\rho}_1)(\lambda_2, \bar{\rho}_2)$$

$$= (\lambda_1\lambda_2 - \bar{\rho}_1 \cdot \bar{\rho}_2, \lambda_1\bar{\rho}_2 + \lambda_2\bar{\rho}_1 + \bar{\rho}_1 \times \bar{\rho}_2) \tag{4-26}$$

Note that in general multiplication is not commutative. Two special quaternions may be defined, the unit quaternion q_u, and the zero quaternion q_o:

$$q_u = (1, \bar{0}) \qquad q_o = (0, \bar{0}) \tag{4-27}$$

Obviously

$$qq_u = q_u q = q \qquad q_o q = qq_o = q_o \tag{4-28}$$

Further, if $q \neq q_o$, there exists a unique inverse or reciprocal q^{-1} such that $qq^{-1} = q^{-1}q = q_u$:

$$q^{-1} = \frac{1}{|q|^2} q^* \tag{4-29}$$

Two relations follow from the definitions of conjugate and inverse:

$$(q_1 q_2)^* = q_2^* q_1^* \qquad (q_1 q_2)^{-1} = q_1^{-1} q_2^{-1} \tag{4-30}$$

If the quaternions q_I and q_b are defined by

$$q_I = (a_I, \overline{V}_I) \qquad q_b = (a_b, \overline{V}_b) \tag{4-31}$$

and related through the quaternion q having unit magnitude.

$$q = (\lambda, \bar{\rho}) \qquad \lambda^2 + \rho^2 = 1 \tag{4-32}$$

by the transformation

$$q_i = q q_b q^* \tag{4-33}$$

then

$$(a_I, \overline{V}_I) = [\, a_b,\ \overline{V}_b + 2\lambda\bar{\rho} \times \overline{V}_b + 2\bar{\rho} \times (\bar{\rho} \times \overline{V}_b)] \tag{4-34}$$

The scalars of q_I and q_b are equal, and the vectors are related by

$$\overline{V}_I = \overline{V}_b + 2\lambda\bar{\rho} \times \overline{V}_b + 2\bar{\rho} \times (\bar{\rho} \times \overline{V}_b) \tag{4-35}$$

Writing out Eq. (4-18) in vector notation, and using $\bar{r}$ as the unit vector along the axis of rotation gives

$$\begin{aligned}
\overline{V}_I &= \overline{V}_b \cos A + (\bar{r} \cdot \overline{V}_b)\, \bar{r}\, (1 - \cos A) + \bar{r} \times \overline{V}_b \sin A \\
&= \overline{V}_b + \bar{r} \times \overline{V}_b \sin A + [\, (\bar{r} \cdot \overline{V}_b)\bar{r} - (\bar{r} \cdot \bar{r})\overline{V}_b\,](1 - \cos A) \\
&= \overline{V}_b + \bar{r} \times \overline{V}_b \sin A + \bar{r} \times (\bar{r} \times \overline{V}_b)(1 - \cos A) \\
&= \overline{V}_b + 2 \sin \frac{A}{2} \cos \frac{A}{2}\, \bar{r} \times \overline{V}_b + 2 \sin^2 \frac{A}{2}\, \bar{r} \times (\bar{r} \times \overline{V}_b)
\end{aligned} \tag{4-36}$$

If λ in Eq. (4-35) is identified with $\cos \frac{A}{2}$ in Eq. (4-36), and $\bar{\rho}$ with $\bar{r} \sin \frac{A}{2}$, then the transformation Eq. (4-32) corresponds to the rotation of $\overline{V}_b$ about an axis $\bar{r}$ through an angle A. Writing q out gives

$$q = (\cos \tfrac{A}{2},\ \bar{r} \sin \tfrac{A}{2}) = \cos \tfrac{A}{2} + \sin \tfrac{A}{2}\, (i r_1 + j r_2 + k r_3) \tag{4-37}$$

Extending Euler's formula for exponentials of complex quantities suggests the notation

$$e^{\frac{A}{2}(i r_1 + j r_2 + k r_3)} = \cos \tfrac{A}{2} + \sin \tfrac{A}{2}\, (i r_1 + j r_2 + k r_3) \tag{4-38}$$

with $r_1^2 + r_2^2 + r_3^2 = 1$, so that the transformation Eq. (4-33) may be written

$$q_I = e^{\frac{A}{2}(ir_1 + jr_2 + kr_3)} \; q_b \; e^{-\frac{A}{2}(ir_1 + jr_2 + kr_3)}$$

The quaternions representing successive rotations may be combined as follows:

$$q_2 = q_{A_2}[q_{A_1} q_1 q_{A_1}^*] \, q_{A_2}^* = (q_{A_2} q_{A_1}) \, q_1 \, (q_{A_2} q_{A_1})^* \tag{4-40}$$

The non-commutativity of finite rotations is evident from the non-commutativity of quaternion multiplication.

The rates of change of the rotation quaternion parameters must now be related to the angular velocity of the body-fixed coordinate system with respect to inertial space. Let q be the quaternion representing the rotation that carries the body-fixed space into the inertial frame at time t. The quaternion representing the opposite rotation is then q^*. Let the quaternion representing the rotation carrying the body-fixed frame into inertial space at time $|t + \Delta t|$ be q'. The quaternion representing the rotation of the body-fixed axes during the time Δt is therefore q'q*:

$$\begin{aligned} q'q^* &= (\cos\frac{\Delta A}{2}, \; \sin\frac{\Delta A}{2}\, \bar{r}_{\Delta t}) = (\lambda + \Delta\lambda, \; \bar{\rho} + \Delta\bar{\rho})(\lambda, -\bar{\rho}) \\ &= [(\lambda, \bar{\rho}) + (\Delta\lambda, \Delta\bar{\rho})](\lambda, -\bar{\rho}) \\ &= (1, \bar{0}) + (\Delta\lambda, \Delta\bar{\rho})(\lambda, -\bar{\rho}) \end{aligned} \tag{4-41}$$

or

$$(\cos\frac{\Delta A}{2} - 1, \; \sin\frac{\Delta A}{2}\, \bar{r}_{\Delta t}) = (\Delta\lambda, \Delta\bar{\rho})(\lambda, -\bar{\rho}) \tag{4-42}$$

Dividing this equation by Δt and allowing Δt to approach zero gives

$$\lim_{\Delta t \to 0} \frac{1}{2}\left[\left(\frac{\cos\frac{\Delta A}{2} - 1}{\Delta A/2}\cdot\frac{\Delta A}{\Delta t}, \bar{r}_{\Delta t}\right) \; \frac{\sin\frac{\Delta A}{2}}{\Delta A/2}\cdot\frac{\Delta A}{\Delta t}\right] = \left(\frac{\Delta\lambda}{\Delta t}, \frac{\Delta\rho}{\Delta t}\right)(\lambda, -\bar{\rho})$$

$$= \frac{1}{2}\,(0, \lim_{t\to 0} r_{\Delta t}\, \frac{\Delta A}{\Delta t}) = (\dot{\lambda}, \dot{\rho})(\lambda, -\rho) \tag{4-43}$$

Since $\lim_{\Delta t \to 0} \bar{r}_{\Delta t}\, \frac{\Delta A}{\Delta t} \triangleq \bar{\omega}$, Eq. (4-43) becomes

$$\frac{1}{2}(0,\bar{\omega}) = (\dot{\lambda},\ \dot{\bar{\rho}})(\lambda,-\bar{\rho}) \tag{4-44}$$

or, post-multiplying by $(\lambda,\bar{\rho})$

$$(\dot{\lambda},\dot{\bar{\rho}}) = \frac{1}{2}(0,\bar{\omega})(\lambda,\bar{\rho}) \tag{4-45}$$

whence

$$\dot{\lambda} = -\frac{1}{2}\bar{\omega}\cdot\bar{\rho}$$

and

$$\dot{\bar{\rho}} = \frac{1}{2}(\lambda\bar{\omega} + \bar{\omega}\times\bar{\rho}) \tag{4-46}$$

4.C.2 Cayley-Klein Parameters

The foregoing discussion provides a method for describing a rotation with four parameters. One is redundant; the redundancy is removed by the constraint that the quaternion $q = (\lambda,\bar{\rho})$ have unit magnitude [Eq. (4-32)]. This formulation suffers from the fact that quaternions are not at all widely known. To obviate this difficulty, Cayley-Klein parameters may be introduced; they retain the simplicity of quaternions while eliminating Hamilton's i, j, k. Defining the Cayley-Klein parameters by

$$\begin{aligned} \alpha &= \lambda - i\rho_3 \\ \beta &= -\rho_2 - i\rho_3 \\ \gamma &= +\rho_2 - i\rho_3 \\ \delta &= \lambda + i\rho_3 \end{aligned} \tag{4-47}$$

and from them, forming the complex matrix Q,

$$Q = \begin{pmatrix} \alpha & \beta \\ \gamma & \delta \end{pmatrix} = \begin{pmatrix} \alpha & \beta \\ -\beta^* & \alpha^* \end{pmatrix} \tag{4-48}$$

gives a matrix which is unitary and has determinent +1:

$$\begin{aligned} Q^{*T} &= Q^A = Q^{-1} \\ |Q| &= \alpha\alpha^* + \beta\beta^* = \lambda^2 + \rho_3^2 + \rho_2^2 + \rho_1^2 = \lambda^2 + \rho^2 = +1 \end{aligned} \tag{4-49}$$

Here, Q^* is the complex conjugate of Q, Q^T is the transpose of Q, and Q^A is the adjoint of Q. When using Cayley-Klein parameters, vectors are represented as Hermition, or self-adjoint, matrices:

$$\bar{V} \longleftrightarrow V = \begin{pmatrix} V_3 & V_1 - iV_2 \\ V_1 + iV_2 & -V_3 \end{pmatrix} \tag{4-50}$$

Note that the trace of the matrix V is zero, and the determinant of V is the negative of the square of the magnitude of the vector V:

$$|V| = -(V_1^2 + V_2^2 + V_3^2) = -\bar{V}^2 \tag{4-51}$$

Using the matrix Q, a similarity transformation may be performed on the matrix V_b, yielding another matrix V_I:

$$V_I = QV_bQ^A \tag{4-52}$$

Under similarity transformations, the Hermition property of a matrix is preserved, as are the trace and determinant. Therefore, V_I must be of the same form as V_b [Eq. (4-50)], and further

$$-\bar{V}_b^2 = |V_b| = |V_I| = -\bar{V}_I^2 \tag{4-53}$$

Eq. (4-53) is the orthogonality condition. Thus the transformation Eq. (4-52) is equivalent to the transformation Eq. (4-33).

The differential equations for the Cayley-Klein parameters follow directly from the defining equation [Eq. (4-47)] and the rates of change of the quaternion parameters[Eq. (4-46)].

4.D Vector Representation

Another useful representation of a rotation is the vector $\bar{\sigma}$

$$\bar{\sigma} = \bar{r} \tan \frac{A}{4} \tag{4-54}$$

where $\bar{r}$ and A are defined above. In terms of the scalar and vector of the rotation quaternion

$$\bar{\sigma} = \bar{r}\,\frac{\sin\frac{A}{4}}{\cos\frac{A}{4}} = \bar{r}\,\frac{\sin\frac{A}{2}}{2\cos^2\frac{A}{4}} = \frac{\bar{\rho}}{1+\cos\frac{A}{2}} = \frac{\bar{\rho}}{1+\lambda} \tag{4-55}$$

The inverse relations are

$$\lambda = \cos\frac{A}{2} = 2\cos^2\frac{A}{4} - 1 = \frac{2}{\sec^2\frac{A}{4}} - 1 = \frac{2-\sec^2\frac{A}{4}}{\sec^2\frac{A}{4}}$$

$$= \frac{2 - (1 + \tan^2 \frac{A}{4})}{1 + \tan^2 \frac{A}{4}} = \frac{1 - \sigma^2}{1 + \sigma^2}$$

and (4-56)

$$\bar{\rho} = (1 + \lambda)\,\bar{\sigma} = \frac{2}{1 + \sigma^2}\,\bar{\sigma}$$

Substituting these expressions for λ and $\bar{\rho}$ into Eq. (4-35) gives

$$\overline{V_I} = \overline{V_b} + 2\,\frac{1 - \sigma^2}{1 + \sigma^2}\left(\frac{2\bar{\sigma}}{1 + \sigma^2}\right) \times \overline{V_b} + 2\left(\frac{2\bar{\sigma}}{1 + \sigma^2}\right) \times \left[\left(\frac{2\bar{\sigma}}{1 + \sigma^2}\right) \times \overline{V_b}\right]$$

or

$$\overline{V_I} = \overline{V_b} + \frac{4(1 - \sigma^2)}{(1 + \sigma^2)^2}\,\bar{\sigma} \times \overline{V_b} + \frac{8}{(1 + \sigma^2)^2}\,\bar{\sigma} \times (\bar{\sigma} \times \overline{V_b}) \qquad (4\text{-}57)$$

The vector representation of a rotation requires only three numbers; there is no redundancy. There is a singularity, however, at $|A| = 2\pi$, corresponding to a full rotation. This singularity may be eliminated by defining another vector $\bar{\sigma}'$:

$$\bar{\sigma}' = -\frac{\bar{\sigma}}{\sigma^2}$$

(4-58)

$$\bar{\sigma}' = \frac{-\bar{r}}{\tan \frac{A}{4}} = (-\bar{r}) \cot \frac{A}{4} = (-\bar{r}) \tan\left(\frac{\pi}{2} - \frac{A}{4}\right)$$

$$\bar{\sigma}' = (-\bar{r}) \tan \frac{2\pi - A}{4} \qquad (4\text{-}59)$$

Since a rotation of A in one direction is equivalent to a rotation of 2π -A in the opposite direction, $\bar{\sigma}$ and $\bar{\sigma}'$ describe the same rotation, and Eq. (4-57) holds with $\bar{\sigma}'$ substituted for $\bar{\sigma}$.

The differential equation relating the rate of change of $\bar{\sigma}$ to the angular velocity of the body-fixed coordinate frame may be obtained by differentiation of Eq. (4-55):

$$\dot{\bar{\sigma}} = \frac{\dot{\bar{\rho}}}{1 + \lambda} - \frac{\dot{\lambda}\,\bar{\rho}}{(1 + \lambda)^2}$$

$$= \frac{1}{2}\left[\frac{\lambda\bar{\omega} + \bar{\omega}\times\rho}{1+\lambda} + \frac{(\bar{\omega}\cdot\bar{\rho})\bar{\rho}}{(1+\lambda)^2}\right]$$

$$= \frac{1}{2}\left[\frac{1-\sigma^2}{2}\,\bar{\omega} + \bar{\omega}\times\bar{\sigma} + (\bar{\omega}\cdot\bar{\sigma})\bar{\sigma}\right] \qquad (4\text{-}60)$$

$$= \frac{1}{2}\left[\frac{1-\sigma^2}{2}\,\bar{\omega} + \bar{\omega}\times\sigma + (\omega\times\sigma)\times\sigma + \sigma^2\bar{\omega}\right]$$

$$\dot{\bar{\sigma}} = \frac{1}{2}\left[\frac{1+\sigma^2}{2}\,\bar{\omega} + \bar{\omega}\times\bar{\sigma} + (\bar{\omega}\times\bar{\sigma})\times\bar{\sigma}\right]$$

Clearly, the same differential equation holds for $\bar{\sigma}'$:

$$\dot{\bar{\sigma}}' = \frac{1}{2}\left[\frac{1+\sigma'^2}{2}\bar{\omega} + \bar{\omega}\times\bar{\sigma}' + (\bar{\omega}\times\bar{\sigma}')\times\bar{\sigma}'\right] \qquad (4\text{-}61)$$

4.E Comparison

The preceding three sections of this chapter have presented several methods for transforming a vector from one Cartesian coordinate frame to another, and derived the differential equations for the transformation parameters in terms of the angular velocity of one frame with respect to another. These transformations and their differential equations are collected below for comparison.

4.B Direction Cosines

Transformation

$$\bar{V}_I = C\bar{V}_b \qquad (4\text{-}1)$$

Direction Cosine Differential Equation

$$\dot{C} = -C\Omega \qquad (4\text{-}10)$$

Six-fold Redundant, with Six Constraints

$$C^T C = I \qquad (4\text{-}12)$$

Euler Angle Differential Equation

$$\dot{A}_Z = \omega_1 \frac{\sin A_z}{\sin A_L} + \omega_2 \frac{\cos A_z}{\sin A_L}$$

$$\dot{A}_L = \omega_1 \cos A_z + \omega_2 \sin A_z \qquad (4\text{-}14)$$

$$\dot{A}_z = -\omega_1 \cot A_L \sin A_z - \omega_2 \cot A_L \cos A_z + \omega_3$$

No redundancy; singularity at $\sin A_L = 0$

4.C Four Parameters

Quaternion Transformation

$$\bar{\bar{V}}_I = \bar{\bar{V}}_b + 2\lambda\bar{\rho} \times \bar{\bar{V}}_b + 2\bar{\rho} \times (\bar{\rho} \times \bar{\bar{V}}_b) \tag{4-35}$$

$$\lambda = \cos \frac{A}{2} \qquad \bar{\rho} = \bar{r} \sin \frac{A}{2} \tag{4-37}$$

Cayley-Klein Transformation

$$\begin{pmatrix} V_{I3} & V_{I1} - V_{I2} \\ V_{I1} + iV_{I2} & -V_{I3} \end{pmatrix} = \begin{pmatrix} \lambda - i\rho_3 & -\rho_2 - i\rho_1 \\ \rho_2 - i\rho_1 & \lambda + i\rho_3 \end{pmatrix} \begin{pmatrix} V_{b3} & V_{b1} - iV_{b2} \\ V_{b1} + iV_{b2} & -V_{b3} \end{pmatrix} \begin{pmatrix} \lambda + i\rho_3 & \rho_2 + i\rho_1 \\ -\rho_2 + i\rho_1 & \lambda - i\rho_3 \end{pmatrix} \tag{4-52}$$

Differential Equation

$$\dot{\lambda} = -\frac{1}{2}\,\bar{\omega} \cdot \bar{\rho}$$

$$\dot{\bar{\rho}} = \frac{1}{2}(\lambda\bar{\omega} + \bar{\omega} \times \bar{\rho}) \tag{4-46}$$

Once redundant with one constraint

$$\dot{\lambda}^2 + \rho^2 = 1 \tag{4-32)(4-49}$$

4.D Vectors

Transformation

$$\bar{\bar{V}}_I = \bar{\bar{V}}_b + 4\frac{1 - \sigma^2}{(1 + \sigma^2)^2}\,\bar{\sigma} \times \bar{\bar{V}}_b + \frac{8}{(1 + \sigma^2)^2}\,\bar{\sigma} \times (\bar{\sigma} \times \bar{\bar{V}}_b) \tag{4-57}$$

$$\bar{\sigma} = \bar{r} \tan \frac{A}{4} \tag{4-54}$$

or

$$\bar{\bar{V}}_I = \bar{\bar{V}}_b + 4\frac{1-\sigma'^2}{(1 + \sigma'^2)^2}\,\bar{\sigma} \times \bar{\bar{V}}_b + \frac{8}{(1 + \sigma'^2)^2}\,\bar{\sigma}' \times (\bar{\sigma}' \times \bar{\bar{V}}_b) \tag{4-57a}$$

$$\bar{\sigma}' = -\frac{\bar{\sigma}}{\sigma^2} \tag{4-58}$$

Differential Equation

$$\dot{\bar{\sigma}} = \frac{1}{2}\left[\frac{1+\sigma^2}{2}\bar{\omega} + \bar{\omega}\times\sigma + (\bar{\omega}\times\bar{\sigma})\times\bar{\sigma}\right] \qquad (4\text{-}60)$$

$$\dot{\bar{\sigma}}' = \frac{1}{2}\left[\frac{1+\sigma'^2}{2}\bar{\omega} + \bar{\omega}\times\bar{\sigma}' + (\bar{\omega}\times\bar{\sigma}')\times\bar{\sigma}'\right] \qquad (4\text{-}61)$$

These transformations will now be examined with a view to determining which is most suitable for machine computation. The basic criterion to be used in this determination is the size of computer required. Further, since the information being dealt with is incremental, incremental computation will be the basis of decision unless general propose computation seems particularly appropriate.

The most straightforward computation employs the direct direction cosine formulation. The transformation requires nine incremental integrators, since each component of the vector to be transformed has magnitude ΔV. The generation of the direction cosines requires eighteen incremental integrators. If Euler angles are generated, then the sine and cosine of each angle is also required; further, the sines and cosines must be combined to give the direction cosines as well as the factors in the differential equations. The use of incremental devices requires forty-six integrators. This does not handle any problems raised by the singularity at $\sin A_L = 0$

Twelve incremental integrators are necessary to generate the four parameters used in the quaternion and Cayley-Klein parameter representation. If the direction cosines are formed from these parameters, an additional twelve integrators are required. Nine more complete the transformation. Thus, thirty-three incremental integrators are required in all, as opposed to twenty-seven for the direction cosine computation. If the formal Cayley-Klein similarity transformation is used, the first multiplication can be performed by twelve incremental integrators. An arithemetic computation seems best for the second matrix multiplication; it requires twelve multiplications and nine additions.

Twenty-one incremental integrators are required to generate the

three components of the vector used to represent a rotation; the vector transformation requires twenty-five more. In addition, an arithmetic section is required to perform the branching operation used to remove the singularity.

The foregoing discussion indicates that the direction cosine computation using a total of twenty-seven integrators is most compact. For this reason, this formulation will be the only one considered in designing the transformation computer.

CHAPTER V

TRANSFORMATION COMPUTER

5.A Introduction

In Chapter IV, the various ways of representing coordinate rotations were derived and compared to determine their suitability for machine computation. As a result of this comparison, the matrix transformation was chosen to be instrumented. The rotation matrix is to be generated by direct computation of the direction cosines. The matrix differential equation to be instrumented is

$$\dot{C} = -C\Omega \tag{5-1}$$

where C is the matrix of direction cosines, a dot ($\cdot$) over a quantity denotes time differentiation, and Ω is the angular velocity matrix.

$$\Omega = \begin{pmatrix} 0 & \omega_3 & -\omega_2 \\ -\omega_3 & 0 & \omega_1 \\ \omega_2 & -\omega_1 & 0 \end{pmatrix} \tag{5-2}$$

The angular velocity is resolved into body axes.

Eq. (5-1) represents nine separate equations; there are three sets of the form

$$\begin{aligned} \dot{C}_{i1} &= C_{i2}\omega_3 - C_{i3}\omega_2 \\ \dot{C}_{i2} &= C_{i3}\omega_1 - C_{i1}\omega_3 \\ \dot{C}_{i3} &= C_{i1}\omega_2 - C_{i2}\omega_1 \end{aligned} \tag{5-3}$$

Multiplication of Eq. (5-3) by dt and integration of the result yields

$$\begin{aligned} C_{i1} &= \int C_{i2} d\theta_3 - \int C_{i3} d\theta_2 \\ C_{i2} &= \int C_{i3} d\theta_1 - \int C_{i1} d\theta_3 \\ C_{i3} &= \int C_{i1} d\theta_2 - \int C_{i2} d\theta_1 \end{aligned} \tag{5-4}$$

5.B Algorithms Available

Equations (5-4) show that each direction cosine is the difference of two integrals, each the integral of a direction cosine with respect to rotation about a body axis. Since the gyro outputs are equal increments of rotation about body axes, the integrals may be approximated by quadrature rules using equal $\Delta\theta$ increments.

5.B.1 Quadrature Rules

Almost any standard text on numerical analysis (Refs. 41, 46-48, 52, 54, for example) gives the more common quadrature rules. Since only the integrand will be available, no rules employing derivatives of the integrand, such as Taylor's series, will be considered. The most common quadrature rules using present and past values of the integrand are the rectangular rule,

$$\int_{\theta(n-1)}^{\theta(n)} C(\theta) d\theta = \Delta\theta C[\theta(n-1)] \tag{5-5}$$

the trapezoidal rule,

$$\int_{\theta(n-1)}^{\theta(n)} C(\theta) d\theta = \frac{\Delta\theta}{2} \{ C[\theta(n-1)] + C[\theta(n)] \} \tag{5-6}$$

and Simpson's one-third rule,

$$\int_{\theta(n-2)}^{\theta(n)} C(\theta)d\theta = \frac{\Delta\theta}{3}\{C[\theta(n-2)]+4C[\theta(n-1)]+C[\theta(n)]\} \qquad (5\text{-}7)$$

The first is an open rule; that is, the value of the integrand at the present time does not appear. The remaining two are closed rules. Each integration rule fits a (p-1) degree polynomial through the p points of the integrand appearing in the formula; for this reason, these rules are called (p-1) order polynomial rules. The rectangular rule is called a zero-order rule; the trapezoidal rule and Simpson's one-third rule are first- and second-order rules respectively.

At each step, the approximation to the integral is in error by some amount. This error, arising from not considering higher derivatives or differences, is called truncation error. For the three rules above, the truncation error made at each step is (Ref. 47, p. 73):

Rectangular	$E_n = 0(\Delta\theta^2)$
Trapezoidal	$E_n = 0(\Delta\theta^3)$
Parabolic	$E_n = 0(\Delta\theta^5)$

This notation means that for the rectangular rule, the truncation error at each step is on the order of $\Delta\theta^2$. The term "on the order of" means that the limit of $E_n/\Delta\theta^2$ remains finite as $\Delta\theta^2$ approaches zero.

5.B.2 Influence of Size of Step

The rather fast pulse rate required in the gyro loops suggests that using higher order integration rules with larger increments would reduce the speed requirement on the computer as well as decreasing the truncation error. For example, if rectangular integration were used with a step length $\Delta\theta$, the truncation error at each step would be $0(\Delta\theta^2)$. If trapezoidal integration were used with a step length of 5 $\Delta\theta$, the error at each step would be $0(125\Delta\theta^3)$ which is significantly less than the rectangular error. This increase in step size permits reduction of computer speed by about a factor of two. However, there is an irreducible uncertainty in the gyro information

of $0(\Delta\theta^2)$ in each pulse, so that the apparent increase in accuracy may not, in fact, be attained. As is shown in Chapter III, Section 3.B, each output pulse of a gyro is $\int_{(n-1)T_s}^{nT_s} \omega_i dt$, the integral of one component of angular velocity resolved into body coordinates. Since addition of rotations is not commutative,

$$\int_{(n-1)T_s}^{nT_s} \bar{\omega} dt \neq \bar{i} \int_{(n-1)T_s}^{nT_s} \omega_1 dt + \bar{j} \int_{(n-1)T_s}^{nT_s} \omega_2 dt + \bar{k} \int_{(n-1)T_s}^{nT_s} \omega_3 dt \qquad (5\text{-}8)$$

in general. In one sampling period, the angular velocity could be equal about all three axes, or there could be successive rotations about all axes in any order; each input gives the same output. Eq. (5-8) adds these rotations as though they were vectors. The error thus made is $0(\Delta\theta^2)$ (Ref. 34, p. 97). The conclusion to be drawn, therefore, is that rectangular integration of Eq. (5-1) is the most suitable algorithm because the angular information is available in rotational increments. Note that this comment applies to any digital computation where the rotations are handled in this way; it is not restricted to delta-modulated gyro information. In special cases, however, the use of higher order integration rules to reduce truncation error may be of some advantage.

The equations to be instrumented to generate the direction cosines are three sets of the form

$$\begin{aligned} \Delta C_{i1} &= C_{i2}\Delta\theta_3 - C_{i3}\Delta\theta_2 \\ \Delta C_{i2} &= C_{i3}\Delta\theta_1 - C_{i1}\Delta\theta_3 \\ \Delta C_{i3} &= C_{i1}\Delta\theta_2 - C_{i2}\Delta\theta_1 \end{aligned} \qquad (5\text{-}9)$$

5.C Digital Differential Analyzers

The computer chosen to generate and perform the coordinate transformation must be fast and accurate. The accuracy requirement, with present equipment, eliminates analog computation from

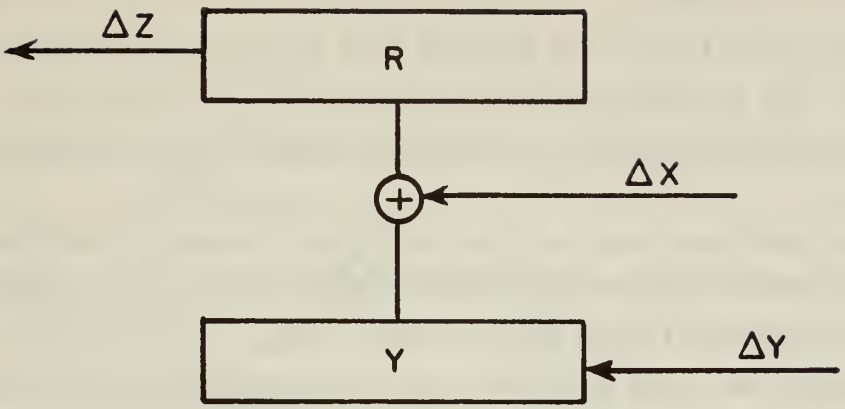

(a)

Register Arrangement

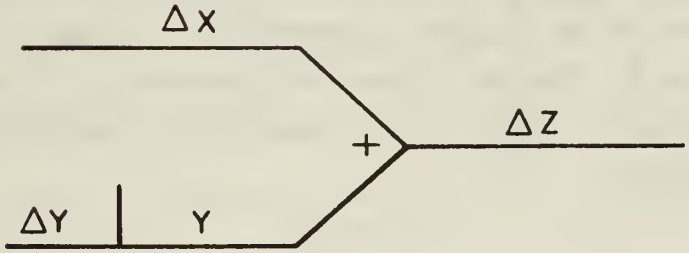

(b)

Schematic

Fig. 5-1 DDA Integrators

consideration; the speed requirement, based on the necessity for processing each pulse as it comes from the gyro, calls for a computer whose cycle time is no greater than the sampling period of the gyro loop. The sampling period, as determined in Chapter III, Sec. 3.B.4, is the quotient of maximum angular velocity and angular increment.

A very fast and compact type of digital computer, and one particularly well suited to the solution of Eq. (5-9), is the digital differential analyzer (DDA) (Refs. 43-45, 53).

The DDA has been described as an analog computer in digital form; it has the advantage found in the Bush differential analyzer (Ref. 42) of not requiring time to be the independent variable of integration. The basic element of DDA computers is the DDA integrator, usually shown diagrammatically as in Fig. 5-1(a). The blocks labeled R and Y are storage registers. The line labelled ΔY carries pulses representing a change (positive or negative according to the sign associated with the pulse) in the least significant bit in Y. The ΔX line carries pulses representing equal increments in X; when a ΔX pulse occurs, the contents of the Y register are added into the R register or subtracted from the R register, depending on the sign associated with the ΔX pulse. The contents of the Y register are left unchanged by this operation. The ΔZ line carries overflow pulses from the R register representing a change in the least significant bit in Z. The ΔZ pulses may be used as ΔX or ΔY pulses in another integrator. The name "integrator" is applied to this unit because it computes

$$\Delta Z = Y\Delta X \qquad (5\text{-}10)$$

This is an increment of rectangular integration of Y with respect to X [See Eq. (5-5)].

Each of the variables X, Y, and Z represents a physical quantity to some scale. If the Y register is n bits long, so is the R register. The least significant bit in the R register, ΔR, is related to ΔY and ΔX by

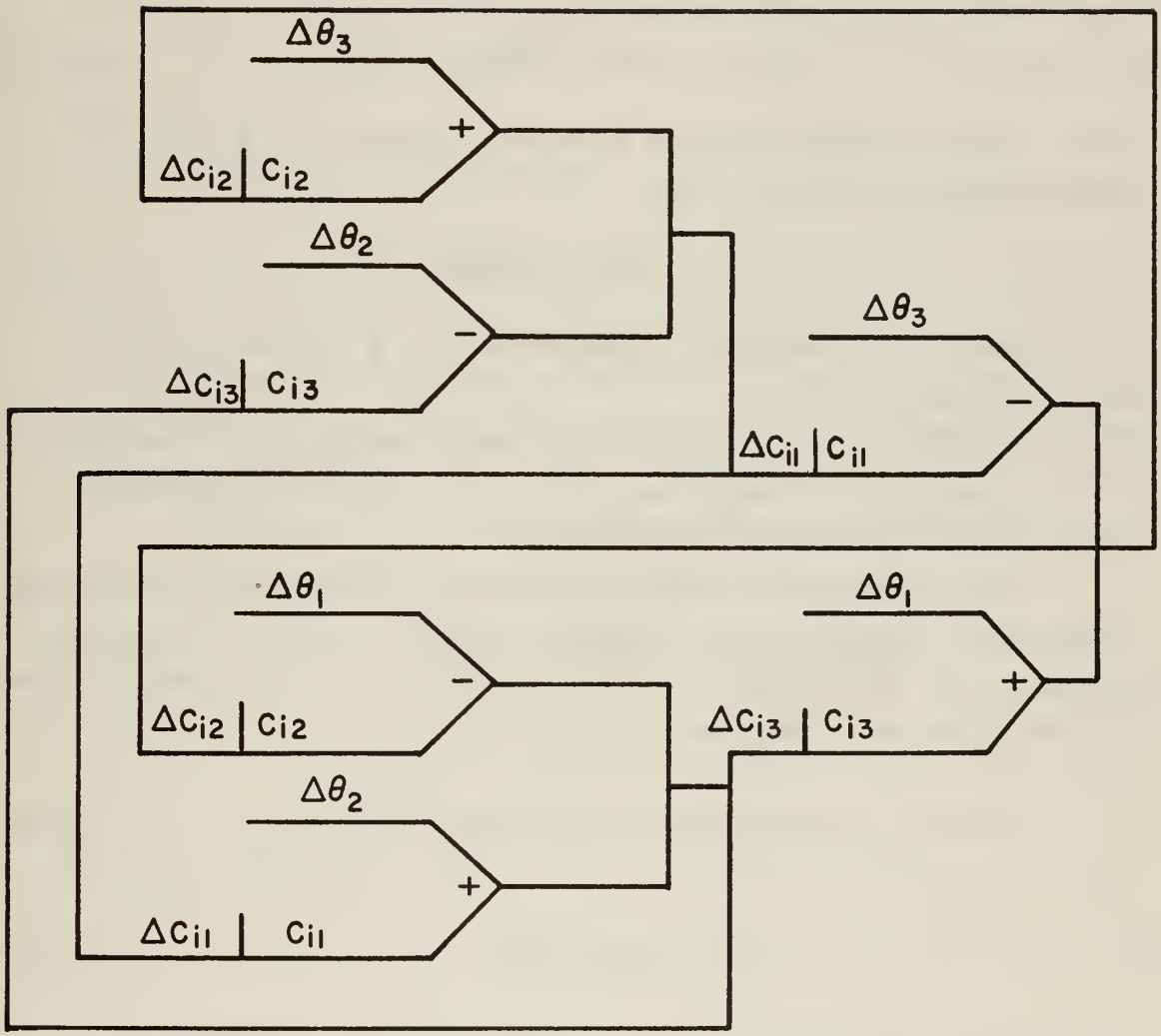

Fig. 5-2 Arrangement for DDA Solution of Equation (5-9)

$$\Delta R = \Delta X \Delta Y \tag{5-11}$$

The overflow logic for the R register causes an overflow pulse when the content of the R register exceeds ΔZ. The simplest kind of overflow logic scales ΔZ so that

$$\Delta Z = 2^n \Delta R \tag{5-12}$$

Thus, the ΔZ overflow occurs when the R register fills up. ΔZ is then related to ΔX and ΔY by

$$\Delta Z = 2^n \Delta X \Delta Y \tag{5-13}$$

The usual schematic representation for a DDA integrator is shown in Fig. 5-1 (b).

The solution of Eq. (5-9) requires six incremental integrators for each value of i arranged as in Fig. 5-2. Note that no order of performing the additions is specified.

There is feedback in this arrangement; hence there are scaling consistency equations to be satisfied, just as in the case of analog computation. The integrators are identical; thus consideration of the loop with the $\Delta\theta_3$ integrators leads to

$$\Delta\theta_3 \Delta C_{i1} 2^n = \Delta\theta_3^2 \, \Delta C_{i2} 2^{2n} = \Delta C_{i2} \tag{5-14}$$

or

$$\Delta\theta_3 = 2^{-n} \tag{5-15}$$

by repeated application of Eq. (5-13). A similar result holds for $\Delta\theta_1$ and $\Delta\theta_2$. Thus for simplest overflow logic, $\Delta\theta$ should be chosen as a negative integral power of 2. The value which $\Delta\theta$ must not exceed may be found from system specifications, and n, the length of the Y and R registers, is determined. Requiring that the scaling of the velocity increments be the same in both coordinate frames yields $\Delta C = 2^{-n}$.

5.D Analysis

With the form and function of the transformation computer determined, an analysis of its operation must be made. Three points are usually considered in the analysis of a computer: dominant mode, truncation error, and round-off or quantization error. These will be taken up in turn after a frequency domain model for the computer has been developed.

5.D.1 Frequency Domain Model

Computers operating in real time have been characterized as sampled-data systems and transfer functions derived for them (Ref. 51). Since the equations that the computer is solving are difference equations, they may be transformed in a way similar to that used in transforming time sequences or samples of continuous functions (Ref. 61, Ch. 1).

The equations describing the computer operation with $\omega_1 = \omega_2 = 0$, $\omega_3 \neq 0$ are

$$\begin{aligned} C_{i1}(n) &= C_{i1}(n-1) + \Delta\theta_3 C_{i2}(n-1) \\ C_{i2}(n) &= C_{i2}(n-1) - \Delta\theta_3 C_{i1}(n) \end{aligned} \tag{5-16}$$

Let $Z_3 = e^{-s\frac{\Delta\theta}{\omega_3}}$ where s is the Laplace complex frequency variable. Then, if

$$C_{ij}(z) = \Sigma C_{ij}(n) z^n \tag{5-17}$$

Eq. (5-16) may be transformed into

$$\begin{aligned} C_{i1}(z_3) &= \frac{\Delta\theta_3 z_3}{1 - z_3} C_{i2}(z_3) \\ C_{i2}(z_3) &= -\frac{\Delta\theta_3}{1 - z_3} C_{i1}(z_3) \end{aligned} \tag{5-18}$$

If $\omega_1 = 2\omega_2$, $\omega_3 = 0$, the transformed set of equations is (see App. C, Sec. C. 1.b)

$$C_{il}(z) = - \frac{\Delta\theta z \; 1 + \frac{\Delta\theta^2 z^2}{1 - z^2}}{(1 - z)(1 + z) \; 1 + \Delta\theta^2 \; 1 + \frac{z}{1 - z}} \; C_{i3}(z)$$

$$C_{i2}(z) = \frac{\Delta\theta z}{1 - z} \; C_{i3}(z) \tag{5-19}$$

$$C_{i3}(z) = \frac{\Delta\theta}{1 - z^2} \; C_{il} \; z - \frac{\Delta\theta}{1 - z} \; C_{i2}(z)$$

where $z = e^{-s \frac{\Delta\theta}{\omega_1}}$ and $z^2 = e^{-s \; 2 \frac{\Delta\theta}{\omega_1}} = e^{-s \frac{\Delta\theta}{\omega_2}}$.
This set of equations may be well approximated by

$$C_{il}(z) = - \frac{\Delta\theta z}{1 - z^2} \; C_{i3}(z)$$

$$C_{i2}(z) = \frac{\Delta\theta z}{1 - z} \; C_{i3}(z) \tag{5-20}$$

$$C_{i3}(z) = \frac{\Delta\theta}{1 - z^2} \; C_{il}(z) - \frac{\Delta\theta}{1 - z} \; C_{i2}(z)$$

If the variables z_1 and z_2 are defined by $z_1 = e^{-s \frac{\Delta\theta}{\omega_1}}$ and $z_2 = e^{-s \frac{\Delta\theta}{\omega_2}}$, then Eq. (5-20) may be written

$$C_{il}(z) = - \frac{\Delta\theta z}{1 - z_2} \; C_{i3}(z)$$

$$C_{i2}(z) = \frac{\Delta\theta z}{1 - z_1} \; C_{i3}(z) \tag{5-21}$$

$$C_{i3}(z) = \frac{\Delta\theta}{1 - z_2} \; C_{il}(z) - \frac{\Delta\theta}{1 - z_1} \; C_{i2}(z)$$

where z represents the delay between the cycling of integrators. If the components of angular velocity are related by

$$k\omega_1 = \ell\omega_2 = m\omega_3 = \omega \tag{5-22}$$

where k, ℓ, and m are integers, and if $z_i = e^{-s\frac{\Delta\theta}{\omega_i}}$, then the z_i's are related by

$$z_1^{\ell m} = z_2^{km} = z_3^{k\ell} = z^{k\ell m} \tag{5-23}$$

Here again z represents the delay between the cycling of the integrators. With the above relations between angular velocity components satisfied the set of equations [cf. Eq. (5-9)]

$$\begin{aligned} C_{i1}(n) &= C_{i1}(n-1) + \Delta\theta_3 C_{i2}(n-1) - \Delta\theta_2 C_{i3}(n-1) \\ C_{i2}(n) &\quad C_{i2}(n-1) + \Delta\theta_1 C_{i3}(n-1) - \Delta\theta_3 C_{i1}(n) \\ C_{i3}(n) &\quad C_{i3}(n-1) + \Delta\theta_2 C_{i1}(n) \quad - \Delta\theta_1 C_{i2}(n) \end{aligned} \tag{5-24}$$

may be approximately transformed into

$$\begin{aligned} C_{i1}(z) &= \frac{\Delta\theta z}{1-z_3} C_{i2}(z) - \frac{\Delta\theta z}{1-z_2} C_{i3}(z) \\ C_{i2}(z) &= \frac{\Delta\theta z}{1-z_1} C_{i3}(z) - \frac{\Delta\theta}{1-z_3} C_{i1}(z) \\ C_{i3}(z) &= \frac{\Delta\theta}{1-z_2} C_{i1}(z) - \frac{\Delta\theta}{1-z_1} C_{i2}(z) \end{aligned} \tag{5-25}$$

With $\omega_1 = 2\omega_2$, $\omega_3 = 0$, this set is identical with Eq. (5-21), which is a good approximation to Eq. (5-19). Similarly with $\omega_1 = \omega_2 = 0$, $\omega_3 \neq 0$, Eq. (5-21) becomes Eq. (5-18). Note that if $\omega_i = 0$, the terms in z_i are taken as zero.

Eq. (5-25) may be represented by a signal flow graph as shown in Fig. 5-3. When the angular velocity of the system is specified, the substitutions indicated by Eq. (5-22) and Eq. (5-23) may be made. For example, with $\omega_1 = 2\omega_2 = 3\omega_3$, k = 1, ℓ = 2, m = 3, and the appropriate signal flow graph is shown in Fig. 5-4.

The use of Mason's method for reducing signal flow graphs (Ref. 60, Ch. 4) shows that the characteristic equation for the computer under these conditions is

$$1 + \frac{\Delta\theta^2 z}{(1-z)^2} + \frac{\Delta\theta^2 z}{(1-z^2)^2} + \frac{\Delta\theta^2 z}{(1-z^3)^2} - \frac{\Delta\theta^3 z}{(1-z^2)(1-z^3)} = 0 \qquad (5\text{-}26)$$

and, in general, the reduction of the signal flow graph in Fig. 5-3 leads to the characteristic equation for the computer

$$1 + \frac{\Delta\theta^2 z}{(1-z_1)^2} + \frac{\Delta\theta^2 z}{(1-z_2)^2} + \frac{\Delta\theta^2 z}{(1-z_3)^2} - \frac{\Delta\theta^3 z(1-z)}{(1-z_1)(1-z_2)(1-z_3)} = 0 \qquad (5\text{-}27)$$

With the node-to-node transfer functions determined, the remainder of the analysis can proceed.

5. D. 2 Determination of Dominant Mode

The various normal modes of the transformation computer are determined from the roots of the characteristic equation. Each root ζ leads to a time sequence of the form ζ^{-n} with coefficients chosen to fit initial conditions. If ζ is complex, its conjugate will also be a root, and an oscillatory term will be present. If $|\zeta| > 1$ then the mode will decay, while if $|\zeta| < 1$ there will be exponential growth.

The initial conditions as the various nodes appear as step inputs; for this reason, the roots near z = 1 will provide the dominant modes, while other modes, which occur near the various n^{th} roots of unity, will have magnitude $\Delta\theta$. Thus the dominant mode of the computer comes from the roots near z = +1.

Fig. 5-3 Signal Flow Graph

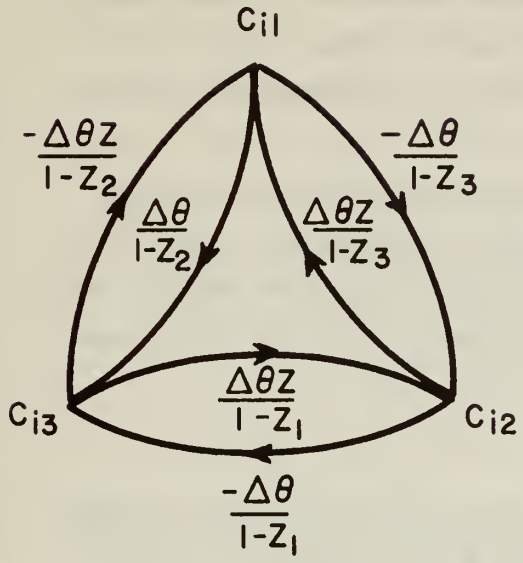

Fig. 5-3 Signal Flow Graph for Computer

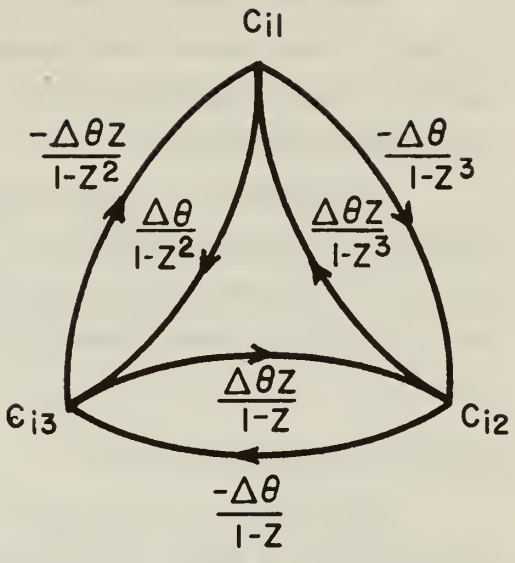

Fig. 5-4 Signal Flow Graph for $\omega_1 = 2\omega_2 = 3\omega_3$

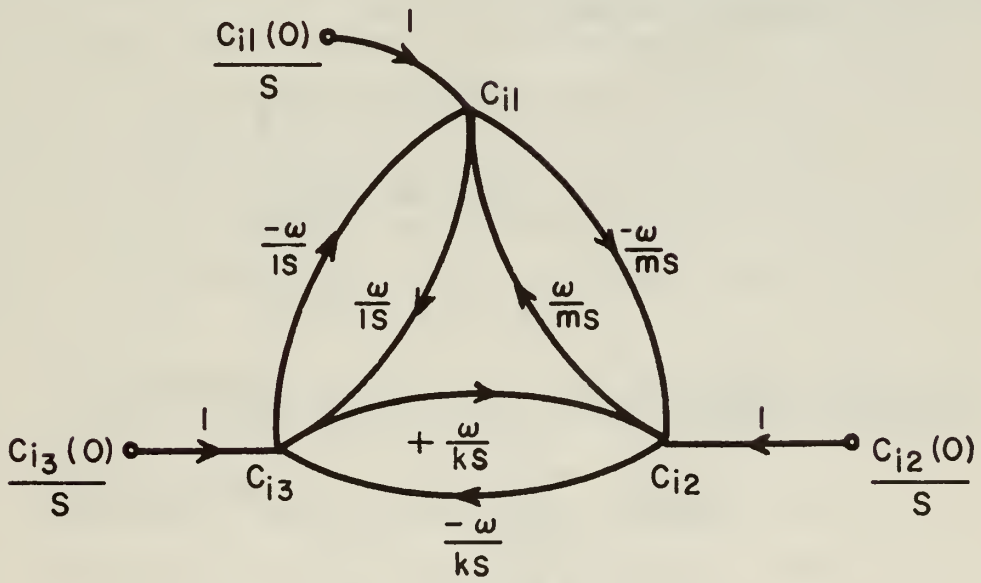

Fig. 5-5 Analog Computer Flow Graph

The magnitude of the roots and their associated modes may be found by root-locus techniques. Since the loop gain, $\Delta\theta^2$, is so small, linear approximations must be used in conjunction with the graphical technique..

In Appendix C, the analysis of two situations is carried out using root-locus techniques. For the case of angular velocity ratio two to one, there are extraneous roots near the square roots of unity not +1. In the case of equal rates on all axes, there are only roots near +1.

5.D.3 Truncation Error

Truncation error is the error made by not considering higher derivatives or differences when computing the solution of a differential equation. It is the difference between the exact solution and the computed solution using computer registers with infinite length.

Assumption of the same angular velocity relationships as above [Eq. (5-22)] with the added restriction that the angular velocity be constant, permits the solution of Eq. (5-1). With Eq. (5-22) satisfied, Eq. (5-1) becomes three sets of the form

$$\begin{aligned} \dot{C}_{i1} &= C_{i2}\frac{\omega}{m} - C_{i3}\frac{\omega}{\ell} \\ \dot{C}_{i2} &= C_{i3}\frac{\omega}{k} - C_{i1}\frac{\omega}{m} \\ \dot{C}_{i3} &= C_{i1}\frac{\omega}{\ell} - C_{i2}\frac{\omega}{k} \end{aligned} \tag{5-28}$$

Applying a Laplace transformation to Eq. (5-28) yields

$$\begin{aligned} C_{i1}(s) &= \frac{1}{s}\left[\frac{\omega}{m}C_{i2}(s) - \frac{\omega}{\ell}C_{i3}(s) + C_{i1}(0)\right] \\ C_{i2}(s) &= \frac{1}{s}\left[\frac{\omega}{k}C_{i3}(s) - \frac{\omega}{m}C_{i1}(s) + C_{i2}(0)\right] \\ C_{i3}(s) &= \frac{1}{s}\left[\frac{\omega}{\ell}C_{i1}(s) - \frac{\omega}{k}C_{i2}(s) + C_{i3}(0)\right] \end{aligned} \tag{5-29}$$

where the $C_{ij}(0)$ are initial conditions. Converting this set of equations to a signal flow graph leads to Fig. 5-5. The initial conditions are taken as inputs at appropriate nodes. Flow graph reduction may be used to derive expressions for the signals at each node. For example,

$$C_{il}(s) = \frac{C_{il}(0)\left[s^2 + \frac{\omega^2}{k^2}\right] + \omega\left[\frac{C_{i3}(0)}{\ell} - \frac{C_{i2}(0)}{m}\right] s + \omega^2\left[\frac{C_{i3}(0)}{km} + \frac{C_{i2}(0)}{k\ell}\right]}{(k^2 + \ell^2 + m^2)\omega^2 s\left[\frac{s^2}{(k^2 + l^2 + m^2)\omega^2} + 1\right]} \tag{5-30}$$

These expressions can be transformed into the time domain and the exact solution to the differential equations found.

The solution to the difference equations instrumented by the computer may be found by taking the z-transform of the solution, as determined by root-locus methods, and writing down the corresponding time sequences. There will be truncation error from three causes; the roots near unity may not have the proper argument, they may not be on the unit circle, and there may be other roots. The error in argument of the root near unity makes the oscillations of the direction cosines the wrong frequency. If these roots are not quite on the unit circle, the oscillations will not be of constant amplitude as they should. The other roots may lead to exponential or oscillatory terms; in any case the size of the corresponding mode may be determined.

When finding the z-transform of the computer output, the last root-locus construction, to find the roots of the computer characteristic equation, deals with a loop that has a gain of $\Delta\theta^2$. Since $\Delta\theta^2$ is very small, the construction cannot be carried out exactly, but linear approximations may be made analytically. These approximations are sufficient to make the truncation errors predicted inexact. However, the order of the errors predicted is correct and the growth rate is correct, but an exact error analysis is not provided. A more

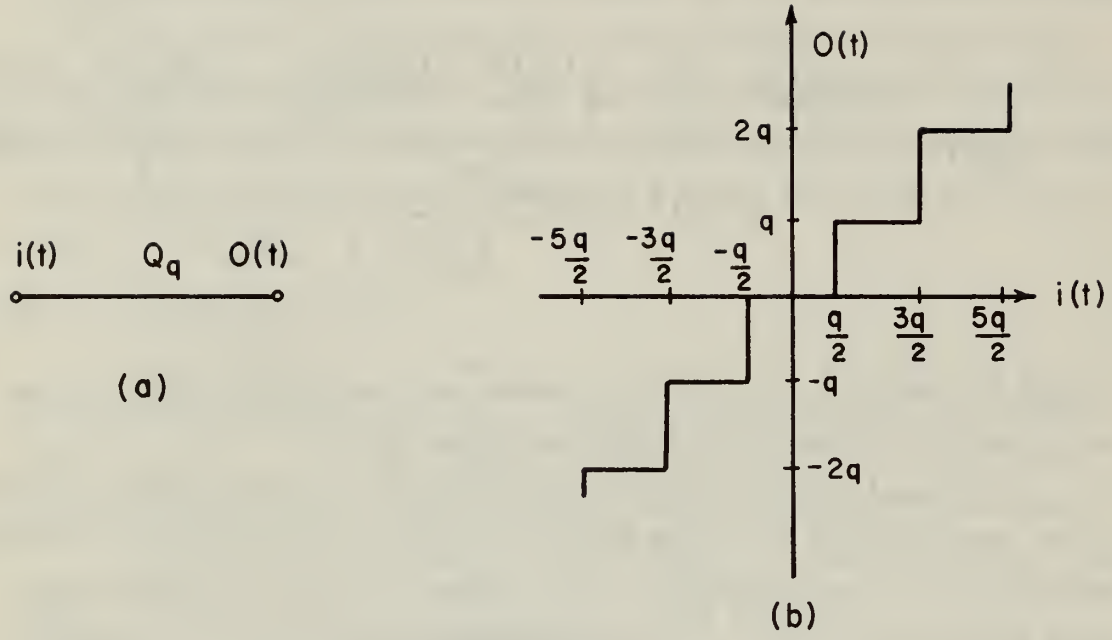

Fig. 5-6 Quantization

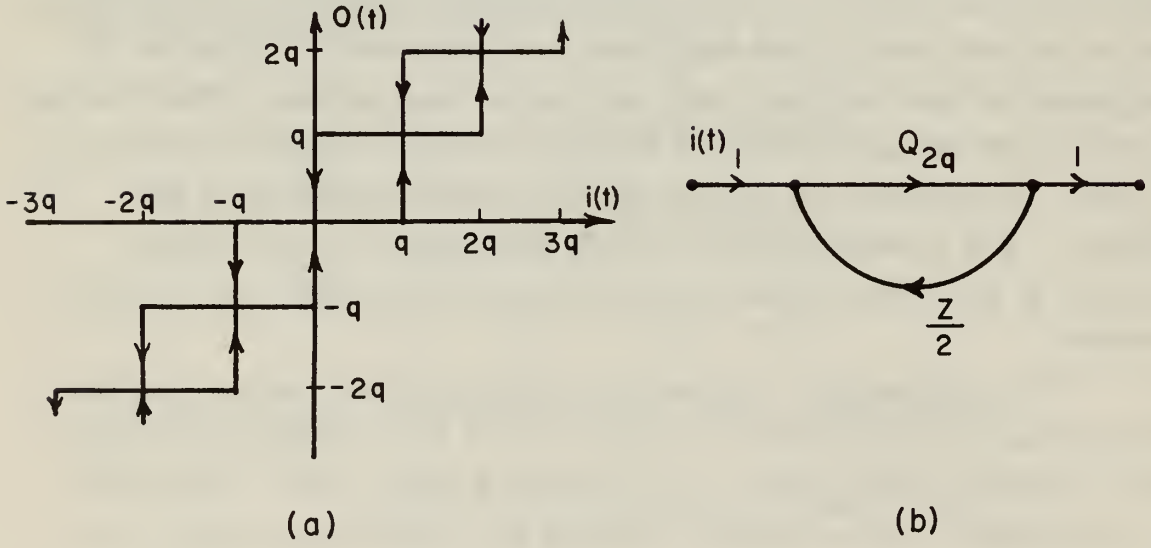

Fig. 5-7 Quantization with Half-Grain Hysteresis

nearly exact error analysis may be had by finding the roots of the characteristic equation exactly, and finding the magnitudes of the modes by root-locus techniques, but the present analysis provides enough information to form a basis for engineering decisions.

5. D. 4 Quantization Error

Quantization, or round-off as it is sometimes termed by numerical analysts, occurs whenever a number is assigned to a physical variable. Through the quantization process the value of the variable is represented as the nearest integral number of the basic units in which the variable is being measured. If this basic unit be q, the quantization process may be represented by the input-output relationship shown in Fig. 5-6.

While this is the basic quantization process, the overflow logic of many computers causes hysteresis in the quantization process. This hysteretic quantization has the characteristic shown in Fig. 5-7(a). The hysteresis may be represented by feedback around the basic quantizer as shown in Fig. 5-7(b). Note that the quantizer has grain size 2q. The z in the feedback loop represents a delay of one cycle time of the computer.

Since quantization distorts the signal, although in a deterministic way, the distortion may be thought of as noise. Widrow (Ref. 55) shows that if the amplitude of the input to the quantizer ranges over more than three quantization boxes, the quantization noise, to a good approximation, may be treated as an additive first order random process, q(t). The probability density distribution of the quantization noise is shown in Fig. 5-8. The expressions for the autocorrelation function and the power spectral density of quantization noise are

$$\phi_{qq}(\tau) = \frac{q^2}{12}\,\delta(t)$$

$$\Phi_{qq}(z) = \frac{q^2}{12} \qquad (5\text{-}31)$$

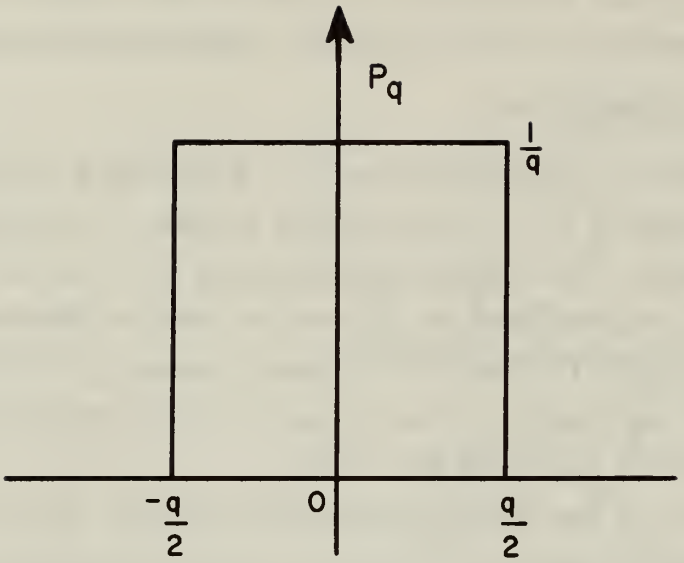

Fig. 5-8 Probability Density Distribution of Quantization

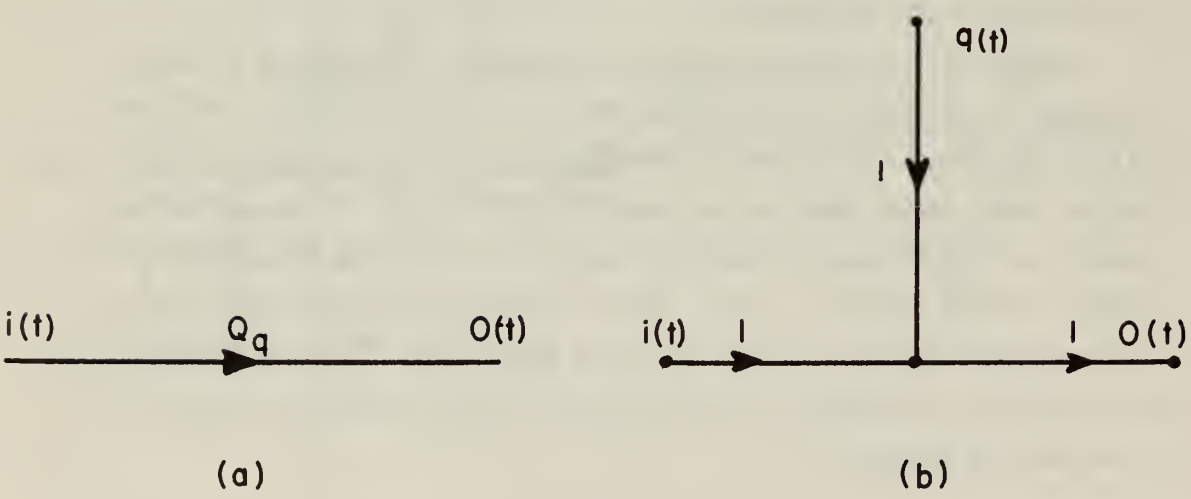

Fig. 5-9 Representation of a Quantizer by Independent Additive Noise

Fig. 5-9 shows the representation of a quantizer as independent additive noise.

Although one attempt was made to apply Widrow's theory to DDA's in real time (Refs. 49, 50), some difficulty was encountered in applying it to interconnected DDA's.

The appropriate signal-flow graph for the computer with non-hysteretic quantization is shown in Fig. 5-10, and Fig. 5-11 shows the quantizers replaced by their equivalent gains and additive noise.

If hysteretic quantization is used, a self-loop with gain $+z/2$ must be included at each node. With integrators cycling at different rates, the z used in the self-loop must correspond to the fastest basic rate: the z of Eq. (5-23) must be used.

Care must be taken to insure that a zero value of the variable actually corresponds to the zero of the computer. In many cases a bias of $\frac{1}{2}q$ is introduced because of an ambiguity of initial conditions (Ref. 49, p. 51).

Using the statistical model of quantization and the sampled-data model of the transformation computer, an expression for the power spectral density of quantization noise may be developed. For example, with $\omega_1 = 2\omega_2 = 3\omega_3$, the power spectral density of quantization in C_{il} is

$$\Phi_{il}(z) = \left| \frac{\frac{\Delta\theta^2 z}{(1-z)^2} + \frac{\Delta\theta z}{1-z^3} - \frac{\Delta\theta z}{1-z^2} + \frac{\Delta\theta^2 z^2}{(1-z)(1-z^3)} + \frac{\Delta\theta^2 z}{(1-z)(1-z^2)}}{1 + \frac{\Delta\theta^2 z}{(1-z)^2} + \frac{\Delta\theta^2 z}{(1-z^2)^2} + \frac{\Delta\theta^2 z}{(1-z^3)^2} - \frac{\Delta\theta^3 z}{(1-z^2)(1-z^3)}} \right|^2 \frac{\Delta\theta^2}{12} \tag{5-32}$$

with similar expressions for power spectral densities at other nodes. Note that for the case of the computer, the quantization grain size is $\Delta\theta$.

The mean square quantization error may be obtained by forming the sum of the squares of the sequence represented by the

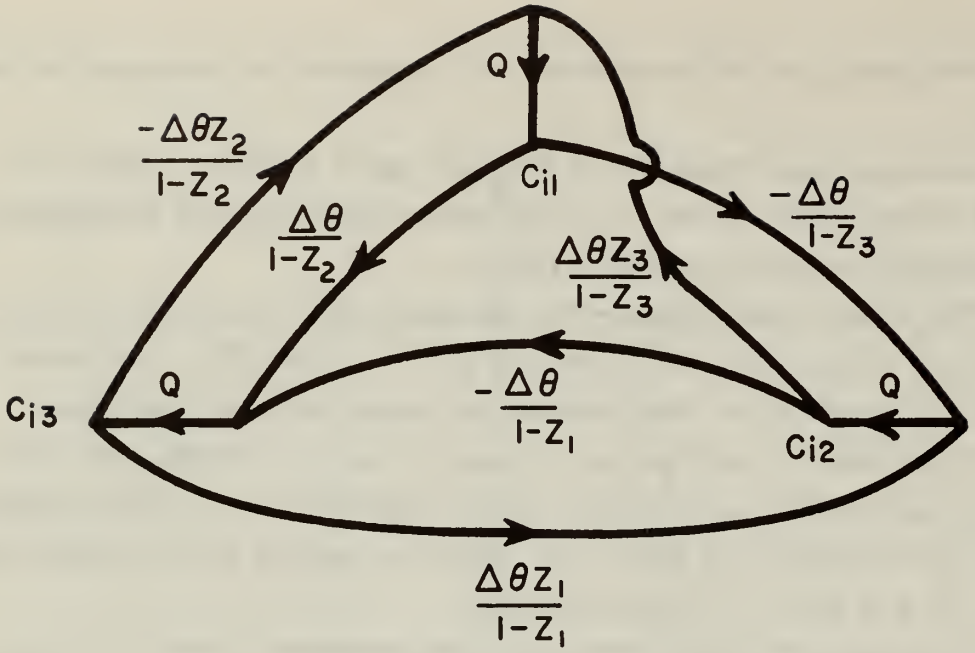

Fig. 5-10 Computer with Quantizers

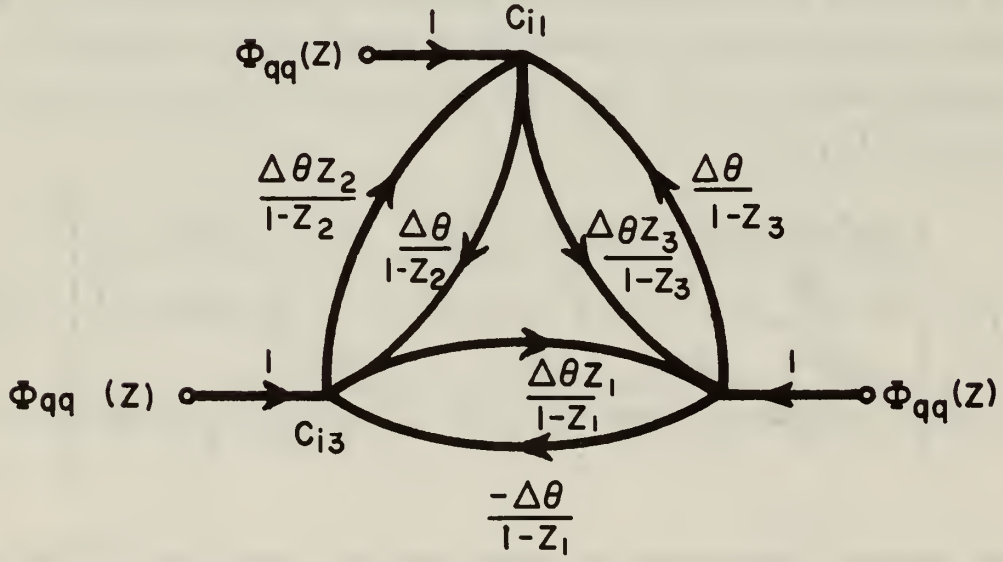

Fig. 5-11 Computer with Quantization Noise

transfer function in Eq. (5-32) and multiplying this sum by the mean square of the quantization noise (Ref. 61, Ch. 7). Since in the case of this computer the roots of the characteristic equation have magnitude close to unity, this mean square value may become very large. Thus, it is appropriate to consider only a finite number of terms in the sum-of-squares series corresponding to a finite number of steps in the computation. With the series truncated after a finite number of terms, an estimate of the error may be obtained. An example is shown in Appendix C, Section C. 3. It is found that quantization error is much smaller than the truncation error; the number of steps required to make the rms quantization error equal to $\Delta\theta$ is $0(\Delta\theta^{-2})$.

In the same section (Section C. 3), an expression for hysteretic quantization error is derived. It is found that the mean square value of hysteretic quantization error is greater than that of non-hysteretic quantization by a factor of four because of the larger quantization box. For this reason, non-hysteretic overflow logic should be used in the transformation computer.

5. D. 5 Reversibility

Up to this point, the analysis has assumed that all the $\Delta\theta$ pulses have been of the same sign. Of course, this will never be the case, and some examination must be made of the effects of negative pulses.

In the sine-cosine generators shown in Fig. 5-12, first one variable is updated, and then the other variable is updated. Thus, Fig. 5-12(a) implies the difference equations

$$\begin{aligned} \cos(n\Delta\theta) &= \cos[(n-1)\Delta\theta] - \Delta\theta \sin[(n-1)\Delta\theta] \\ \sin(n\Delta\theta) &= \sin[(n-1)\Delta\theta] + \Delta\theta \cos(n\Delta\theta) \end{aligned} \tag{5-33}$$

If a positive pulse is followed by a negative pulse, there should result

$$\cos[(n+1)\Delta\theta] = \cos[(n-1)\Delta\theta] \tag{5-34}$$

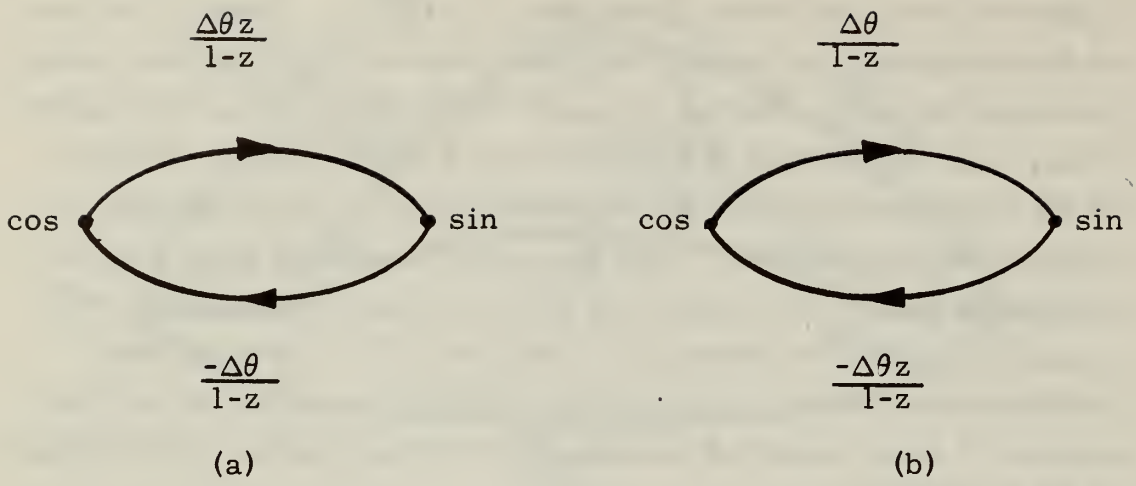

Fig. 5-12 Reversibility of Sine-Cosine Generation

The use of Eq. (5-33) for processing both pulses yields

$$\cos[(n+1)\Delta\theta] = \cos[(n-1)\Delta\theta] + \Delta\theta^2 \cos[(n-1)\Delta\theta] \qquad (5\text{-}35)$$

If positive pulses are processed according to Fig. 5-12(a), however, and negative pulses according to Fig. 5-12(b), Eq. (5-34) is satisfied, the computation is completely reversible, and the truncation and quantization errors for the two steps cancel each other.

This idea may be extended to the direction cosine computation. In Fig. 5-3, all the pulses are assumed positive, and the order of processing the pulses updates C_{il} first, then C_{i2}, then C_{i3}. Since the computation is made up of a number of sine-cosine generators interconnected, the process can be reversed by moving the z in the numerator of each loop transfer function to the other branch; this may be accomplished by updating the variables in reverse order for negative pulses.

There are three pulses, each with two possible signs, which drive the computer. This gives $2^3 = 8$ possible combinations.

There are only three direction cosines in a set; the number of possible orders of updating them is 3! = 6. Thus one pair of combinations cannot be reversed. Using the updating sequence 1, 2, 3, for all positive pulses, the computer cannot reverse $\Delta\theta_2+$; $\Delta\theta_1-$, $\Delta\theta_3-$; and $\Delta\theta_2-$; $\Delta\theta_1+$, $\Delta\theta_3+$. With another sequence representing all pulses positive, another pair could not be reversed; however, any combination of two, as well as any single pulse, can be completely reversed.

The non-reversibility of this computation causes a drift of $0(\Delta\theta^2)$ for each step reversed. Unless the computation is operating with marginal accuracy, the added equipment required to change the order of updating the variables is probably too expensive, in terms of weight, power, and cost, to pay for the additional precision achieved.

5.E Processing ΔV Pulses

At each sampling instant in the accelerometer loop a $\overline{\Delta V}$ vector, resolved into body-fixed components, appears at the accelerometer outputs. If a two-level relay is used in the loops, there will be pulses at each loop output at every sampling instant; if a three-level relay is used, output pulses will occur only at certain times. The $\overline{\Delta V}$ vector may be resolved into inertial coordinates by processing it with the direction cosine matrix:

$$\overline{\Delta V}_I = C\overline{\Delta V}_b \tag{5-36}$$

Since the magnitudes of the ΔV pulses are the same, Eq. (5-36) may be realized by the arrangement shown in Fig. 5-13. The ΔV_I pulses will be accumulated in V_I registers. Errors also arise in this computation, and they may be determined by the methods outlined above.

5.F Summary

In this chapter, the design and analysis of the transformation computer was completed. Various quadrature rules were examined, and the rectangular rule was chosen as the most appropriate for

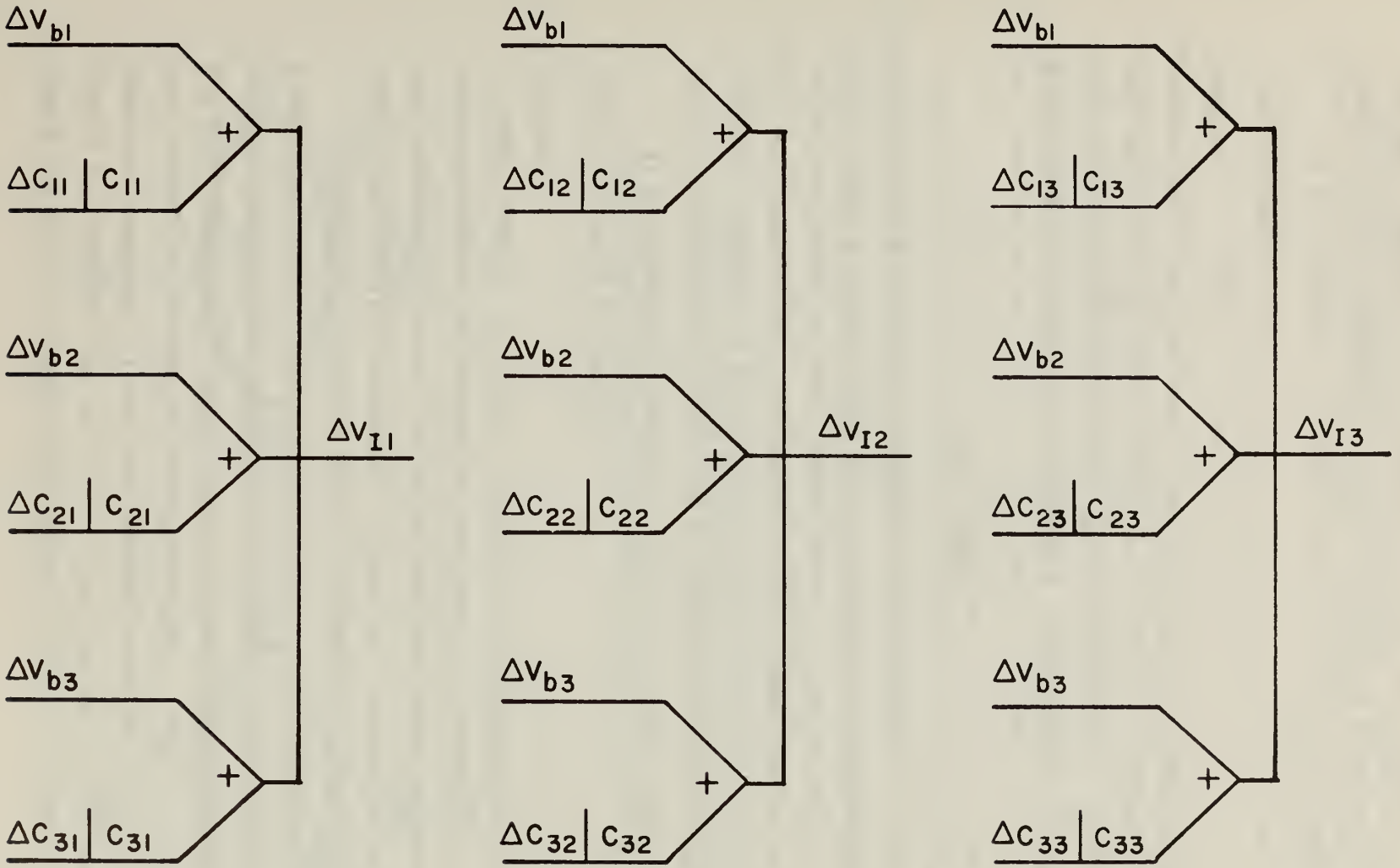
ΔVb1
ΔC11 | C11
ΔVb2
ΔC21 | C21
ΔVb3
ΔC31 | C31
ΔVI1
ΔVb1
ΔC12 | C12
ΔVb2
ΔC22 | C22
ΔVb3
ΔC32 | C32
ΔVI2
ΔVb1
ΔC13 | C13
ΔVb2
ΔC23 | C23
ΔVb3
ΔC33 | C33
ΔVI3

integrating the direction cosines [Eq. (5-9)]. With the angular information available in $\Delta\theta$ pulses, digital differential analyzers seem the most suitable form of computer for the computation (Fig. 5-2). A frequency domain model for the computer was developed (Fig. 5-3) and analyzed. The truncation error was estimated by developing an exact solution for the differential equation, and comparing it with the computer solution as indicated by root-locus plots. Quantization was treated statistically and it was found that hysteretic quantization caused a greater error than non-hysteretic. The integrators were shown to drift by $O(\Delta\theta^2)$ for each computation step reversed. Finally, a method for transforming the $\overline{\Delta V}$ vector was established.

CHAPTER VI

SYSTEM DESIGN

6.A General Considerations

The previous chapters have described and analyzed the component parts of the system; the design parameters must now be chosen so that the system operates in an optimum manner to carry out the mission assigned. Two decisions may be made without reference to the mission which the system will perform: whether the instruments should limit cycle, and how the clocks in the gyro and accelerometer loop should be related to each other.

6.A.1 Limit-Cycling Instruments

In Chapter V, Section 5.D.5, it is shown that for each step reversed in the direction-cosine computation, the integrators drift by an amount $0(\Delta\theta^2)$. For this reason, it is desirable not to have the gyros limit cycling. With a three-level relay in the gyro loop, the torquer current may be turned off during the quiescent periods, thus saving a great deal of power. Turning the current on and off, however, makes stabilization of the current more uncertain.

Since the velocity pulses are being processed by DDA's, there may be a drift of $0(\Delta\theta\Delta V)$ in accumulated velocity for each reversal. Thus, the arguments above indicate the desirability of eliminating the limit cycles in the accelerometer loops.

6.A.2 Instrument Clock Relationships

In general, the clock rate of the accelerometers will be slower than that of the gyros; thus the direction cosine may change many times between Δ V pulses. Processing of the Δ V pulses must occur between changes of direction cosines; this requirement may

be satisfied either by providing buffer storage for the Δ V pulses, or by choosing the clock frequencies and phasing of the gyro and accelerometer loops so that the Δ V pulses will always occur at the same point in the computer cycle. The latter choice is more attractive, since it eliminates the need for buffer storage and the consequent delay in processing information.

6.B Basic Design Parameters

The quantities needed to design a guidance system are the inputs, or maneuvers it will experience, the allowable error at the target, and the time of flight. The input specifications must include the maximum acceleration, velocity, and angular velocity which the guidance system is expected to undergo. From these data, the basic instrument and computer parameters may be determined.

With increment size and clock frequency specified, Chapter III and Chapter V indicate methods for determining the remaining system parameters. In the two sections that follow, computations are carried out to determine clock frequency and increment size for typical aircraft and missile missions. Numbers representing current performance are substituted into the expressions for increment size and clock frequency to provide a notion of the order of the magnitudes involved.

6.C Airplane Flights

Airplane guidance systems are position control systems; their task is to guide the aircraft to a specified position. Thus, errors in position at the target are errors in the controlled quantity. To determine specifications for the instrument increment sizes, it is appropriate to analyze a "worst possible" case, and equate the error made to the error specification.

An airplane is essentially a constant speed vehicle; thus, the worst possible case for the generation of error is a flight at maximum velocity with the direction of the velocity in error by $\frac{1}{2}\Delta\theta$, and the magnitude of the velocity in error by $\frac{1}{2}\Delta V$. If the allowable error in position E_p is the same for gyro and accelerometer quantization, the appropriate calculations are

$$\frac{1}{2}\Delta\theta V_{max} = \frac{E_p}{T_f}$$

and

$$\frac{1}{2}\Delta V = \frac{E_p}{T_f} \tag{6-1}$$

where T_f is the time of flight. Thus the required increment sizes are

$$\Delta\theta = \frac{2E_p}{V_{max} T_f}$$

and (6-2)

$$\Delta V = \frac{2E_p}{T_f}$$

Note that $\Delta\theta$ should be chosen as a power of 2. The clock frequencies are

$$f_g = \frac{W_{max}}{\Delta\theta}$$

and (6-3)

$$f_a = \frac{a_{max}}{\Delta V}$$

Specifications which represent a typical high performance airplane are

$$\begin{aligned} a_{max} &= 5g = 161 \text{ ft/sec}^2 \\ W_{max} &= 3 \text{ rad/sec} \\ V_{max} &= 600 \text{ kt} \\ E_p/T_f &= .1 \text{ kt} \end{aligned} \tag{6-4}$$

Substitution gives

$$\Delta\theta = 333 \ \mu\text{rad}$$

$$\Delta V = .2 \text{ kt} = .333 \text{ fps.}$$

Since $\Delta\theta$ should be chosen as a negative integral power of two, take

$$\Delta\theta = 2^{-12} = 244 \ \mu\text{rad}$$

Then the clock frequencies are

$$f_g = 12.3 \text{ kc}$$

$$f_a = 482 \text{ cps}$$

Since it is desirable to have f_a a subharmonic of f_g set,

$$f_a = \frac{12300}{25} = 492 \text{ cps}$$

The complete set of design parameters is

$$\begin{aligned} \Delta\theta &= 244\ \mu\text{rad.} \\ f_g &= 12.3 \text{ kc} \\ \Delta V &= .333 \text{ fps} \\ f_a &= 492 \text{ cps} \end{aligned} \qquad (6\text{-}5)$$

The period of the gyro loop is 81.3 microseconds. With 18 additions to be made in the transformation computer in this time, an add time of 4.5 microseconds per word is required. Since a first-rate arithmetic computer with central control would be required in toto to accomplish this task, a DDA is clearly the best machine for this job. It will be smaller, faster, and easier to build.

For serial addition of a word with thirteen bits (twelve plus one for sign) in four and a half microseconds, a bit rate of about three megacycles is required. This performance is available in present DDA's.

With increment sizes and clock frequencies fixed, the remaining parameters may be quickly determined.

6.D Missile Flights

In contrast to an airplane guidance system, a missile guidance system is essentially a velocity control system, and a specified error in point of impact must be translated into an error in velocity at thrust termination. Relations between increment sizes and velocity error at cutoff are determined and translated down range using linear perturbation techniques to find impact error.

The relationship between trajectory parameters and point of impact is called the hit equation (Ref. 65). The perturbation factors are called range derivatives and are obtained by differentiating the hit equation. The velocity range derivative, $\delta R/\delta V$, is the one of interest in the following computation.

The worst possible case to be analyzed here is where the velocity

is in error by $\frac{1}{2}\ \Delta V$ in the direction of maximum range derivative, and where the error due to gyro quantization is a velocity error of $\frac{1}{2} V_{co} \Delta\theta$ in the direction of maximum range derivative. The origin of the first error is rather obvious; the origin of the second is not.

Suppose that as each ΔV pulse is processed, the direction cosines are in error by $\frac{1}{2}\ \Delta C = \frac{1}{2}\Delta\vartheta$, then the error at each step is $\frac{1}{2}\Delta\theta\Delta V$. Summing this over the total velocity accumulation yields

$$E(V) = \Sigma\ \frac{1}{2}\ \Delta\theta\Delta V = \frac{1}{2}\Delta\theta\ \Sigma\Delta V = \frac{1}{2}\Delta\theta V_{co} \tag{6-6}$$

The appropriate calculations for increment size are

$$\frac{1}{2}\ \Delta\theta V_{co}\ \frac{\delta R}{\delta V} = E_p$$

and (6-7)

$$\frac{1}{2}\ \Delta V\ \frac{\delta R}{\delta V} = E_p$$

or

$$\Delta\vartheta = \frac{2E_p}{V_{co}\frac{\delta R}{\delta V}}$$

and (6-8)

$$\Delta V = \frac{2E_p}{\frac{\delta R}{\delta V}}$$

The clock frequencies are then

$$f_g = \frac{W_{max}}{\Delta\theta}$$
$$f_a = \frac{a_{max}}{\Delta V} \tag{6-9}$$

Typical specifications for an 1800 nautical mile missile are

$$a_{max} = 10g = 322\ ft/sec^2$$
$$W_{max} = .2\ rad/sec$$

$$V_{co} = 20,000 \text{fps}$$
$$E_p = 300 \text{ ft} \qquad (6\text{-}10)$$

Substitution gives

$$\Delta\vartheta = 33.3\ \mu\text{rad}$$
$$\Delta V = .333 \text{ fps}$$

Since $\Delta\theta$ should be a negative integral power of two, take

$$\Delta\vartheta = 2^{-15} = 30.5\ \mu\text{rad}$$

The clock frequencies are then

$$f_g = 6.55 \text{ kc}$$

and

$$f_a = 484 \text{ cps}$$

Since the accelerometer clock frequency should be a subharmonic of the gyro clock frequency, take

$$f_a = \frac{6550}{13} = 504 \text{ cps}$$

The complete set of parameters is

$$\Delta\theta = 30.5\ \mu\text{rad}$$
$$f_g = 6.55 \text{ kc}$$
$$\Delta V = .333 \text{ fps} \qquad (6\text{-}11)$$
$$f_a = 504 \text{ cps}$$

As in the case of the airplane mission, the computer must be quite fast, requiring an add time of about eight and a half microseconds per word. Again, the logical choice for the computer is the DDA, since an airborne computer must be compact. Further, the advantage of flexibility associated with an arithmetic machine would not be realized because of the fast add time required. For a serial DDA to perform eighteen additions of words sixteen bits long in the computer cycle time, a bit rate of about two megacycles is required. This performance is available in present DDA's.

CHAPTER VII

SUMMARY AND CONCLUSIONS; SUGGESTIONS FOR FURTHER STUDY AND DEVELOPMENT

7.A Summary and Conclusions

This work has been concerned with a broad theoretical analysis of gimballess inertial reference equipment using delta-modulated instruments. The equipment considered consists of three body-mounted, delta-modulated, single-degree-of-freedom integrating gyros, three body-mounted, delta-modulated, single-axis pendulum accelerometers, and a transformation computer. The delta-modulated gyros deliver output pulses representing increments of rotation and the delta-modulated accelerometers deliver output pulses representing increments of velocity. This representation leads naturally to the choice of an incremental computer to perform the coordinate transformation. An examination of performance required from the equipment concludes the investigation. Following is a brief summary of the specific points covered, and the specific conclusions reached.

1. Gimballess inertial reference equipment is theoretically feasible, and the required computation can be done with DDA's currently available. The major obstacle to the realization of practical gimballess inertial reference equipment is the lack of inertial instruments specifically designed for this application.

2. Delta modulation is a pulse modulation system in which each output pulse represents a fixed increment in the input, or one of its integrals or derivatives. The analysis of a delta-modulated loop proceeds in a straightforward manner, using a moding plot to determine the modes of the system and Bergen's technique for finding the detailed behavior of the limit cycles. In a loop with a three-level relay, the width of the zero level may be adjusted to eliminate the limit cycle. The response of the loop to inputs may be found by determining bounds on the consecutive numbers of pulses possible under certain conditions.

The output sequences may be verified by a modified form of Bergen's method. For small inputs a modified step-by-step transient approach is best. This technique relies on detailed knowledge of the system's modes.

3. Delta-modulated integrating gyros and accelerometers are useful inertial instruments. They deliver digital outputs in synchronism with a clock, and can be scaled as necessary to meet computational requirements. Delta-modulated instruments are fixed level torquing, which is much more accurate than analog torquing; and the measurement of integrated torque, which indicates the system output, is merely a pulse-counting process.

4. The transformation of the Δ V vector from a body-fixed coordinate frame to an inertial coordinate frame is best accomplished through a direction cosine matrix transformation. The direct application of the matrix differential equation is most suitable for digital computation. Other methods considered for transforming vectors, while providing valuable insight into the problem, are computationally cumbersome.

5. Since the instrument outputs are incremental in form, the digital differential analyzer is the most attractive choice for instrumenting the solution of the matrix differential equation. Their speed and compactness are attractive features for airborne computers.

6. Integration rules with order higher than zero, using a larger increment, cannot be used to attain a slower computer speed with increased accuracy because of an irreducible uncertainty in gyro information. This uncertainty is a consequence of the digital form of the angular information. Thus, rectangular integration, being the simplest, is the best for this application.

7. The transformation computer may be analyzed using frequency domain techniques. With the assumption that the angular rate about one axis is a rational multiple of that about another, the computer may be modeled as a sampled-data system, and a simple signal flow graph drawn for it. This signal flow graph provides great insight into

the computer operation, showing the dominant mode, and giving an estimate of truncation error. Quantization may be treated statistically.

7.B Suggestions for Further Study and Development

The areas of further study and development which can contribute to the realization of practical gimballess inertial reference equipment are listed below.

1. Development of gyroscopes designed specifically for gimballess applications should be pursued. The severe angular velocity environment to which these instruments will be subjected provides enough design problems to warrant a separate design. A torque generator providing high torque very accurately is the most important element in such a design.

2. Moving-coil and flapper-type torque and signal generators should be developed. Their advantages of small size and greater sensitivity combine to make them an attractive choice for use in inertial instruments.

3. The frequency domain analysis of the transformation computer should be extended to more complicated systems. A method should be developed which generalizes the results for rates which are not related to each other as rational multiples to cases where the rates are irrational multiples and to cases where the rates have varying relationships.

4. The reversibility of the computation is an interesting point which deserves further study. The logic required in the computer, as well as the actual method of computation, should be considered.

5. Stability in the large of the limit cycles of delta-modulated loops should be investigated.

APPENDIX A

DETAILED ANALYSIS OF A DELTA-MODULATED LOOP WITH A TWO-LEVEL RELAY

The system to be analyzed is shown in Fig. A-1. This is the loop considered by many investigators with $T_s = \tau = 1$ second, $D = 1$. The moding analysis has been carried out in Chapter II, Fig. 2-4. The Moding Plot indicates the existence of the 1-1, 2-2, and 3-3 modes.

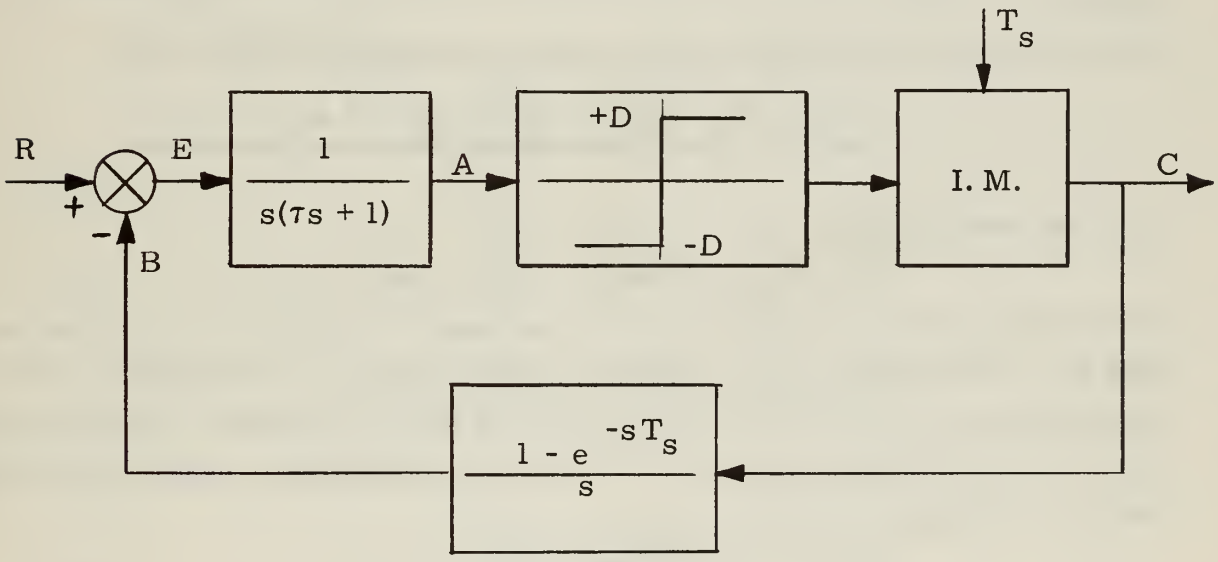

Fig. A-1 Delta-Modulated Loop to be Analyzed

A.1 Zero Input Behavior

A detailed analysis of the 3-3 mode follows:

The output of the sampler is

$$C(z) = \frac{(1 + z + z^2)(1-z^3)}{1 - z^6} \qquad \text{(A-1)}$$

Here z is a unit delay, $z = e^{-sT_s}$.

The output of the linear plant is

$$A(s,z) = -C(z)G(s) + \frac{A_o}{s} + \frac{\tau\dot{A}_o}{s(\tau s+1)} \qquad (A-2)$$

The z-transform of A, giving the samples of A, is

$$A(z) = -C(z)\, G^*(s) + \left[\frac{A_o}{s} + \frac{\tau\dot{A}_o}{s(\tau s+1)}\right]^*$$

$$= -\left[\frac{(1+z+z^2)\,(1-z^3)\,(1-z)}{1-z^6}\right]\left[\frac{T_s z}{(1-z)^2} - \frac{\tau}{1-z} + \frac{\tau}{1-\alpha z}\right] \qquad (A-3)$$

$$+ \frac{A_o}{1-z} + \tau\dot{A}_o\left[\frac{1}{1-z} - \frac{1}{1-\alpha z}\right]$$

where $\alpha = e^{\frac{-T_s}{\tau}}$.

If the 3-3 mode is possible, A(z) must be expressible in the form

$$A(z) = \frac{A_o + A_1 z + A_2 z^2 + A_3 z^3 + A_4 z^4 + A_5 z^5}{1 - z^6} \qquad (A-4)$$

with the constraints

$$A_o > 0\ A_1 > 0\ A_2 > 0\ \ A_3 < 0\ A_4 < 0\ A_5 < 0 \qquad (A-5)$$

so that the postulated relay action is sustained. If Eq. (A-3) is to be put into the form of Eq. (A-4), the factor $(1-\alpha z)$ must be eliminated from the denominator of Eq. (A-3). For this factor to be eliminated, the numerator, $M_1(z)$, of the terms having $(1-z^6)(1-\alpha z)$ as denominator must contain that factor. The numerator is

$$M(z) = -(1-z^3)^2\tau - (1-z^6)\,\tau\dot{A}_o$$

$$= -\tau\,(1-z^3)[1-z^3 + \dot{A}_o(1+z^3)] \qquad (A-6)$$

$$= -\tau\,(1+\dot{A}_o)\,(1-z^3)\left(1 - \frac{1-\dot{A}_o}{1+\dot{A}_o} z^3\right)$$

If M(z) is to contain $(1-\alpha z)$ as a factor $\dot{A}_o$ must be such that

$$\frac{1-\dot{A}_o}{1+\dot{A}_o} = \alpha^3$$

or

$$\dot{A}_o = \frac{1-\alpha^3}{1+\alpha^3} = .905 \tag{A-7}$$

This is one condition on the state of the linear plant for no transient in the limit cycle. With this condition satisfied, the output of the linear plant is

$$A(z) = -\frac{(1-z^3)^2}{1-z^6}\left(\frac{T_s z}{(1-z)^2} - \frac{\tau}{1-z}\right) + \frac{1+z+z^2+z^3+z^4+z^5}{1-z^6}(A_o+\tau\dot{A}_o)$$

$$- \frac{2\tau}{1+\alpha^3}\cdot\frac{(1+\alpha z+\alpha^2 z^2)(1-z^3)}{1-z^6} \tag{A-8}$$

The last term in Eq. (A-8) corresponds to M(z) after cancellation. Collecting powers of z in Eq. (A-8) gives

$$(1-z^6)\ A(z) = A_o$$

$$+ (A_o - \frac{2\alpha\tau}{1+\alpha^3} + \frac{1-\alpha^3}{1+\alpha^3}\tau - T_s + \tau)z$$

$$+ (A_o - \frac{2\alpha^2\tau}{1+\alpha^3} + \frac{1-\alpha^3}{1+\alpha^3}\tau - 2T_s + \tau)\ z^2$$

$$+ (A_o + \frac{2\tau}{1+\alpha^3} + \frac{1-\alpha^3}{1+\alpha^3}\tau - 3T_s - \tau)\ z^3$$

$$+ (A_o + \frac{2\alpha\tau}{1+\alpha^3} + \frac{1-\alpha^3}{1+\alpha^3}\tau - 2T_s - \tau)\ z^4$$

$$+ (A_o + \frac{2\alpha^2\tau}{1+\alpha^3} + \frac{1-\alpha^3}{1+\alpha^3}\tau - T_s - \tau)\ z^5 \tag{A-9}$$

The numbers above $T_s = \tau = 1$ sec) lead to

$$(1-z^6)\ A(z) = A_o + (A_o + .204)z + (A_o - .353)z^2 + (A_o - 1.195)z^3$$

$$+ (A_o - 1.394)z^4 + (A_o - .837)z^5 \tag{A-10}$$

By applying the inequalities Eq. (A-5) to Eq. (A-10) the following bounds on A_o are found:

$$.353 < A_o < .837 \qquad \text{(A-11)}$$

Thus, with initial conditions as specified in Eq. (A-7) and Eq. (A-11), the 3-3 mode will occur without transient.

Similar computations lead to no transient initial conditions for the 1-1 and 2-2 modes:

1-1 mode: $0 < A_o < .076$

$$\dot{A}_o = \frac{1-\alpha}{1+\alpha} = .463 \qquad \text{(A-12)}$$

2-2 mode: $0 < A_o < .475$

$$\dot{A}_o = \frac{1-\alpha^2}{1+\alpha^2} = .762 \qquad \text{(A-13)}$$

Further computations show that no other modes are possible.

A.2 Transient Response

A.2.a Impulse Response

The impulse response of the loop is found by a modified step-by-step computation. After an input impulse, the output pulses remain one sign for a number of pulses determined by the strength of the impulse, as the increments of the output corresponding to the integrated impulse build up. As the output impulses pass through the zero order hold, they become a step. Thus, the appropriate calculation to find the state of the linear plant as the error dies out is a combination of step and impulse response.

For a numerical example, assume that the loop is in the 1-1 mode centered at the origin. Let the input impulse be applied halfway between sampling instants, as the linear plant output is crossing from negative to positive. Let the imput impulse have strength S = 5.5.

With t = 0 at the clock pulse just preceding the application of the impulse, the following equations describe the linear plant output

$$A(t) = t - .038 - 1.463(1-e^{t}) \quad 0 \leqq t \leqq .5 \qquad \text{(A-14a)}$$

$$A(t) = t - .377 + 4.612 (1-e^{-(t-.5)}) \quad .5 \leqq t \leqq 1 \qquad \text{(A-14b)}$$

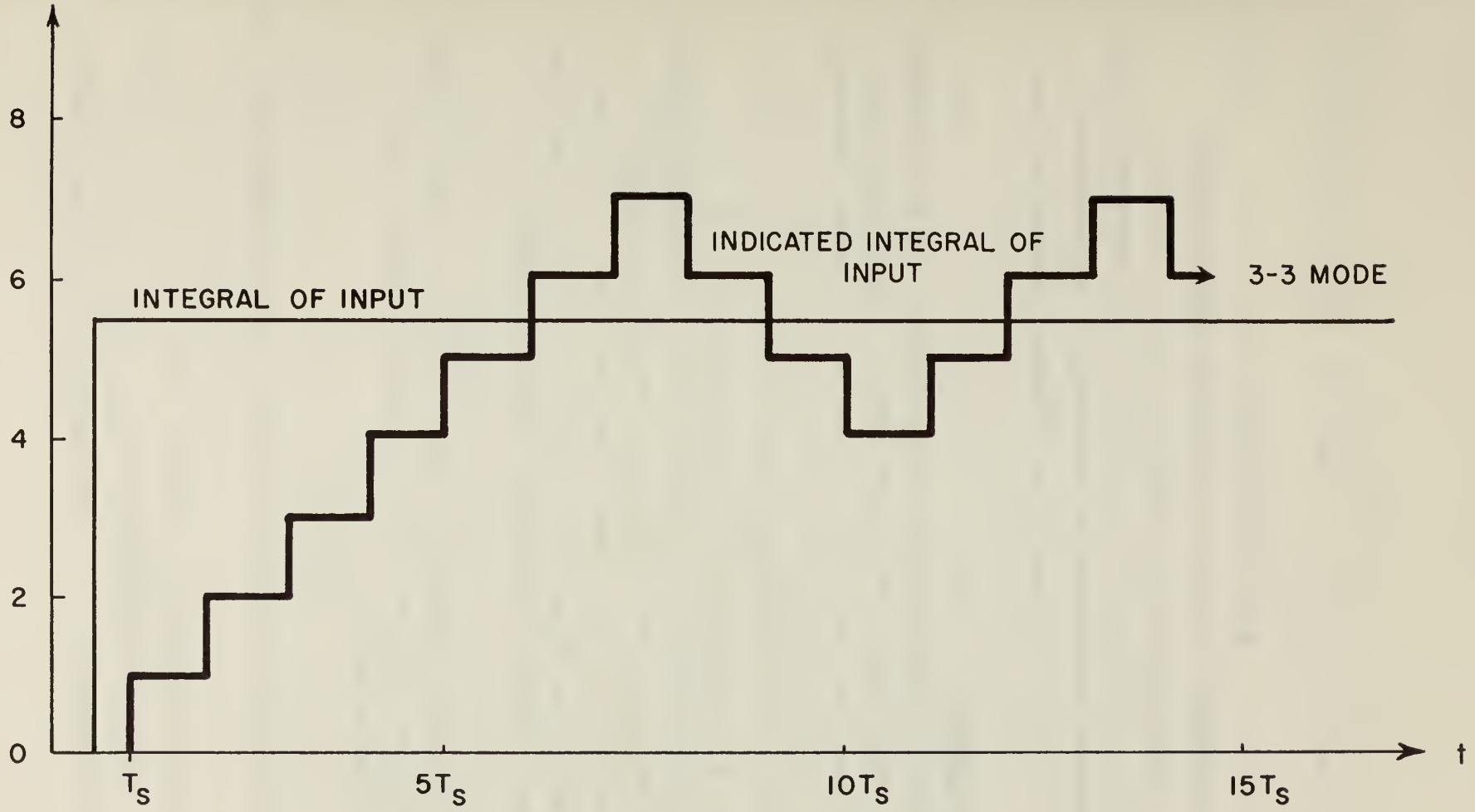

Fig. A-2 Response of Loop to Impulse: $R(t) = 5.5\delta(t)$

$$A(t) = -(t-1) + 2.403 + 3.8(1-e^{-(t-1)}) \quad 1 \leqq t \tag{A-14c}$$

Eq. (A-14c) changes sign between t = 7 and t = 8. At t = 8, the state of the system is

$$A(8) = .792 \text{ and } \dot{A}(8) = -1 \tag{A-15}$$

These initial conditions lead to the 3-3 mode, as may be seen by comparison with Eq. (A-7) and Eq. (A-11).

Note that the input integral is only determined to within three units. This is a quantization uncertainty due to moding. If the system had settled into the 1-1 mode, the quantization uncertainty would have been only one unit.

A.2.b Step Response

The first task in determining the step response of the loop is finding the upper and lower bounds on the number of consecutive pulses of one sign. To determine the upper bound on the number of pulses of one sign the maximum velocity and displacement of the linear plant output are assumed, and the number of pulses required to drive the plant across null is counted. If the magnitude of the input step is R = rD, the maximum rate that the system can attain is D(1+r). If a sampling instant occurs just before the system crosses null, the maximum possible displacement is $D(1+r)T_s$. With these initial conditions on the linear plant and the linear plant being driven negatively by a step of magnitude D(-1+r), the time response of the system may be written as

$$A(nT_s) = D(-1+r)nT_s + D(1+r)T_s + 2D\tau(1-e^{-n\frac{T_s}{\tau}}) \tag{A-16}$$

If n is to be the upper bound on consecutive positive pulses, it must be the least integer such that

$$A(nT_s)<0 \tag{A-17}$$

For this to be the case, the relation between r, n, and the loop parameters must be

$$r > \frac{n-1-2\frac{\tau}{T_s}(1-e^{-n\frac{T_s}{\tau}})}{n+1} \tag{A-18}$$

Note that D does not appear in the above expression. For the numerical

example above this relation is

$$r > \frac{n-3+2^{e-n}}{n+1} \tag{A-19}$$

Table A-1 is the result of substitution of various n in Eq. (A-19).

While this eliminates some possible sequences, the number remaining to be tested is still quite large; thus it is desirable to place a lower bound on the number of pulses of one sign which can follow a given number of pulses of the opposite sign.

The computation to determine this lower bound is similar to that above. The initial conditions to be used are minima. The initial position is taken as zero plus, and the minimum velocity after n_1 negative pulses, resulting from maximum velocity at the previous switching time, is

$$\dot{A}_o(n_1) = D(1+r)-2De^{-\frac{T_s}{\tau}n_1} \tag{A-20}$$

With the above initial conditions, the expression for the linear plant output is

$$A(nT_s) = D(-1+r)nT_s + 2D\tau(1-e^{-\frac{T_s}{\tau}n_1})(1-e^{-\frac{T_s}{\tau}n}) \tag{A-21}$$

As before, if n is to be the required lower bound, it must be the least n for which Eq. (A-17) is valid. The required relationship is

$$r < 1 - \frac{2D\frac{\tau}{T_s}(1-e^{-\frac{T_s}{\tau}n_1})(1-e^{-\frac{T_s}{\tau}n})}{n} \tag{A-22}$$

The ranges of r for various n and n_1 are shown for the numerical example above in Table A-2.

The response of the loop for $r = \frac{1}{2}$ will now be computed. For $r = \frac{1}{2}$, Table A-1 shows that while the feedback and input act together, the maximum number of pulses (which are negative) is two, and when they

TABLE A-1

UPPER BOUND ON CONSECUTIVE POSITIVE PULSES

n	range of r
1	r<-.634
2	-.634<r<-.233
3	-.233<r< .025
4	.025<r< .207
5	.207<r< .336
6	.336<r< .429
7	.429<r< .5

TABLE A-2

LOWER BOUND ON CONSECUTIVE POSITIVE PULSES
FOLLOWING A GIVEN NUMBER OF NEGATIVE PULSES

	range of r			
n_1 / n	1	2	3	4
1	- 1 <r<.2	- 1 <r<.095	- 1 <r<-.2	- 1 <r<.24
2	.2 <r<.456	-.095<r<.251	-.2 <r<.18	-.24 <r<.15
3	.456<r<.6	.261<r<.456	.18 <r< .4	.15 <r<.38
4	.6 <r<.688	.452<r<.579	.4 <r<.533	.38 <r<.518
5	.688<r<.749	.579<r<.656	.533<r< .622	.518<r<.611

NOTE: Bounds on negative pulses may be found by changing the sign of r and entering the tables again.

are in opposition the maximum number permitted is seven. For the feedback and input acting together, one is the lower bound on the number of negative pulses following any number of positive pulses, according to Table A-2. However, at least three positive pulses must follow one negative pulse, and at least four positive pulses must follow two negative pulses.

For $r = \frac{1}{2}$, the following is a partial list of sequences which have the required average:

Period	Sequences
$4T_s$	3,1
$8T_s$	4,1,2,1; 5,1,1,1; 6,2.
$12T_s$	4,1,3,1,2,1; 4,1,2,1,3,1; 5,1,3,1,1;1;
	5,1,1,1,3,1; 6,2,3,1; 7,1,2,2; 7,2,2,1.

According to the bounds found above, the only sequences which are possible are 3,1 and 6,2. The sequence 3,1 will be verified in a manner similar to that used in verifying modes above.

The output of the loop is

$$C(z) = \frac{1+z+z^2-z^3}{1-z^4} \tag{A-23}$$

The output of the linear plant is

$$A(s,z) = [R(s) - C(z)G_2(s)]G_1(s) + \frac{A_o}{s} + \frac{\tau \dot{A}_o}{s(\tau s+1)} \tag{A-24a}$$

The samples of the linear plant are given by

$$A(z) = D[r-C(z)(1-z)]\left[\frac{T_s z}{(1-z)^2} - \frac{\tau}{1-z} + \frac{\tau}{1-\alpha z}\right] + \frac{A_o + \tau \dot{A}_o}{1-z} - \frac{\tau \dot{A}_o}{1-\alpha z} \tag{A-24b}$$

If the postulated sequence is possible, then $A(z)$ must be expressible as

$$A(z) = \frac{A_o + A_1 z + A_2 z^2 + A_3 z^3}{1-z^4} \qquad \text{(A-25)}$$

with

$$A_o > 0 \quad A_1 > 0 \quad A_2 > 0 \; A_3 < 0 \qquad \text{(A-26)}$$

For this to be the case, the factor $(1-\alpha z)$ must be eliminated from the denominator of Eq. (A-24). The numerator of terms with denominator $(1-z^4)(1-\alpha z)$ is

$$\begin{aligned} M(z) &= [.5(1-z^4) - (1+z+z^2-z^3)(1-z)]\tau - \tau\dot{A}_o(1-z^4) \\ &= \tau(1-z)[(.5-A_o)(1+z+z^2+z^3) - (1+z+z^2-z^3)] \\ &= -\tau(.5+\dot{A}_o)(1-z)\left(1+z+z^2 - \frac{1.5-A_o}{.5+\dot{A}_o} z^3\right) \end{aligned} \qquad \text{(A-27)}$$

For $(1-\alpha z)$ to be a factor of M(z), it is necessary that:

$$\frac{1.5-\dot{A}_o}{.5+\dot{A}_o} = \alpha+\alpha^2+\alpha^3$$

or

$$\dot{A}_o = \frac{1 + .5(1-\alpha-\alpha^2-\alpha^3)}{1+\alpha+\alpha^2+\alpha^3} \qquad \text{(A-28)}$$

With $\dot{A}_o$ as in Eq. (A-28), A(z) may be written as

$$A(z) = \frac{.5(1-z^4) - (1+z+z^2-z^3)(1-z)}{1-z^4}\left[\frac{T_s z}{(1-z)^2} - \frac{\tau}{1-z}\right] + \frac{A_o+\tau\dot{A}_o}{1-z}$$

$$- \frac{2\tau}{1+\alpha+\alpha^2+\alpha^3}(1-z)[1+(1+\alpha)z + (1+\alpha+\alpha^2)z^2] \qquad \text{(A-29)}$$

Collecting powers of z yields

$$(1-z^4)A(z) = A_o + (A_o+\tau\dot{A}_o + .5\tau - .5T_s - \frac{2\alpha\tau}{1+\alpha+\alpha^2+\alpha^3})z$$

$$+(A_o+\tau\dot{A}_o+.5\tau-T_s - \frac{2\alpha^2\tau}{1+\alpha+\alpha^2+\alpha^3})z^2$$

$$+(A_o+\tau\dot{A}_o - 1.5\tau - 1.5T_s + \frac{2(1+\alpha+\alpha^2)}{1+\alpha+\alpha^2+\alpha^3}) z^3 \qquad (A-30)$$

Substitution of the numbers of the example into Eq. (A-30) yields

$$(1-z^4)A(z) = A_o+(A_o+1.312)z = (A_o+3.113)z^2 + A_o - .25)z^3 \qquad (A-31)$$

Application of the inequalities Eq. (A-26) shows that for 3, 1 to be an output sequence, the acceptable range of initial plant values is

$$0 > A_o > .25 \qquad (A-32)$$

Similar computations show that 6, 2 is also a possible output sequence, but that none of the others is possible.

The above analysis, as noted in Chapter II, is useful only for inputs larger than about 10% of the saturating signal. For example, an input step of one-twentieth of the saturating signal would have an output sequence of some multiple of forty sampling periods, which implies a formidable computation.

For small inputs, the modified step-by-step transient analysis described in Chapter II is the most useful. The key to the analysis is the fact that a small input may be viewed as a small disturbance of the prevailing limit cycle.

For a numerical example, assume the system analyzed above is in the 1-1 mode with zero average and that an input step of R = .01D is applied at the sampling instant when the linear plant is positive.

The plant is assumed to move under the influence of the input alone using the initial value of linear plant output and the velocity of the plant relative to the limit cycle as initial conditions. These initial conditions are

$$A_o = .038 \qquad \dot{A}_o = 0 \qquad (A-33)$$

and the equation describing the motion is

$$A(t) = .01Dt + .036 - .01D\tau(1-e^{-\frac{t}{\tau}}) \qquad (A-34)$$

The mode will change when the plant output sample which is now negative becomes positive. When this occurs, $t = (2K=1)T_s$, and

$A[(2K+1)T_s] > .076$, that is, the linear plant output sample gets outside its permitted range for sustaining the 1-1 mode [see Eq. (A-12)].

$$A[(2K+1)T_s] = .01D(2K+1)T_s + .036 - .01D\tau(1-e^{-(2K+1)\frac{T_s}{\tau}}) \tag{A-35}$$

For $K = 2$, $A[2K+1)T_s] = .07607$, and the mode will change. The velocity of the linear plant at this time is the drive velocity, .01, plus the limit cycle velocity, -.463, [see Eq. (A-12)], and the position of the linear plant is .07607 - .076, since the plant output which was negative is now being considered. One sampling period later, the linear plant output is (shifting the time origin)

$$A(T_s) = -.99 + .00007 + (-.453 + .99)(1-e^{-1})$$

$$A(T_s) = -.651 \tag{A-36}$$

The plant velocity at this time is

$$\dot{A}(T_s) = -.792 \tag{A-37}$$

By comparing this state of the linear plant with the mode initial conditions, it is seen that the system will settle into the 3-3 mode. Again, the plant is assumed to move under the influence of the input alone, with initial conditions which are the actual plant position and the velocity of the plant relative to the limit cycle. Thus the initial conditions to be used are

$$A_o = -.651 \qquad \dot{A}_o = -.792 - (-.905) = +.113 \tag{A-38}$$

The equation of motion for the linear plant is (again shifting the time origin)

$$A(t) = .01Dt - .651 + \tau(.103)(1-e^{-\frac{t}{\tau}}) \tag{A-39}$$

The mode will change when the linear plant output sample which is least negative becomes positive. This occurs at $t = (6K+2)T_s$. At this time, the linear plant output will leave the region leading to the 3-3 mode so that $A[(6K+2)T_s] > -.353$ [see Eq. (A-11)].

$$A[6K+2)T_s] = .01D(6K+2)T_s - .651 + \tau(.103)(1-e^{-(6K+2)\frac{T_s}{\tau}}) \tag{A-40}$$

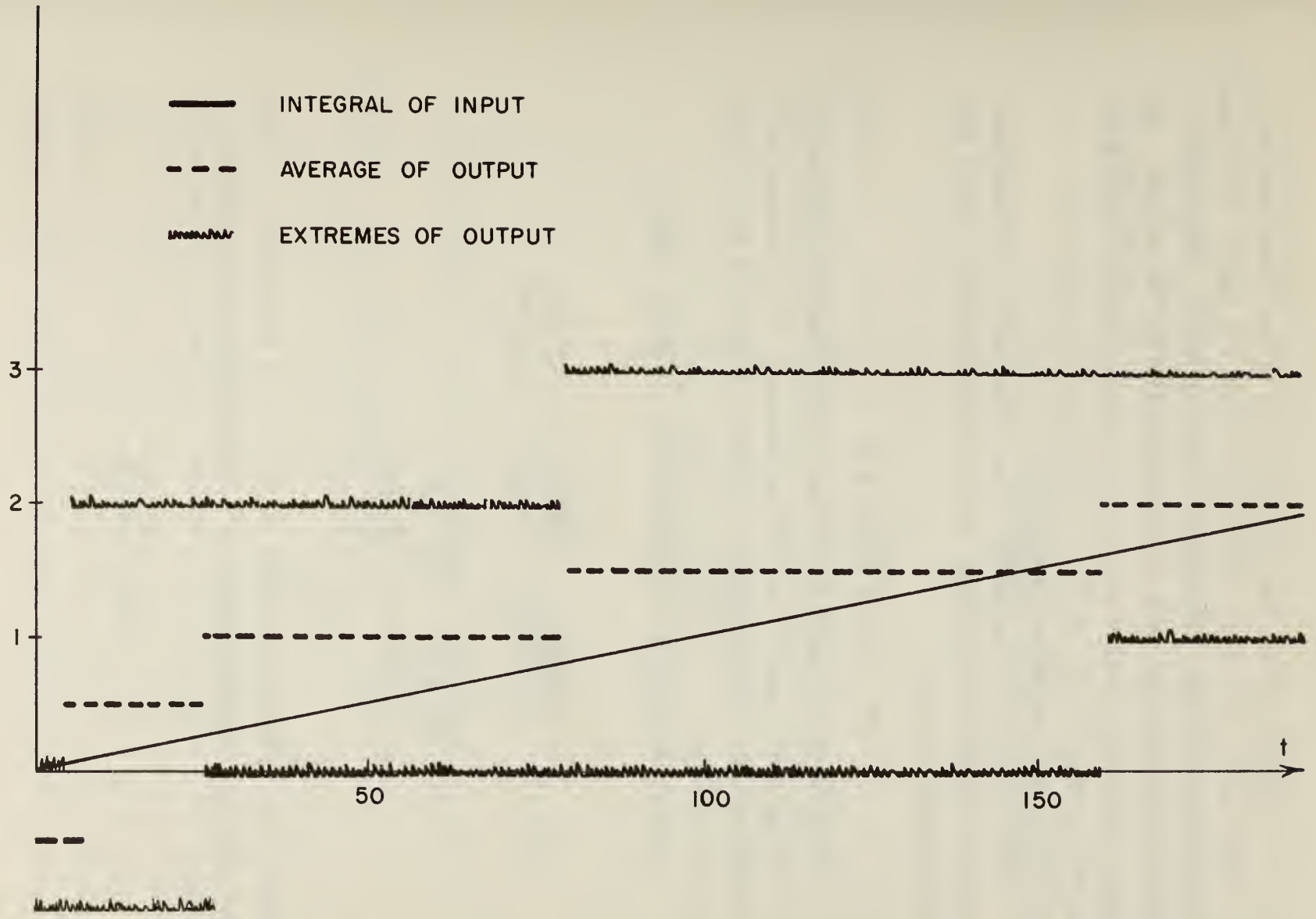

Fig. A-3 Response of Loop to Step: $R(t) = 0.01u_{-1}(t)$

For K = 3, $A[(6K+2)T_s] = .348$, and the state of the linear plant is $A_o = .005$, and $\dot{A}_o = +.739$, which leads to the 2-2 mode. This mode prevails for 80 periods, when the 3-3 mode appears. This mode persists for 50 periods, then 2-2 mode prevails for 50 periods. The average output has changed one unit in a hundred periods, giving the required average of .01. A plot of this is shown in Fig. A-3.

A.2.C Effects of Imperfect Integration

With imperfect integration in the linear plant, the integrator is replaced by a first order lag. In that case the linear plant in the forward path becomes

$$G_1(s) = \frac{1}{(\tau_1 s + 1)(\tau_2 s + 1)} \tag{A-41}$$

To show that a small input cannot be detected, a sequence with zero average and a small input will be assumed. The inequalities resulting from the output sequence will show the size of the input that cannot be detected.

Assume an input R = rD and test the 1-1 mode. Then

$$A(z) = \left(r - \frac{(1-z)^2}{1-z^2}\right)\left(\frac{1}{1-z} - \frac{\frac{1}{1-\tau_2/\tau_1}}{1-\alpha_1 z} - \frac{\frac{1}{1-\tau_1/\tau_2}}{1-\alpha_2 z}\right)$$
$$+\frac{\frac{A_o+\tau_2\dot{A}_o}{1-\tau_2/\tau_1}}{1-\alpha_1 z} + \frac{\frac{A_o+\tau_1\dot{A}_o}{1-\tau_1/\tau_2}}{1-\alpha_2 z} \tag{A-42}$$

where $\alpha_1 = e^{-\frac{T_s}{\tau_1}}$ and $\alpha_2 = e^{-\frac{T_s}{\tau_2}}$

If the postulated output sequence is to be sustained, A(z) must be of the form

$$A(z) = \frac{A_o + A_1 z}{1-z^2} \tag{A-43}$$

with

$$A_o > 0 \qquad A_1 < 0 \tag{A-44}$$

Again the $(1-\alpha z)$ factors must be eliminated from the denominator of Eq. (A-42). The constraints on the initial conditions which lead to that elimination are

$$A_o + \tau_2 \dot{A}_o = r + \frac{1-\alpha_1}{1+\alpha_1}$$

$$A_o + \tau_1 \dot{A}_o = r + \frac{1-\alpha_2}{1+\alpha_2} \tag{A-45}$$

With these conditions met, the output of the linear plant may be written as

$$(1-z^2)\, A(z) = \left(r + \frac{\tau_1 \frac{1-\alpha_1}{1+\alpha_1} - \tau_2 \frac{1-\alpha_2}{1+\alpha_2}}{\tau_1 - \tau_2} \right) + \left(r - \frac{\tau_1 \frac{1-\alpha_1}{1+\alpha_1} - \tau_2 \frac{1-\alpha_2}{1+\alpha_2}}{\tau_1 - \tau_2} \right) z \tag{a-46}$$

For the postulated mode to be sustained, the limits on r are

$$|r| < \left| \frac{\tau_1 \frac{1-\alpha_1}{1+\alpha_1} - \tau_2 \frac{1-\alpha_2}{1+\alpha_2}}{\tau_1 - \tau_2} \right| = |A_o| \quad r = 0 \tag{A-47}$$

Similar calculations show that the magnitude of input which cannot be detected is that which would, in the steady state, drive the sample of the linear plant output closest to zero just to zero. For design, the dead zone for each mode must be found and the largest used as a limit. As was seen in the response of the loop for a small input, each mode was present, and the largest dead zone would have stopped the output. As the above discussion shows, elastic restraint causes an

error in the output. The average position of the linear plant and the elastic restraint constant combine to give an average force on the linear plant which is subtracted from the input. Thus, the output indicates the integral of the difference between the input and the average elastic force.

A.3 Frequency Response

The describing function of the loop shown in Fig. A-1 will be generated, following the method outlined in Chapter II.

The input to the relay is assumed to be sinusoidal. In complex notation

$$A(t) = Ae^{j\omega t} \tag{A-48}$$

Consequently

$$C(t) = \frac{4}{\pi} e^{j\omega t} \tag{A-49}$$

The error signal is

$$E(t) = \frac{A}{G(j\omega)} e^{j\omega t} = \frac{A}{|G(j\omega)|} e^{j(\omega t - \underline{/G(j\omega)})} \tag{A-50}$$

The feedback signal is

$$B(t) = \frac{4}{\pi} \frac{\sin \frac{\omega T_s}{2}}{\frac{\omega T_s}{2}} e^{(j\omega t - \frac{\omega T_s}{2})} \tag{A-51}$$

The input is the sum of the error and the feedback signal:

$$R(T) = E(t) + B(t)$$

$$= \left(\frac{A}{|G(j\omega)|} e^{-j\underline{/G(j\omega)}} + \frac{4}{\pi} \frac{\sin \frac{\omega T_s}{2}}{\frac{\omega T_s}{2}} e^{-j\frac{\omega T_s}{2}} \right) e^{j\omega t} \tag{A-52}$$

The describing function is the ratio of output to input amplitude

$$\frac{C}{R}(\omega, R) = \frac{\frac{4}{\pi}}{\frac{A(R,\omega)}{|G(j\omega)|} e^{-j\underline{/G(j\omega)}} + \frac{4}{\pi} \frac{\sin \frac{\omega T_s}{2}}{\frac{\omega T_s}{2}} e^{j\frac{\omega T_s}{2}}} \tag{A-53}$$

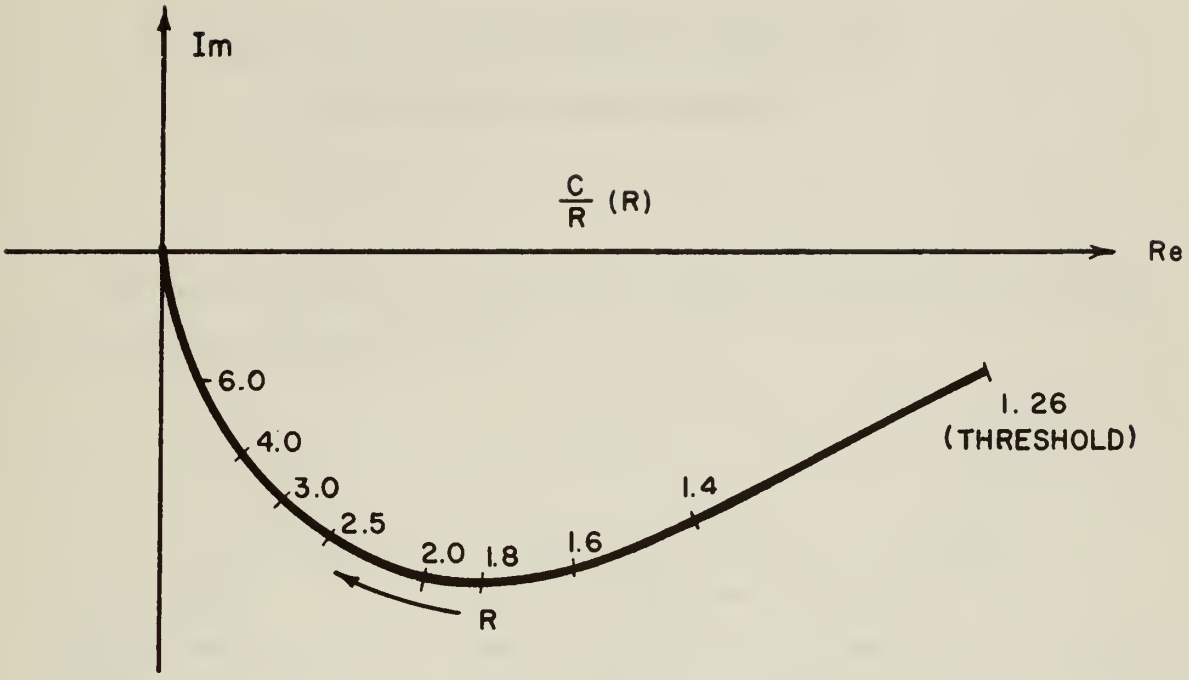

R	1.26	1.4	1.6	1.8	2.0	2.5	3.0	4.0	6.0
$\frac{C}{R}$	.995	.91	.79	.705	.635	.51	.425	.32	.215
$\frac{C}{R}$	-9^{o}	-26^{o}	-38^{o}	-46^{o}	-51^{o}	-60^{o}	-65^{o}	-70^{o}	-75^{o}

Fig. A-4 Low Frequency Describing Function of Loop

This function is frequency-independent at low frequencies if there is an integration in $G(j\omega)$. A polar plot of this function is shown in Fig. A-4.

APPENDIX B

ANALYSIS OF DELTA-MODULATED LOOP WITH THREE-LEVEL RELAY

The same system as in Appendix A will be analyzed, with a three-level relay as shown in Fig. B-1.

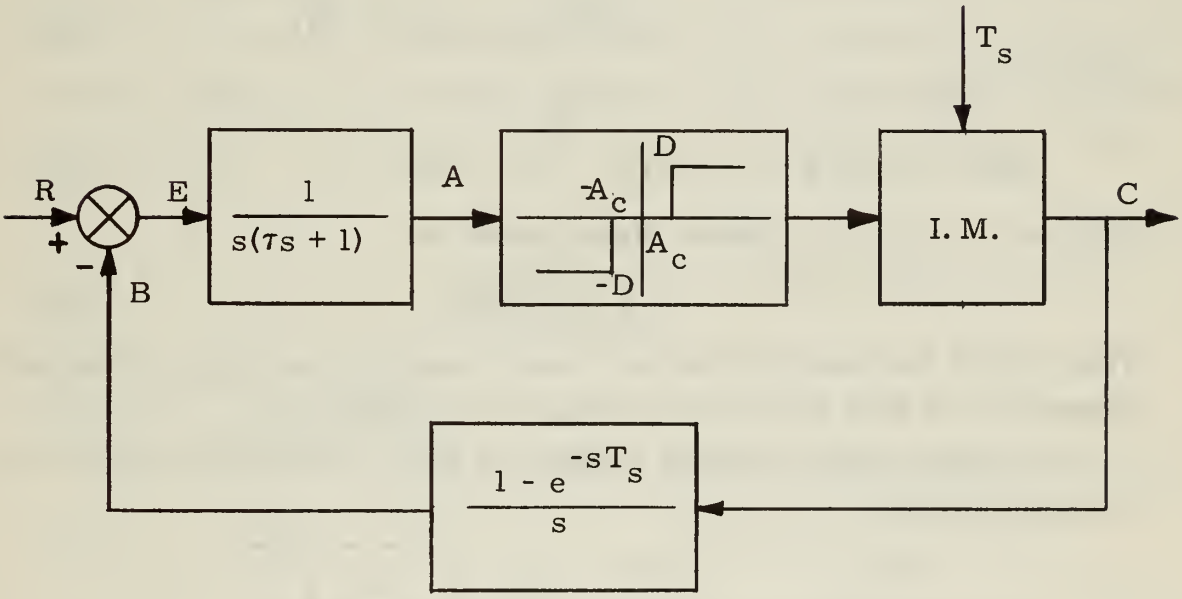

Fig. B-1 Delta-Modulated Loop to be Analyzed

B.1 Choice of Zero-Level Width

As explained in Chapter II, the zero level of the relay should be chosen to be as narrow as possible while eliminating the limit cycle. There are two aspects of limit cycle elimination to be considered: the low-energy region, handled by a transient analysis, and the high-energy

region, handled by a transient analysis, and the high-energy region, handled by a describing function analysis. Each analysis gives a lower limit on the zero level, and the larger is chosen as the size to be used.

The low-energy analysis assumes that the linear plant output is at the edge of the zero level with zero derivative, and that one clock pulse occurs to drive the plant back to null. The zero level is chosen wide enough so that in an infinite time the other edge of the zero level is not reached.

While the clock pulse is driving the plant toward null, the plant output is

$$A(t) = -Dt + A_c + \tau D(1-e^{-\frac{t}{\tau}}) \qquad \text{(B-1)}$$

At $t = T_s$

$$\dot{A}(T_s) = -D(1-e^{-\frac{T_s}{\tau}}) \qquad \text{(B-2)}$$

After $t = T_s$

$$A(t) = -DT_s + A_c + \tau D(1-e^{-\frac{T_s}{\tau}}) - \tau D(1-e^{-\frac{t}{\tau}}) \qquad \text{(B-3)}$$

if $A(\infty) > -A_c$, A_c must be chosen such that

$$A_c > \frac{1}{2} DT_s \qquad \text{(B-4)}$$

This will be the result of any low-energy analysis, no matter what the dynamics, as long as the plant contains one integration.

The high-energy analysis makes use of the describing function for the relay which is

$$N(A) = \frac{4D}{\pi A}\sqrt{1 - \left(\frac{A_c}{A}\right)^2} \qquad \text{(B-5)}$$

This has a maximum, and hence $\frac{1}{N}$ has a minimum at $A = \sqrt{2}A_c$ where

$$N(\sqrt{2}A_c) = \frac{2D}{\pi A_c} \qquad \text{(B-6)}$$

The size of the zero level is chosen so that there is no intersection of the $-\frac{1}{N}$ locus with the extended $G(j\omega)$ locus. The magnitude of the $G(j\omega)$ locus is critical for the 3-3 mode, the possible mode with the

largest amplitude. At that frequency

$$\left|G(j\frac{\omega_s}{6})\right| = \frac{1}{\left|j\frac{\omega_s}{6}(1 + j\frac{\omega_s}{6}\tau)\right|} = \frac{3T_s}{\left[1 + (\frac{\pi}{3}\frac{\tau}{T_s})^2\right]^{1/2}} \qquad (B\text{-}7)$$

Equating $|G(j\frac{\omega_s}{6})|$ and $\frac{1}{|N|}$ yields

$$A_c > \frac{1}{2} DT_s \left\{\frac{3}{\left[1 + (\frac{\pi}{3}\frac{\tau}{T_s})^2\right]^{1/2}}\right\} \qquad (B\text{-}8)$$

For slow systems ($\frac{T_s}{\tau} < 1$), this width for the zero level is smaller than the low-energy requirement, and for faster systems it is somewhat larger. However, the factor multiplying $\frac{1}{2}DT_s$ depends on the highest permissible mode. For the case being considered here ($T_s = \tau$) Eq. (B-8) becomes

$$A_c > \frac{1}{2} DT_s \ (2.08) = 1.04 \qquad (B\text{-}9)$$

Since this is larger than the size specified by Eq. (B-4), it will be taken as the size of A_c for this example.

B.2 Transient Response

B.2.a Impulse Response

The impulse response is again handled in a step-by-step transient manner, recognizing that an impulse input changes the derivate of the input instantaneously by the strength of the input.

For a numerical example, take the input impulse strength as 5.5 and assume zero initial conditions. At the end of one sampling period, the linear plant state is

$$A(T_s) = 5.5D\tau(1-e^{-\frac{T_s}{\tau}}) = 3.48$$

$$\dot{A}(T_s) = 5.5De^{-\frac{T_s}{\tau}} = 2.02 \qquad (B\text{-}10)$$

At this time the feedback signal appears; the linear plant output is

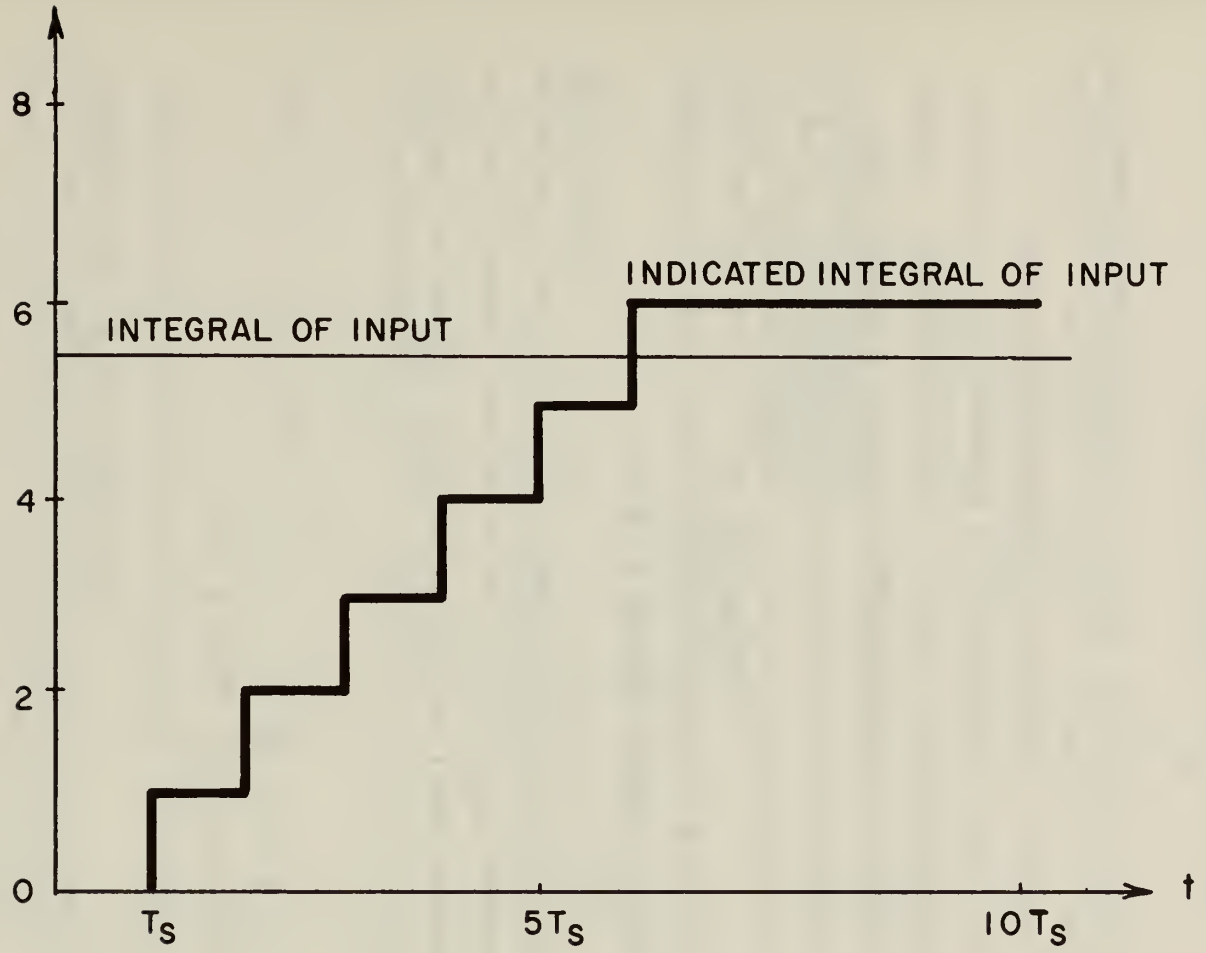

Fig. B-2 Response of Loop to Impulse: $R(t) = 5.5\delta(t)$

$$A(nT_s) = -DnT_s + 5.5D\tau(1-e^{-\frac{T_s}{\tau}}) + D\tau(5.5e^{-\frac{T_s}{\tau}} + 1)$$
$$(1-e^{-n\frac{T_s}{\tau}}) \qquad \text{(B-11)}$$

The feedback signal will cease when $A(nT_s) < A_c$ or n = 6 in this example. The state of the linear plant is then

$$A(6T_s) = .5$$
$$\dot{A}(6T_s) = -1 \qquad \text{(B-12)}$$

The plant continues under the influence of the remaining velocity, but no feedback signal:

$$A(t) = .5DT_s - \tau D(1-e^{-\frac{t}{\tau}})$$

and (B-13)

$$\dot{A}(\infty) = .5DT_s - \tau D = -.5$$

Thus no negative pulse is generated.

A plot of the loop's impulse response is shown in Fig. B-2.

B.2.B Step Response

The step response of the loop with a three-level relay is computed in much the same way as that of the loop with a two-level relay. The bounds to be determined in this case are the number of consecutive output pulses of the sign of the input permitted and the number of consecutive pulses of sign opposite to the input.

The first computation proceeds from the assumption that the linear plant output has travelled a full sampling period under the influence of the input alone at maximum velocity. This leads to initial conditions as the feedback signal appears

$$A_o = A_c + DrT_s$$
$$\dot{A}_o = Dr \qquad \text{(B-14)}$$

The linear plant output is then

$$A(nT_s) = -D(1-r)nT_s + A_c + DrT_s + \tau D(1-e^{-\frac{T_s}{\tau}}) \qquad \text{(B-15)}$$

The maximum number of output pulses of the same sign as the input

is that n for which $A(nT_s) \leq A_c$. If this is the case, then

$$r > \frac{n - \frac{\tau}{T_s}\left(1 - e^{-n\frac{T_s}{\tau}}\right)}{n+1} \qquad \text{(B-16)}$$

Substitution of various n into Eq. (B-16) yields Table B-1, which shows limits on r for a given maximum number of output pulses of the same sign as the input.

Table B-1
Limits on Size of Input, Given
Number of Consecutive Output Pulses
of Same Sign as Input

n	Range of r
1	$\|r\| > 0$
2	$\|r\| > .181$
3	$\|r\| > .378$
4	$\|r\| > .501$
5	$\|r\| > .604$
6	$\|r\| > .668$

The possibility of pulses of opposite sign from the input must be considered. If the feedback and input act in opposition for a full sampling period before switching occurs, the state of the linear plant is

$$A_o = A_c - D(1-r)T_s$$
$$\dot{A}_o = -D(1-r) \qquad \text{(B-17)}$$

Even for the smallest input, $A_o > -A_c$ so there will be no feedback signal initially. Thus the linear plant output is

$$A(nT_s) = DrnT_s + A_c - D(1-r)T_s - \tau D\left(1 - e^{-n\frac{T_s}{\tau}}\right) \qquad \text{(B-18)}$$

If ever $A(nT_s) < -A_c$, there will be a negative pulse; thus the expression

$$0 > r > \frac{1 + \frac{\tau}{T_s}\left(1 - e^{-n\frac{T_s}{\tau}}\right) - \frac{2A_c}{DT_s}}{n+1} \qquad \text{(B-19)}$$

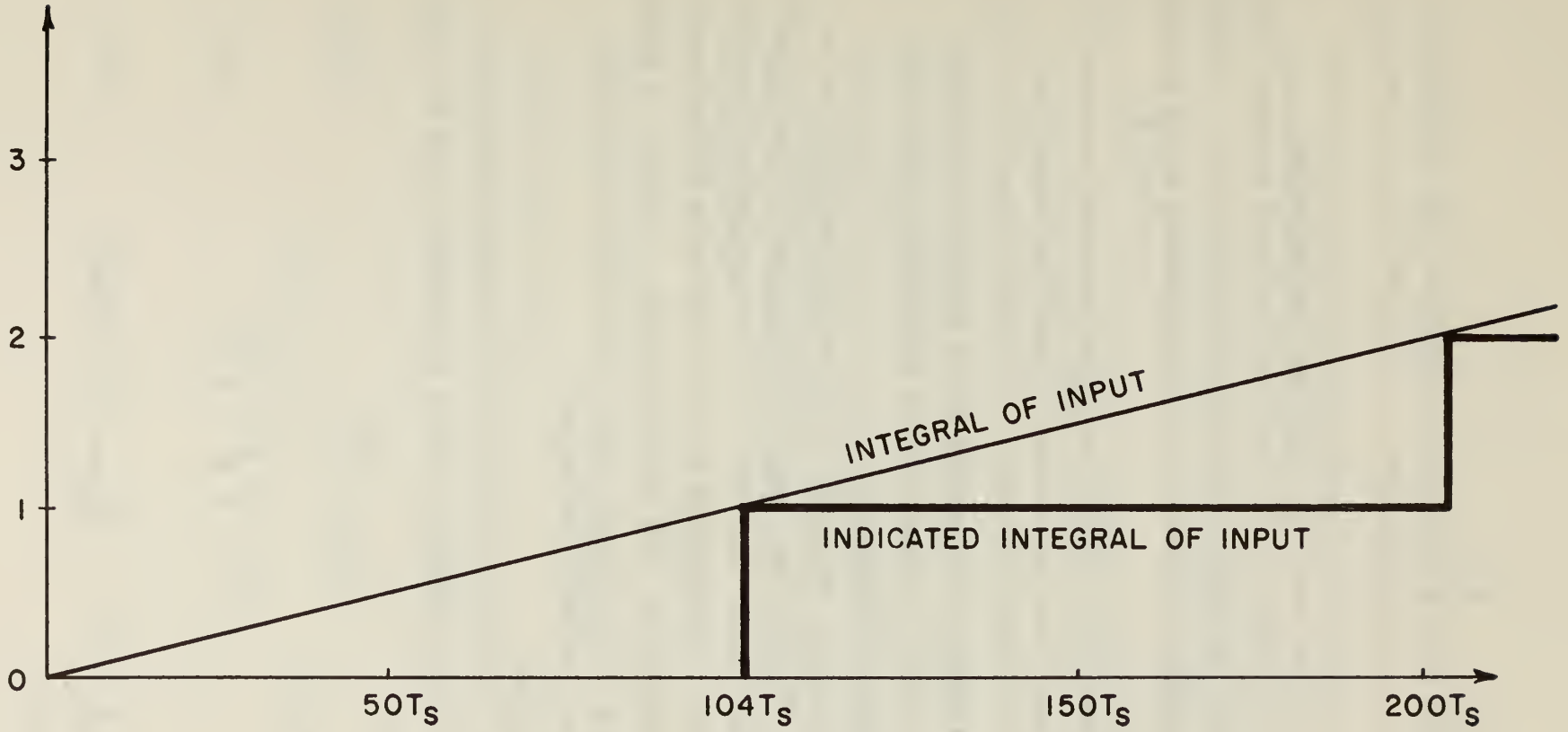

Fig. B-3 Response of Loop to Step: $R(t) = 0.0u_{-1}(t)$

is of interest. Clearly r has been assumed positive. For the present example, there can be no negative pulses for a positive input, and vice versa.

The output for an input step $R=\frac{1}{2}$ D will now be computed. According to Table B-1, there may be one, two, or three positive pulses, but not four. However, the only possible output sequences are 1, 1, 0, 0, and 2, 2, 0, 0. These may be verified in the same manner as the sequences tested in Appendix A.

For an input step of R = .01D, the only possible output sequence is 1, 99, 0, 0. That no more than one consecutive positive output pulse is possible is clear from Table B-1; thus, the above sequence alone is permitted. A short transient calculation shows that the first output pulse will occur at $t = 104T_s$, because of the width of the zero level.

B.2.C Effects of Imperfect Integration

As in the previous case, the effect of imperfect integration is to mask a small input. The limit on detectable inputs can be determined by comparing the steady-state response of the linear plant with the zero-level width of the relay. Inputs which cause steady-state displacement of the linear plant less than A_c will not be detected. Further, as before, an input corresponding to the average value of the linear plant output will be subtracted from the indicated output.

B.3 Frequency Response

As in Appendix A, a frequency dependent describing function may be calculated for the loop, beginning with an assumption about the relay input. Assume this is

$$A(t) = Ae^{j\omega t} \tag{B-20}$$

The output of the loop is

$$C(t) = \frac{4}{\pi}\sqrt{1 - \left(\frac{A_c}{A}\right)^2} \tag{B-21}$$

the error signal is

$$E(t) = \frac{A}{G(j\omega)}\, e^{j\omega t} = \frac{A}{|G(j\omega)|}\, e^{j(\omega t - \angle G(j\omega))} \tag{B-22}$$

and the feedback signal is

$$B(t) = \frac{4}{\pi}\sqrt{1 - \left(\frac{A_c}{A}\right)^2}\;\frac{\sin\frac{\omega T_s}{2}}{\frac{\omega T_s}{2}}\,e^{j\left(\omega t - \frac{\omega T_s}{2}\right)} \qquad \text{B-23)}$$

The input is the sum of the feedback and error signals, so that the describing function of the loop is

$$\frac{C}{R}(A,\omega) = \frac{\frac{4}{\pi}\sqrt{1 - \left(\frac{A_c}{A}\right)^2}}{\frac{A}{|G(j\omega)|}\,e^{-j\angle G(j\omega)} + \frac{4}{\pi}\sqrt{1 - \left(\frac{A_c}{A}\right)^2}\;\frac{\sin\frac{\omega T_s}{2}\,e^{-j\frac{\omega T_s}{2}}}{\frac{\omega T_s}{2}}} \qquad \text{(B-24)}$$

This may be plotted as a function of R for each frequency. Unlike the describing function for the loop with a two-level relay, this is not freqency independent for low frequencies.

Due to the zero level of the relay, there is a magnitude which R must attain, depending on frequency, before any output appears. It is required that

$$A = R|G(j\omega)| > A_c \qquad \text{(B-25)}$$

or

$$R > \frac{A_c}{|G(j\omega)|} \qquad \text{(B-26)}$$

for an output to occur.

APPENDIX C

ANALYSIS OF TRANSFORMATION COMPUTER

C.1 Roots of Characteristic Equation

The roots of the computer's characteristic equation for two different inputs will be determined using the root-locus method.

C.1.a Equal Rates on All Axes

In this case $\omega_1 = \omega_2 = \omega_3$, so $z_1 = z_2 = z_3 = z$. Eq. (5-27) becomes

$$1 + 3\Delta\theta^2 \frac{z}{(1 - z)^2} - \Delta\theta^3 \frac{z}{(1 - z)^2} = 0 \qquad \text{(C-1)}$$

As is shown in Fig. C-1 the roots of this equation remain on the unit circle. This indicates a non-decaying oscillatory behavior, as expected of direction cosines.

C.1.b Different Rates on Different Axes

Suppose that the angular velocities are $\omega_1 = 2\omega_2$, $\omega_3 = 0$. The difference equations are then

$$\begin{aligned}
C_{i1}(2n) &= C_{i1}(2n-1) - \Delta\theta C_{i3}(2n-1) \\
C_{i1}(2n+1) &= C_{i1}(2n) \\
C_{i2}(n) &= C_{i2}(n-1) + \Delta\theta C_{i3}(n-1) \\
C_{i3}(2n) &= C_{i3}(2n-1) + \Delta\theta C_{i1}(2n) - \Delta\theta C_{i2}(2n) \\
C_{i3}(2n+1) &= C_{i3}(2n) - \Delta\theta C_{i2}(2n+1) \qquad \text{(C-2)}
\end{aligned}$$

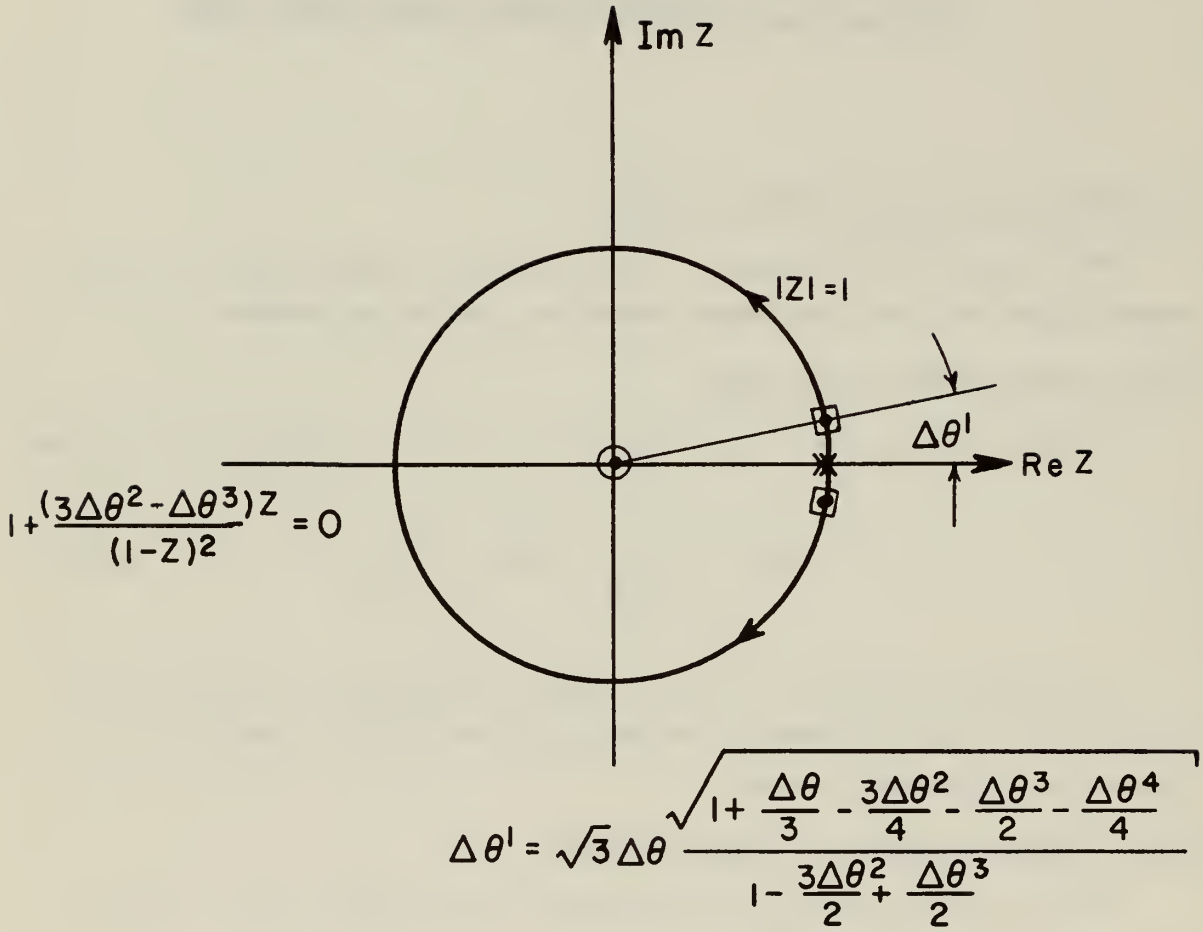

Fig. C-1 Root Locus For Equal Rates on all Axes

To transform these equations into the frequency domain, it is necessary to compute $\sum_{n=0}^{\infty} C_{i3}(2n)z^{2n}$, which is the transformed sequence of every other value of C_{i3}. This is the sequence which is fed into the C_{il} node (register).

$$\Sigma C_{i3}(2n)z^{2n} = \Sigma C_{i3}(n)z^{n} - \Sigma C_{i3}(2n+1)z^{2n+1}$$

$$= \Sigma C_{i3}(n)z^{n} - \Sigma C_{i3}(2n)z^{2n+1} + \Delta\theta C_{i2}(2n+1)z^{2n+1}$$

$$= \Sigma C_{i3}(n)z^{n} - z\Sigma C_{i3}(2n)z^{2n} + \Delta\theta\Sigma C_{i2}(2n)z^{2n+1} + \Delta\theta^{2}\Sigma C_{i3}(2n)z^{2n+1}$$

$$= \Sigma C_{i3}(n)z^{n} - z(1 - \Delta\theta^{2})\Sigma C_{i3}(2n)z^{2n} + \Delta\theta z\Sigma C_{i2}(2n)z^{2n} \qquad (C-3)$$

$$\Sigma C_{i2}(2n)z^{2n} = \Sigma C_{i2}(n)z^{n} - \Sigma C_{i2}(2n+1)z^{2n+1}$$

$$= \Sigma C_{i2}(n)z^{n} - \Sigma C_{i2}(2n)z^{2n+1} - \Delta\theta\Sigma C_{i3}(2n)z^{2n+1}$$

$$\Sigma C_{i2}(2n)z^{2n} = \frac{1}{1+z}\left(\Sigma C_{i2}(n)z^{n} - \Delta\theta z\Sigma C_{i3}(2n)z^{2n}\right) \qquad (C-4)$$

$$\Sigma C_{i3}(2n)z^{2n} = \Sigma C_{i3}(n)z^{n} - z\left[1 + \Delta\theta^{2}\left(1 + \frac{z}{1+z}\right)\right]\Sigma C_{i3}(2n)z^{2n} + \frac{\Delta\theta z}{1+z}\Sigma C_{i2}(n)z^{n}$$

$$\Sigma C_{i3}(2n)z^{2n} = \frac{\Sigma C_{i3}(n)z^{n} + \frac{\Delta\theta z}{1+z}\Sigma C_{i2}(n)z^{n}}{\left(1 + z\left[1 + \Delta\theta^{2}\left(1 + \frac{z}{1+z}\right)\right]\right)} \qquad (C-5)$$

In z-transform theory, the z-transform of a function is defined as $C_{ij}(z) = \sum_{n=0}^{\infty} C_{ij}(n)z^{n}$ (Ref. 61, Ch. 1). Let $C'_{ij}(z) = \sum_{n=0}^{\infty} C_{ij}(2n)z^{2n}$. Then Eq. (C-5) may be written

$$C'_{i3}(z) = \frac{C_{i3}(z) - \frac{\Delta\theta z}{1+z} C_{i2}(z)}{\left(1+z\right)\left(1+\Delta\theta^2\left[1+\frac{z}{1+z}\right]\right)} \tag{C-6}$$

From the difference equations are obtained the relations

$$C'_{il}(z) = \frac{1}{1+z} C_{il}(z) \tag{C-7}$$

$$C_{il}(z) = -\frac{\Delta\theta z}{1-z} C'_{i3}(z) \tag{C-8}$$

$$C_{i2}(z) = \frac{\Delta\theta z}{1-z} C_{i3}(z) \tag{C-9}$$

$$C_{i3}(z) = \frac{\Delta\theta}{1-z} C_{i2}(z) - \frac{\Delta\theta}{1-z} C'_{il}(z) \tag{C-10}$$

Combining Eqs. (C-6) through (C-10) gives the characteristic equation for the computer:

$$1 + \frac{\Delta\theta^2 z}{(1-z)^2} + \frac{\Delta\theta^2 z\left(1 - \frac{\Delta\theta^2 z^2}{1-z^2}\right)}{(1-z)^2(1+z)\left[1+z\left(1+\Delta\theta^2\left[1+\frac{z}{1+z}\right]\right)\right]} = 0 \tag{C-11}$$

Fig. C-2 shows the root-locus diagrams used to find the singularities of Eq. (C-11). There are four important zeros of this equation, marked with squares in Fig. C-2(b). The pair of roots near unity represent the dominant mode of the system. The pair near -1 are oscillatory with magnitude $1 - \frac{\Delta\theta}{2}$. This gives rise to a time sequence $(1 - \frac{\Delta\theta}{2})^{-n}$. Since the magnitude of the mode is $O(\Delta\theta)$ the pair of roots gives rise to an error growing as $n\Delta\theta^2$. This leads to an increment of error in about one revolution.

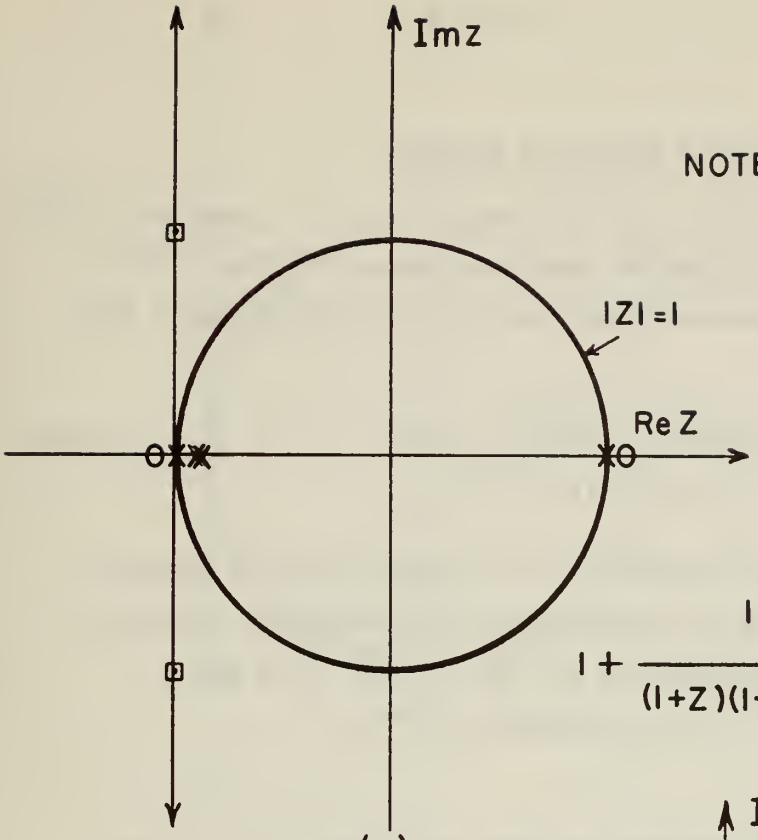

NOTE: DISTANCES OF SINGULARITIES FROM +1 AND −1 ARE $O(\Delta\theta^2)$.

$$1+\frac{1-\frac{\Delta\theta^2 Z^2}{1-Z^2}}{(1+Z)(1+Z\left[1+\Delta\theta^2(1+\frac{Z}{1+Z})\right])}=0$$

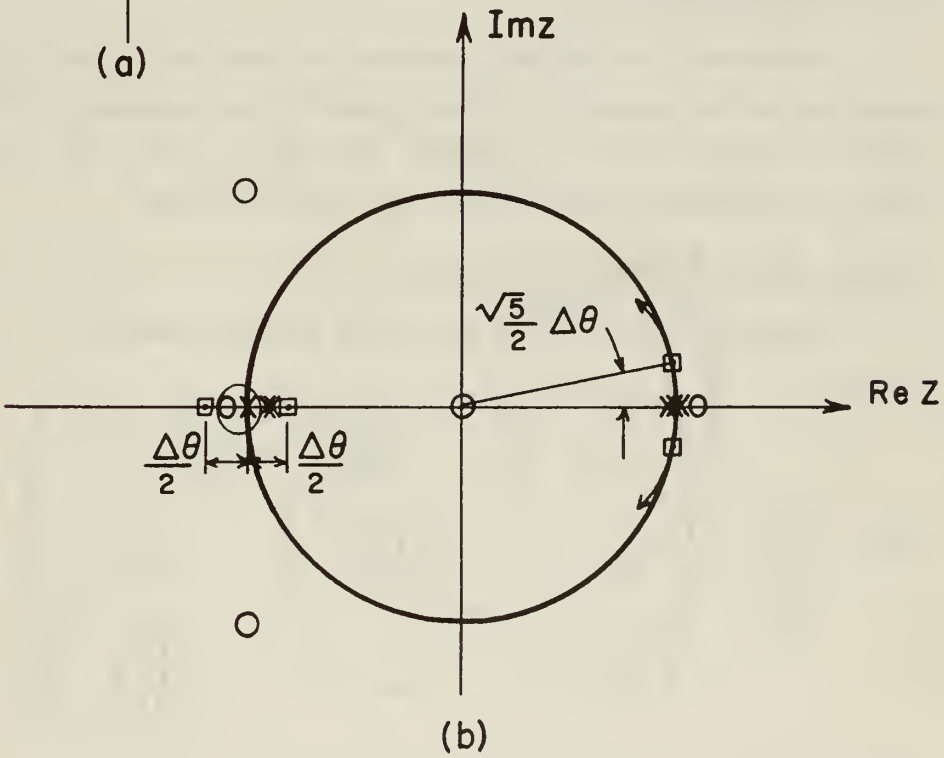

$$1+\frac{\Delta\theta^2 Z}{(1-Z)^2}\left(1+\frac{1-\frac{\Delta\theta^2 Z^2}{1-Z^2}}{(1+Z)(1+Z\left[1+\Delta\theta^2\left[1+\frac{Z}{1+Z}\right]\right])}\right)=0$$

Fig. C-2 Exact Root Locus for $\omega_1=2\omega_2, \omega_3=0$

C.1.c Approximate Analysis of Multirate System

For $\omega_1 = 2\omega_2$, $\omega_3 = 0$, Eq. (5-22) shows k = 1, $\ell = 2$, and Eq. (5-23) shows $z_1^2 = z_2 = z^2$. Substitution of these relations into Eq. (5-25) yields Eq. (5-21). The characteristic equation corresponding to this set is

$$1 + \frac{\Delta\theta^2 z}{(1-z)^2} + \frac{\Delta\theta^2 z}{(1-z^2)^2} = 0 \qquad \text{(C-12)}$$

Comparison of this equation with Eq. (C-11) shows that it is approximately correct. The root locus diagram for this equation, shown in Fig. C-3, is practically the same as for Eq. (C-11). The extra dipoles appearing in Fig. C-2 have negligible effect.

C.2 Truncation Error

Following the method outlined in Chapter V, Sec. 5.D.3, an analysis of the truncation error made by the computer will be made, first for equal rates on all axes, then for $\omega_1 = 2\omega_2$, $\omega_3 = 0$. In each case, the initial condition C(0) = I, will be used.

C.2.a Equal Rates on All Axes

The exact solution to Eq. (5-1) in this case is

$$C(s) = \frac{1/s}{\frac{s^2}{3\omega^2}+1} \begin{pmatrix} \frac{1}{3}\left(\frac{s^2}{\omega^2}+1\right) & -\frac{s}{3\omega}+\frac{1}{3} & \frac{s}{3\omega}+\frac{1}{3} \\ +\frac{s}{3\omega}+\frac{1}{3} & \frac{1}{3}\left(\frac{s^2}{\omega^2}+1\right) & -\frac{s}{3\omega}+\frac{1}{3} \\ -\frac{s}{3\omega}+\frac{1}{3} & \frac{s}{3\omega}+\frac{1}{3} & \frac{1}{3}\left(\frac{s^2}{\omega^2}+1\right) \end{pmatrix} \qquad \text{(C-13)}$$

The time solution is then

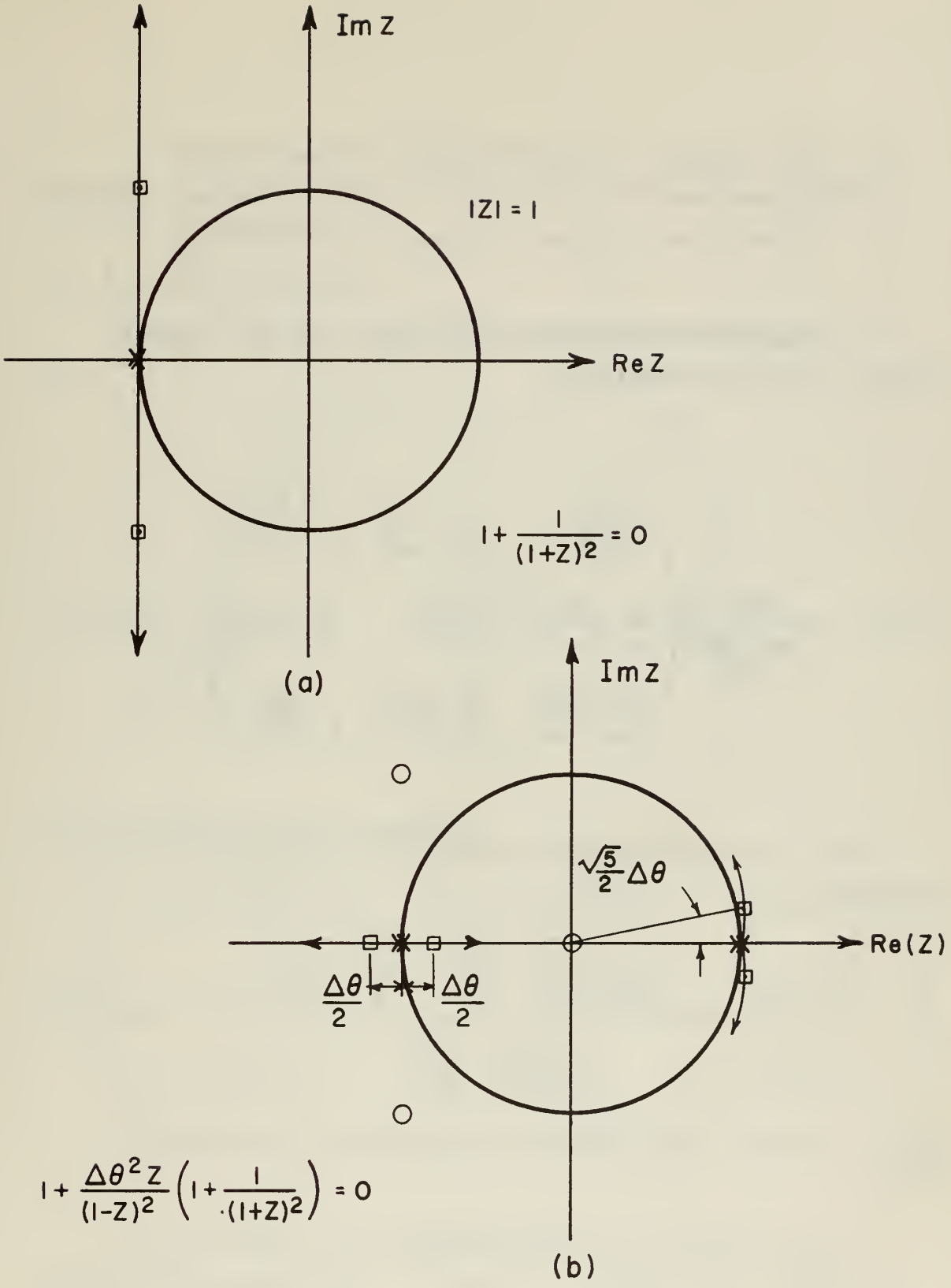

Fig. C-3 Approximate Root Locus for $\omega_1 = 2\omega_2, \omega_3 = 0$

$$C(t) = \frac{1}{3}\begin{pmatrix} 1 + 2\cos\sqrt{3}\,\omega t & 1 - \cos\sqrt{3}\,\omega t - \sqrt{3}\sin\sqrt{3}\,\omega t & 1 - \cos\sqrt{3}\,\omega t + \sqrt{3}\sin\sqrt{3}\,\omega t \\ 1 - \cos\sqrt{3}\,\omega t + \sqrt{3}\sin\omega t & 1 + 2\cos\sqrt{3}\,\omega t & 1 - \cos\sqrt{3}\,\omega t - \sqrt{3}\sin\sqrt{3}\,\omega t \\ 1 - \cos\sqrt{3}\,\omega t - \sqrt{3}\sin\omega t & 1 - \cos\sqrt{3}\,\omega t + \sqrt{3}\sin\sqrt{3}\,\omega t & 1 + 2\cos\sqrt{3}\,\omega t \end{pmatrix} \qquad \text{(C-14)}$$

According to the flow graph shown in Fig. 5-4, the computer solution, without quantization is

$$C(z) = \frac{\frac{1}{(1-z)}}{1 + \frac{(3\Delta\theta^2 + \Delta\theta^3)z}{(1-z)^2}} \begin{pmatrix} 1 + \frac{\Delta\theta^2 z}{(1-z)^2} & -\frac{\Delta\theta}{1-z} + \frac{\Delta\theta^2 z}{(1-z)^2} & \frac{\Delta\theta}{1-z} + \frac{\Delta\theta^2}{(1-z)^2} \\ \frac{\Delta\theta z}{1-z} + \frac{\Delta\theta^2 z}{(1-z)^2} & 1 + \frac{\Delta\theta^2 z}{(1-z)^2} & -\frac{\Delta\theta}{1-z} + \frac{\Delta\theta^2}{(1-z)^2} \\ -\frac{\Delta\theta z}{1-z} + \frac{\Delta\theta^2 z^2}{(1-z)^2} & \frac{\Delta\theta z}{1-z} + \frac{\Delta\theta^2 z}{(1-z)^2} & 1 + \frac{\Delta\theta^2 z}{(1-z)^2} \end{pmatrix} \qquad \text{(C-15)}$$

The normal modes of this determinant have unit magnitude and argument

$$\Delta\theta' = \sqrt{3}\Delta\theta \frac{\sqrt{1 + \frac{\Delta\theta}{3} - \frac{3\Delta\theta^2}{4} - \frac{\Delta\theta^3}{2} - \frac{\Delta\theta^4}{4}}}{1 - \frac{3\Delta\theta^2}{2} - \frac{\Delta\theta^3}{4}} \qquad \text{(C-16)}$$

Thus the sequence corresponding to Eq. (C-15) is approximately

$$C(n) = \frac{1 - \frac{\Delta\theta}{3}}{3}\begin{pmatrix} 1 + 2\cos n\,\Delta\theta' & 1 - \cos n\,\Delta\theta' - \sqrt{3}\sin n\,\Delta\theta' & 1 - \cos n\,\Delta\theta' + \sqrt{3}\sin n\,\Delta\theta' \\ 1 - \cos n\,\Delta\theta' + \sqrt{3}\sin n\,\Delta\theta' & 1 + 2\cos n\,\Delta\theta' & 1 - \cos n\,\Delta\theta' - \sqrt{3}\sin n\,\Delta\theta' \\ 1 - \cos n\,\Delta\theta' - \sqrt{3}\sin n\,\Delta\theta' & 1 - \cos n\,\Delta\theta' + \sqrt{3}\sin n\,\Delta\theta' & 1 + 2\cos n\,\Delta\theta' \end{pmatrix} \qquad \text{(C-17)}$$

The truncation error arises in this case from the fact that the argument of the roots near +1 is not quite correct. This leads to an error which grows as $n\Delta\theta^2$.

C.2.b Multirate Systems

With $\omega_1 = 2\omega_2$, $\omega_3 = 0$ and $C(0) = I$, the exact solution to Eq. (5-1) is

$$C(s) = \frac{1/s}{\frac{s^2}{\frac{5}{4}\omega^2} + 1} \begin{pmatrix} \frac{s^2 + \omega^2}{\frac{5}{4}\omega^2} & .4 & \frac{.4s}{\omega} \\ .4 & \frac{s^2 + \frac{\omega^2}{4}}{\frac{5}{4}\omega^2} & -.8\frac{s}{\omega} \\ -.4\frac{s}{\omega} & .8\frac{s}{\omega} & 1 \end{pmatrix} \qquad \text{(C-18)}$$

The corresponding time solution is

$$C(t) = \begin{pmatrix} \frac{1}{5}(4 + \cos\frac{\sqrt{5}}{2}\omega t) & \frac{2}{5}(1 - \cos\frac{\sqrt{5}}{2}\omega t) & -\frac{1}{\sqrt{5}}\sin\frac{\sqrt{5}}{2}\omega t \\ \frac{2}{5}(1 - \cos\frac{\sqrt{5}}{2}\omega t) & \frac{1}{5}(1 + 4\cos\frac{\sqrt{5}}{2}\omega t) & \frac{2}{\sqrt{5}}\sin\frac{\sqrt{5}}{2}\omega t \\ \frac{1}{\sqrt{5}}\sin\frac{\sqrt{5}}{2}\omega t & -\frac{2}{\sqrt{5}}\sin\frac{\sqrt{5}}{2}\omega t & \cos\frac{\sqrt{5}}{2}\omega t \end{pmatrix}$$

(C-19)

Under the same conditions the model of the computer is as shown in Fig. C-4.

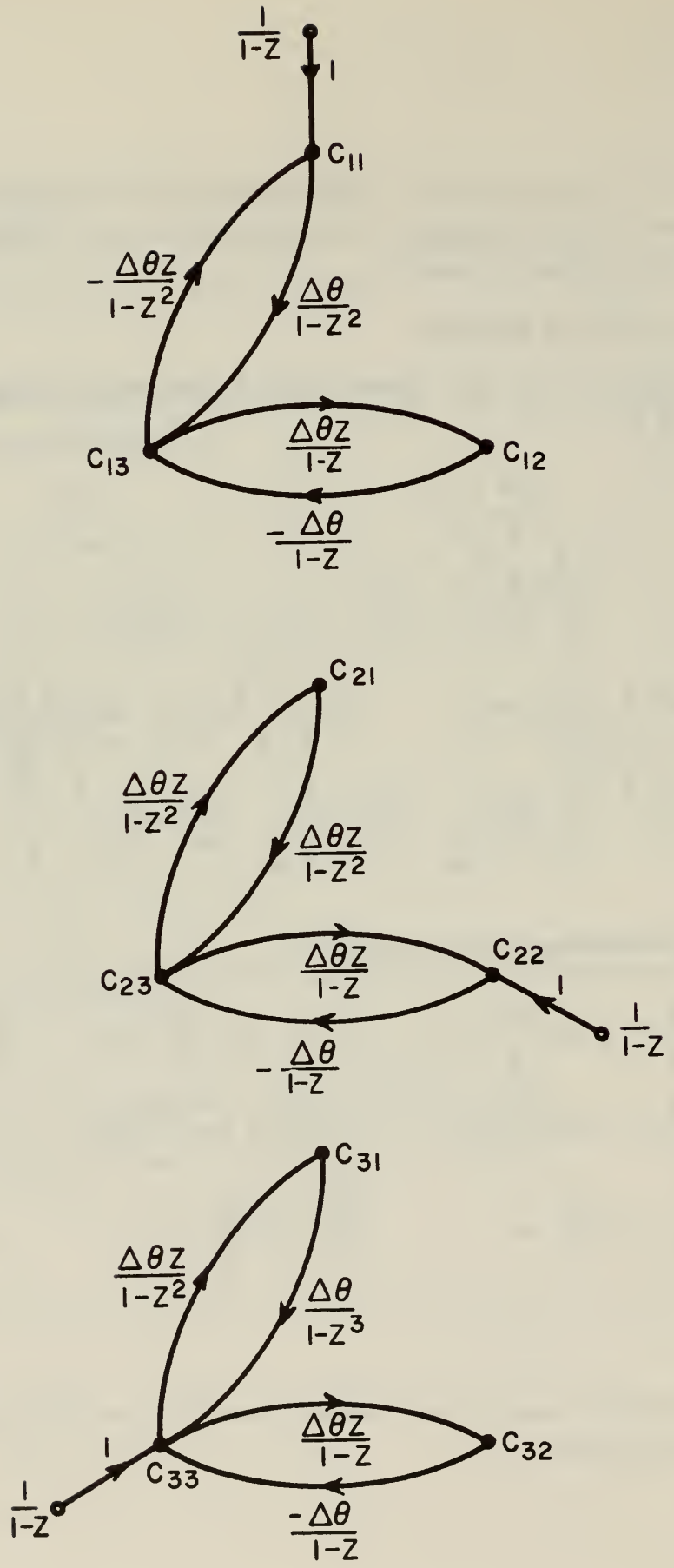

Fig. C-4 Computer Model for $\omega_1=2\omega_2, \omega_3=0$; C(0)=I

$$C(z) = \frac{\frac{1}{1-z}}{1 + \frac{\Delta\theta^2 z}{(1-z)^2} + \frac{\Delta\theta^2 z}{(1-z^2)^2}} \begin{pmatrix} 1 + \frac{\Delta\theta^2 z}{(1-z)^2} & \frac{\Delta\theta^2 z}{(1-z)(1-z^2)} & \frac{\Delta\theta}{1-z^2} \\ \frac{\Delta\theta^2 z}{(1-z)(1-z^2)} & 1 + \frac{\Delta\theta^2 z}{(1-z^2)^2} & -\frac{\Delta\theta}{(1-z)} \\ -\frac{\Delta\theta z}{1-z^2} & \frac{\Delta\theta z}{1-z} & 1 \end{pmatrix} \qquad \text{(C-20)}$$

There are essentially two parts to the time solution of Eq. (C-20). The first, desired part of the solution arises from the roots near +1. The roots near -1 give rise to extraneous, unstable terms. The roots near +1 have magnitude $1 + \frac{1}{8}\Delta\theta^2$, and argument $\Delta\theta' = \frac{\sqrt{5}}{2}\Delta\theta$. The time sequence represented by Eq. (C-20) is approximately

$$C(n) = \left(1 - n\frac{\Delta\theta^2}{8}\right) \begin{pmatrix} \frac{1}{5}(4 + \cos n\Delta\theta') & \frac{2}{5}(1 - \cos n\Delta\theta') & -\frac{1}{\sqrt{5}}\sin n\Delta\theta' \\ \frac{2}{5}(1 - \cos n\Delta\theta') & \frac{1}{5}(1 + 4\cos n\Delta\theta') & \frac{2}{\sqrt{5}}\sin n\Delta\theta' \\ \frac{1}{\sqrt{5}}\sin n\Delta\theta') & -\frac{2}{\sqrt{5}}\sin n\Delta\theta' & \cos n\Delta\theta' \end{pmatrix}$$

$$+n\Delta\theta^2 \begin{pmatrix} \frac{1}{4} & 0 & \frac{1}{2} \\ 0 & 0 & \frac{1}{2} \\ \frac{1}{2} & \frac{1}{2} & \frac{1}{4} \end{pmatrix} - \begin{pmatrix} 0 & \frac{\Delta\theta^2}{8} & 0 \\ \frac{\Delta\theta^2}{8} & \frac{\Delta\theta^2}{8} & 0 \\ 0 & 0 & 0 \end{pmatrix} \qquad \text{(C-21)}$$

Again, an estimate of the truncation error may be had by comparing Eq. (C-21) and Eq. (C-14). The error arises from the presence

of the poles near -1, and the fact that the roots near +1 are not on the unit circle. The truncation error grows as $n\Delta\theta^2$ in each direction cosine. It should be noted that the approximations made in the analysis preclude taking Eq. (C-21) as the exact computer solution.

C.3 Quantization Error

The power spectral density of quantization may be calculated following the procedure indicated in Chapter V, Sec. 5.D.4. However, perhaps a better indication of the error due to quantization is the mean-squared signal appearing at any node due to quantization noise. This will be done for the case of $\omega_1 = 2\omega_2$, $\omega_3 = 0$, using both hysteretic and non-hysteretic quantizers.

C.3.a Non-Hysteretic Quantization

The model to be analyzed is shown in Fig. C-5. The expression for power spectral density at each node is:

$$\Phi_{11} = \left| \frac{1 + \frac{\Delta\theta^2 z}{(1-z)^2} + \frac{\Delta\theta^2 z}{(1-z^2)(1-z)} - \frac{\Delta\theta z}{1-z^2}}{1 + \frac{\Delta\theta^2 z}{(1-z)^2} + \frac{\Delta\theta^2 z}{(1-z^2)^2}} \right|^2 \frac{\Delta\theta^2}{12}$$

$$\Phi_{22} = \left| \frac{1 + \frac{\Delta\theta^2 z}{(1-z^2)^2} + \frac{\Delta\theta^2 z}{(1-z^2)(1-z)} + \frac{\Delta\theta z}{1-z}}{1 + \frac{\Delta\theta^2 z}{(1-z)^2} + \frac{\Delta\theta^2 z}{(1-z^2)^2}} \right|^2 \frac{\Delta\theta^2}{12} \qquad \text{(C-23)}$$

$$\Phi_{33} = \left| \frac{1 + \frac{\Delta\theta z}{1-z^2} - \frac{\Delta\theta}{1-z}}{1 + \frac{\Delta\theta^2 z}{(1-z)^2} + \frac{\Delta\theta^2 z}{(1-z^2)^2}} \right|^2 \frac{\Delta\theta^2}{12}$$

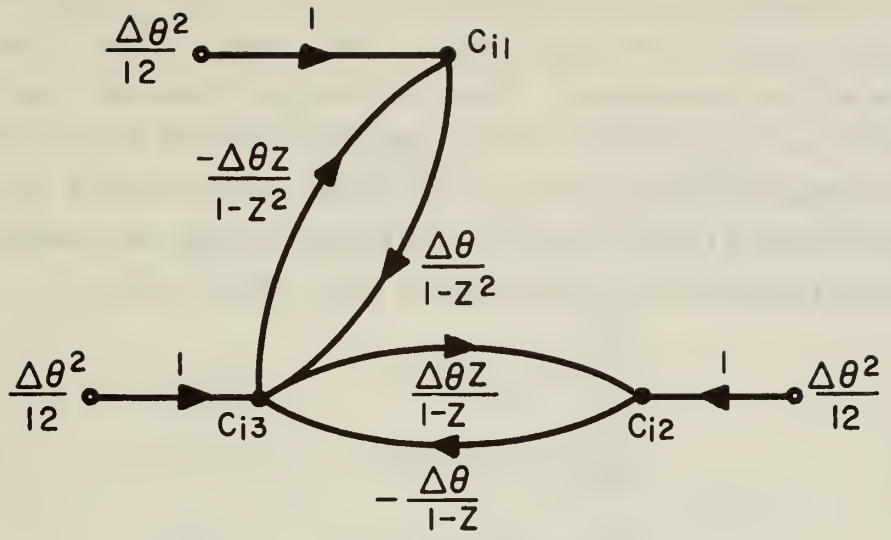

Fig. C-5 Computer Model with Non-Hysteretic Quantization

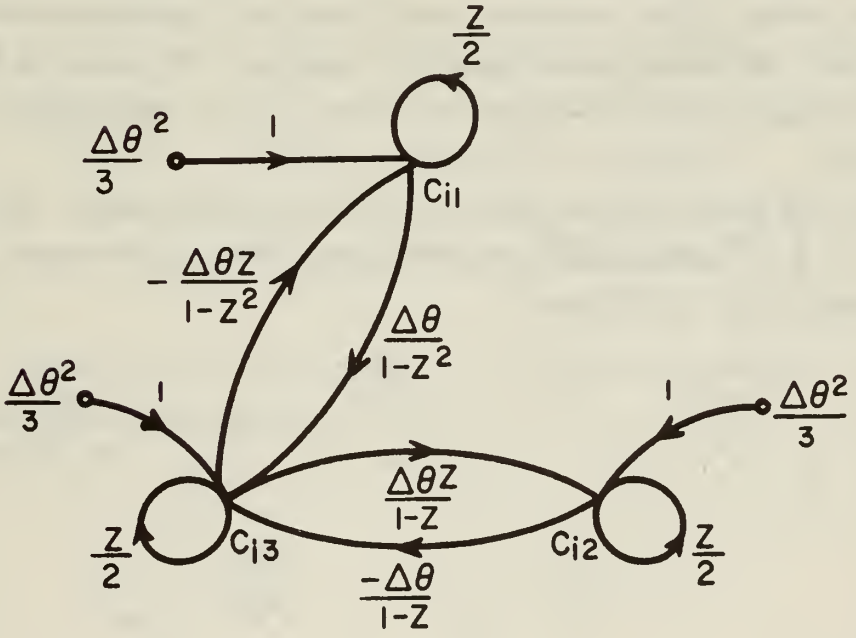

Fig. C-6 Computer Model with Hysteretic Quantization

Since the magnitudes of the roots are very close to unity, the mean square value will be very large. Thus, only n terms in the sum of squares will be considered. Note that the contributions from the roots near +1 are oscillatory, so that the mean square may be taken as half the amplitude squared. Let $\overline{q_{ij}^2}$ be the mean squared value of quantization noise at the ij^{th} node. Carrying through the computations indicated above gives for mean squared value after n steps

$$\overline{q_{ii}^2}(n) = .096\, n\Delta\theta^4$$

$$\overline{q_{i2}^2}(n) = 1.2\, n\Delta\theta^4 \qquad \text{(C-24)}$$

$$\overline{q_{i3}^2}(n) = .0188\, n\Delta\theta^4$$

The rms quantization noise at any node, then, is on the order of $\sqrt{n}\Delta\theta^2$.

C.3.b Hysteretic Quantization

The model of the computer with hysteretic quantization is shown in Fig. C-6. Note the power spectral density of the noise is four times as great as the non-hysteretic noise, due to the larger quantization box.

The self loops may be absorbed into the other paths, giving a factor $1/(1-\frac{1}{2}z)$ multiplying each path gain. The expressions corresponding to Eq. (C-23) are:

$$\Phi_{11} = \left| \frac{1 + \dfrac{\Delta\theta^2 z}{(1-z)^2(1-\frac{1}{2}z)^2} + \dfrac{\Delta\theta^2 z}{(1-z^2)(1-z)(1-\frac{1}{2}z)^2} - \dfrac{\Delta\theta z}{(1-z^2)(1-\frac{1}{2}z)}}{1 + \dfrac{\Delta\theta^2 z}{(1-z)^2(1-\frac{1}{2}z)^2} + \dfrac{\Delta\theta^2 z}{(1-z^2)^2(1-\frac{1}{2}z)^2}} \right|^2 \frac{\Delta\theta^2}{3}$$

$$\Phi_{22} = \left| \frac{1 + \frac{\Delta\theta^2 z}{(1 - z^2)^2 (1 - \frac{1}{2}z)^2} + \frac{\Delta\theta^2 z}{(1 - z^2)(1 - z)(1 - \frac{1}{2}z)} + \frac{\Delta\theta z}{(1 - z)(1 - \frac{1}{2}z)}}{1 + \frac{\Delta\theta^2 z}{(1 - z)^2 (1 - \frac{1}{2}z)^2} + \frac{\Delta\theta^2 z}{(1 - z^2)^2 (1 - \frac{1}{2}z)^2}} \right|^2 \frac{\Delta\theta^2}{3}$$

$$\Phi_{33} = \left| \frac{1 + \frac{\Delta\theta z}{(1 - z^2)(1 - \frac{1}{2}z)} - \frac{\Delta\theta}{(1 - z)(1 - \frac{1}{2}z)}}{1 + \frac{\Delta\theta^2 z}{(1 - z)^2 (1 - \frac{1}{2}z)^2} + \frac{\Delta\theta^2 z}{(1 - z^2)^2 (1 - \frac{1}{2}z)^2}} \right|^2 \frac{\Delta\theta^2}{3} \qquad \text{(C-25)}$$

Performing a sum-of-squares computation similar to the above gives:

$$\overline{q_{i1}^2}(n) = .384\, n\Delta\theta^4 + 1.07\, \Delta\theta^4$$

$$\overline{q_{i2}^2}(n) = 4.8\, n\Delta\theta^4 + 5.23\, \Delta\theta^4$$

$$\overline{q_{i3}^2}(n) = .0752\, n\Delta\theta^4 + .158\, \Delta\theta^4 \qquad \text{(C-26)}$$

The rms error is a factor of two higher than before, and a constant has been added.

ANNOTATED LIST OF REFERENCES

A. Delta-Modulated Loops

1. A. R. Bergen, "Discussion", following Tomg and Meserve's paper (Ref. 19), IRE Transactions on Automatic Control, Sept., 1960, 304.

   Verifies moding of delta-modulated loop using z-transforms. Introduces initial conditions of modes. $z = e^{sT_s}$

2. Frank K. Bowers, "What Use is Delta Modulation to the Transmission Engineer?" Trans AIEE, LXXVI (1957), 142-153.

   General discussion of delta modulation from transmission point of view. Discusses saturation.

3. C.K. Chow, "Contactor Servomechanisms Employing Sampled Data", Trans AIEE Part II, LXXIII (1954), 51-64.

   First published paper using idea of variable delay due to sampling. Works with polar Nyquist diagrams.

4. Andrew R. Cohen, A Design of a Practical Digital Accelerometer, M.S. Thesis, M.I.T. (MIT/IL Rpt. T-200) June, 1958.

5. F. de Jager, "Delta Modulation, A Method of PCM Transmission Using the 1-unit Code", Phillips Res. Rpt. VII (1952), 442-466.

   Detailed discussion of delta modulation from transmission point of view, with one and two integrators in feedback path.

6. Edmonde -Maurice Deloraine, Stanislas von Miers, et Boris Derjavitch, Invention, Brevet d'Invention, Gr. 12-Ct. 4, No. 932140, "Méthode et système de transmission par impulsions." Demandé le 10 août 1946 à Paris, République Française, Ministre de l'Industrie et

du Commerce, Service de la Propriété Industrielle.

French patent of delta modulation with circuit diagrams and waveforms.

7. Robert Hayum, Compensation of a Digital Integrating Accelerometer, M.S. Thesis, M.I.T. (MIT/IL Rpt. T-209A) June, 1959.

Compensation is accomplished by using torque generator microsyn as torquer and sensor.

8. Patrick B. Hutchings, Compensation of a Sampled Data Contactor Servo, M.S. Thesis, M.I.T. (MIT/IL Rpt. T-222) May, 1959.

First attempt to handle inputs. Heuristic discussion provides good insights.

9. K. Izawa and L.A. Weaver, "Relay-type Feedback Control Systems with Dead Time and Sampling," Trans AIEE, Part II, LXXVIII (1959), 49-53.

Phase plane analysis of delta-modulated loops with dead time. Attempts to determine modes.

10. Rudolph E. Kalman, Phase Plane Analysis of Non-Linear Sampled Data Systems, M.S. Thesis, M.I.T., 1954.

Essentially a computer study of a delta-modulated loop, with emphasis on stability in the large.

11. F.J. Mullin and E.I. Jury, "A Phase Plane Approach to Relay Sampled Data Feedback Systems," Trans AIEE Part II, LXXVIII (1959), 517-523.

Phase plane analysis with a nice method for reintroducing time into computation.

12. J.J. Rocchio, Jr., Analysis of a Digital Integrating Pendulous Accelerometer, M.S. Thesis, M.I.T. (MIT/IL Rpt. T-176) June, 1958.

13. Frederick A. Russell, Design Criterion for Stability of Sampled Data On-Off Servomechanisms, Ph.D. Thesis, Columbia University, June, 1953.

Like Chow (Ref. 3), Russell introduces variable delay due to sampling. Uses Bode plots.

14. J.F. Schouten, F. de Jager, and J.A. Greifkes, "Delta Modulation, A New Communications System for Telecommunications" Phillips Tech. Rev., XIII 7 (1952), 237-268.

Discussion of delta modulation and its application to transmission.

15. Stuart C. Schwartz, Analysis of Sampled Data Relay Servomechanisms with Zero and Step Inputs, M.S. Thesis, M.I.T. (MIT/IL Rpt. T-284), May, 1961.

First use of Bergen's method to verify modes of delta-modulated loops. Application of this technique to verify step input behavior.

16. Joseph J. Sliwkowski, A Study of a Delta Modulator, M.S. Thesis, M.I.T. (MIT/IL Rpt. T-287), May, 1961.

Analysis from a transmission point of view. Describing function for amplitude only derived.

17. Richard D. Smallwood, A Pulse Restrained Accelerometer, M.S. Thesis, M.I.T. (MIT/IL Rpt. T-174) June, 1958.

18. Calvin M. Theiss, "The Theory and Analysis of á Digital Accelerometer," Unpublished Ms., 10 January 1961.

Time domain analysis of delta-modulated loop.

19. H.C. Tørng and W.E. Meserve, "Determination of Periodic Modes in Relay Servomechanisms Employing Sampled Data," IRE Transactions on Automatic Control, September, 1960, 298-305.

Uses difference equations to verify moding of loop.

20. Robert B. Meeks, Jr. and Eugene R. Wells Jr, Feasibility of Using a Ternary Mode for Pulse Torquing a Pendulous Accelerometer, M.S. Thesis, M.I.T. (MIT/IL Rpt. T-278), May, 1961.

First discussion of ternary torquing, but limit cycles not eliminated. Discussion of logical compensation.

B. Inertial Instruments

21. Charles S. Draper, Walter Wrigley, and Lester R. Grohe, The Floating Integrating Gyro and its Application to Geometrical Stabilization Problems on Moving Bases, A. Sherman F. Fairchild Fund Paper (FF-13)(Institute of the Aeronautical Sciences, New York), 1955.

General discussion of gyros and their application to platform stabilization. Gyro performance is considered in some detail.

du Commerce, Service de la Propriété Industrielle.

French patent of delta modulation with circuit diagrams and waveforms.

7. Robert Hayum, Compensation of a Digital Integrating Accelerometer, M.S. Thesis, M.I.T. (MIT/IL Rpt. T-209A) June, 1959.

Compensation is accomplished by using torque generator microsyn as torquer and sensor.

8. Patrick B. Hutchings, Compensation of a Sampled Data Contactor Servo, M.S. Thesis, M.I.T. (MIT/IL Rpt. T-222) May, 1959.

First attempt to handle inputs. Heuristic discussion provides good insights.

9. K. Izawa and L.A. Weaver, "Relay-type Feedback Control Systems with Dead Time and Sampling," Trans AIEE, Part II, LXXVIII (1959), 49-53.

Phase plane analysis of delta-modulated loops with dead time. Attempts to determine modes.

10. Rudolph E. Kalman, Phase Plane Analysis of Non-Linear Sampled Data Systems, M.S. Thesis, M.I.T., 1954.

Essentially a computer study of a delta-modulated loop, with emphasis on stability in the large.

11. F.J. Mullin and E.I. Jury, "A Phase Plane Approach to Relay Sampled Data Feedback Systems," Trans AIEE Part II, LXXVIII (1959), 517-523..

Phase plane analysis with a nice method for reintroducing time into computation.

12. J.J. Rocchio, Jr., Analysis of a Digital Integrating Pendulous Accelerometer, M.S. Thesis, M.I.T. (MIT/IL Rpt. T-176) June, 1958.

13. Frederick A. Russell, Design Criterion for Stability of Sampled Data On-Off Servomechanisms, Ph.D. Thesis, Columbia University, June, 1953.

Like Chow (Ref. 3), Russell introduces variable delay due to sampling. Uses Bode plots.

14. J.F. Schouten, F. de Jager, and J.A. Greifkes, "Delta Modulation, A New Communications System for Telecommunications" Phillips Tech. Rev., XIII 7 (1952), 237-268.

Discussion of delta modulation and its application to transmission.

15. Stuart C. Schwartz, Analysis of Sampled Data Relay Servomechanisms with Zero and Step Inputs, M.S. Thesis, M.I.T. (MIT/IL Rpt. T-284), May, 1961.

First use of Bergen's method to verify modes of delta-modulated loops. Application of this technique to verify step input behavior.

16. Joseph J. Sliwkowski, A Study of a Delta Modulator, M.S. Thesis, M.I.T. (MIT/IL Rpt. T-287), May, 1961.

Analysis from a transmission point of view. Describing function for amplitude only derived.

17. Richard D. Smallwood, A Pulse Restrained Accelerometer, M.S. Thesis, M.I.T. (MIT/IL Rpt. T-174) June, 1958.

18. Calvin M. Theiss, "The Theory and Analysis of a Digital Accelerometer," Unpublished Ms., 10 January 1961.

Time domain analysis of delta-modulated loop.

19. H.C. Torng and W.E. Meserve, "Determination of Periodic Modes in Relay Servomechanisms Employing Sampled Data," IRE Transactions on Automatic Control, September, 1960, 298-305.

Uses difference equations to verify moding of loop.

20. Robert B. Meeks, Jr. and Eugene R. Wells Jr, Feasibility of Using a Ternary Mode for Pulse Torquing a Pendulous Accelerometer, M.S. Thesis, M.I.T. (MIT/IL Rpt. T-278), May, 1961.

First discussion of ternary torquing, but limit cycles not eliminated. Discussion of logical compensation.

B. Inertial Instruments

21. Charles S. Draper, Walter Wrigley, and Lester R. Grohe, The Floating Integrating Gyro and its Application to Geometrical Stabilization Problems on Moving Bases, A. Sherman F. Fairchild Fund Paper (FF-13)(Institute of the Aeronautical Sciences, New York), 1955.

General discussion of gyros and their application to platform stabilization. Gyro performance is considered in some detail.

22. William E. Fellows, "Vibration Effects on Gyroscopes and Accelerometers," Minneapolis Honeywell Regulator Co. Aero Document R-Ed 29004-1A, November, 1958.

Detailed discussion of many errors caused by vibrations.

23. Richard H. Frazier, Analysis of Four Pole Torquer with Full Normal to Gap Faces, MIT/IL Rpt. E-700, March, 1958.

24. Richard H. Frazier, Four Pole Alterating Current Signal Generator with Flapper Type Rotor, MIT/IL Rpt. E-703, April, 1958.

Each reportis a brief discussion, with numerical examples, of theory of flapper-rotor instruments in different applications.

25. Albert P. Freeman and Peter J. Palmer, Abridged Nominal Values and Specification for 2FBG-2 Series Floated Gyro Unit, MIT/IL Doc. G7-100-u-2FBG-2C, July, 1959.

26. Philip J. Gilinson Jr., William Denhard, Richard H. Frazier, A Magnetic Support for Floated Inertial Instruments, A Sherman, F. Fairchild Fund Paper (FF-27)(Institute of the Aeronautical Sciences, New York), May, 1960.

Discussion of theory of magnetic suspension system used in many inertial instruments. Numerical examples provided.

27. William B. Haff and Melvin Meltzer, Effects of Angular Vibration on the Performance of a Single-Degree-of-Freedom Integrating Gyroscope, M. S. Thesis, M. I. T. (MIT/IL Rpt. T-257), May, 1960.

Theoretical analysis of vibration effects on gyros. Coning and sculling discussed. Series solution for equation of gyro motion proposed.

28. Robert K. Mueller, Microsyn Electromagnetic Components (Instrumentation Laboratory, M. I. T.), December, 1952.

Fundamental discussion of microsyns in their various forms by the inventor.

29. Herbert Weinstock, A Study of the Response of the Single-Degree-of-Freedom Integrating Gyroscope to Angular Vibrations, MIT/IL Rpt. E-885, January, 1960.

Consideration of simultaneous angular vibrations about several instrument axes at once.

C. Coordinate Transformations

30. Herbert Goldstein, Classical Mechanics (Cambridge, Mass., 1951).

Chapter IV has a complete discussion of matrix transformation, Euler angles, and Cayley-Klein parameters. Good annotated bibliography.

31. Sir William R. Hamilton, Elements of Quaternions (Dublin, 1856).

This treatise introduces quaternions as an extension of complex numbers.

32. A. S. Hardy, Elements of Quaternions (Boston, 1881).

Basic text on quaternions with geometrical applications.

33. H. W. L. Hime, The Outlines of Quaternions (London, 1894).

Quaternions introduced as the quotient of two vectors. Various forms given.

34. Sir Harold Jeffreys and Bertha Swirles (Lady Jeffreys), Methods of Mathematical Physics, (Cambridge, England, 1956).

Chapters 3 and 4 cover matrices and tensors very well. Each chapter is headed by an apt quotation.

35. Myron Kayton, Coordinate Frames in Inertial Navigation, Ph. D. Thesis, M. I. T. (MIT/IL Rpt. T-260) August, 1960.

General discussion of coordinate transformation theory in Chapter 4 using tensors.

36. P. Kelland and P. G. Tait, Introduction to Quaternions (London, 1873).

Written "for those who desire to become mathematicians."

37. J. Halcombe Laning, Jr., The Vector Analysis of Finite Rotations and Angles, MIT/IL Rpt. 6398-S-3, September, 1949.

An interesting development of algebra required for the use of vectors to represent angles and rotations.

38. Philip M. Morse and Herman Feshbach, Methods of Theoretical Physics, 2 vols. (New York, 1953).

Chapter 1 develops some transformation properties and contains a brief mention of quaternions.

39. William R. Weems, An Introduction to the Study of Gyroscopic Instruments. (Department of Aeronautical Engineering, M. I. T.), January, 1948.

Section 8 contains a nice discussion of Euler angles.

40. E. T. Whittaker, A Treatise on the Analytical Dynamics of Particles and Rigid Bodies, 4th ed. (Cambridge, England, 1959).

Chapter 1 contains discussion of rotational transformations using quaternions, Cayley-Klein parameters, and Euler angles.

D. Numerical Analysis and Computers

41. Anonymous, "Modern Computation Methods," Notes on Applied Science, National Physical Laboratory (of England)(New York, 1957).

Complete discussion of numerical analysis as applied to computers. Excellent extensive bibliography.

42. Vannevar Bush, "The Differential Analyzer," J. Franklin Inst., CCXII (1931), 447-488.

Detailed physical description of one of the first analog computers.

43. Vincent Rocco DeMarco, The Effect of Increment Representation on the Accuracy of the Digital Differential Analyzer, M. S. Thesis, M. I. T. (MIT/IL Rpt. T-158), May, 1958.

Complete discussion of errors in DDA with various increment representations. Analysis in time domain.

44. George F. Forbes, The Digital Differential Analyzer, 3rd ed. (Pacoima, Calif., 1956).

Discussion and analysis of DDA.

45. Laurence J. Gitten, Incremental Computer Solution of a Coordinate Conversion Problem, M. S. Thesis, M. I. T., 1959.

Study of a coordinate transformation using a general incremental computer.

46. David R. Hartree, Numerical Analysis, 2nd ed.(Oxford, 1961).

A standard reference, includes a section on organization for automatic computation.

47. Francis B. Hildebrand, Introduction to Numerical Analysis (New York, 1956).

Standard text on numerical analysis.

E. Miscellaneous

56. Lewis Carrol, Through the Looking Glass, and What Alice Found There, illus. John Tenniel (New York, 1941).

The quote is in Chapter I. The explanation, by an early astronaut who had trouble on the launching pad, is in Chapter VI.

57. Harold Chestnut and Robert W. Mayer, Servomechanisms and Regulating System Design, 2 vols. Vol I, 2nd ed. (1959), Vol. II (1955).

Comprehensive text on control system theory and practice.

58. Ralph J. Kochenburger, "A Frequency Response Method for Analyzing and Synthesizing Contactor Servomechanisms," Trans AIEE Part I, LXl (1950), 270-284.

The describing function presented and applied by its originator.

59. Albrecht L. Kosmala, Feasibility Study of a Gimballess Inertial Space Reference, MIT/IL Rpt. R-274, April, 1960.

Early attempts at analysis of gimballess inertial reference equipment.

60. Samuel J. Mason and Henry J. Zimmerman, Electronic Circuits, Signals, and Systems (New York, 1960).

Chapter IV contains detailed discussion of flow graph analysis.

61. Robert W. Sittler et al., Pulsed Data Systems (Course Notes for 6.54, M.I.T., Spring, 1960).

Course notes for sampled data systems. Includes material on sampling, signal recovery, compensation and statistical theory of quantization. $z = e^{-sT}s$

62. Julius J. Tou, Digital and Sampled Data Control Systems (New York, 1959).

Sampled data text. Good section on compensation, especially with digital computers. $z = e^{sT}s$.

63. John G. Truxal, Automatic Feedback Control System Synthesis (New York 1955).

Standard text in the field covering practically all aspects of automatic control.

48. Alton S. Householder, Principles of Numerical Analysis, (New York, 1953).

Numerical methods for sets of linear equations, differentiation and integration. Excellent bibliography and bibliographical notes.

49. Harold E. Maurer, Error Analysis of a Digital Differential Analyzer, E. E. Thesis, M. I. T. (MIT/IL Rpt. T-129), May, 1957.

Attempt to use Widrow's (Ref. 55) statistical characterization of quantization.

50. Harold E. Maurer, An Approximate Analysis of Error Propagation in a Digital Differential Analyzer (MIT/IL Rpt. E-698), March, 1958.

Extension of Ref. 49.

51. John M. Salzer, Treatment of Digital Control Systems and Numerical Processes in the Frequency Domain, Sc. D. Thesis, M. I. T., August, 1951.

A clean way to handle numerical analysis. Presents a design method for computers.

52. James B. Scarborough, Numerical Mathematical Analysis, 4th ed. (Baltimore, 1958).

Standard work on numerical analysis. Full of numerical examples.

53. Wallace E. Vander Velde, "Computers in Inertial Navigation Systems", Section V in Inertial Guidance - Terrestrial and Interplanetary, (Course Notes for 16.45S, M. I. T., Cambridge, Mass., Summer, 1960).

A good basic discussion of all three types of computers, their operative advantages and disadvantages.

54. E. T. Whittaker and G. Robinson, The Calculus of Observations, 4th ed. (Glasgow, 1958).

Covers most numerical analysis topics as well as curve fitting and Fourier series.

55. Bernard Widrow, A Study of Rough Amplitude Quantization by Means of Nyquist Sampling Theory, Sc. D. Thesis, M. I. T., June, 1958.

A detailed analysis of quantization through a statistical model.

64. John G. Truxal, ed., Control Engineer's Handbook (New York, 1958).

As the title implies, this is written for the practicing engineer. Comprehensive coverage.

65. Albert D. Wheelon, "Free Flight of A Ballistic Missile, ARS J., XXIX (1959), 915-926.

One of the few places that range derivatives are discussed in the open literature.

66. Henry F. Blazek, "The Performance of Inertial Components on an Unstabilized Base", Presented at ARS Controllable Satelites Conference, M.I.T., 30 April 1959.

A brief listing of the effects of unstabilized bases on instruments.

BIOGRAPHICAL NOTE

Born on 31 May 1935 in Washington, D. C., Thomas Freud Wiener attended public schools in Trindad and the United States, and was graduated from The Western High School, Washington, D. C., in June, 1953. He matriculated at Brown University in September of that year, where he majored in Engineering. At Brown, he was an Associate Member of Sigma Xi, President of Rhode Island Alpha of Tau Beta Pi and the Brown Engineering Society, and a Francis Wayland Scholar. During the academic year 1957-1958, he held an appointment as Undergraduate Assistant in the Division of Engineering. In June, 1958, Brown University awarded him the degree of Bachelor of Science in Engineering magna cum laude, and he was commissioned Ensign, U. S. Naval Reserve.

After serving in USS GYATT (DDG-1) and USS MEREDITH (DD-890), he was ordered to the Massachusetts Institute of Technology in September, 1959, under the Junior Line Officers' Advanced Scientific Educational Program. In December, 1959, he was promoted to Lieutenant (junior grade), and in March, 1960, accepted a commission in the Regular Navy. In May, 1960, he was elected to Sigma Gamma Tau. He held an appointment as Teaching Assistant for the Spring Term, 1961. He is a member of the Institute of Radio Engineers and the United States Naval Institute.

He is married to the former Louise Ladd of Washington, D. C.